Università degli Studi di Trieste

Dipartimento di Ingegneria e Architettura

Corso di Dottorato in Ingegneria Industriale e dell'Informazione

XXXV ciclo

PhD thesis

Energy modelling and optimization of PEM fuel cells power plants in view of shipping decarbonization

PhD Student:
Chiara Dall'Armi

PhD Supervisor:
Prof. Rodolfo Taccani

PhD Coordinator:
Prof. Alberto Tessarolo

Academic Year 2021/2022

UNIVERSITÀ DEGLI STUDI DI TRIESTE

UNIVERSITÀ DEGLI STUDI DI TRIESTE

XXXV CICLO DEL DOTTORATO DI RICERCA IN

Ingegneria Industriale e dell'Informazione

PO FRIULI VENEZIA GIULIA – FONDO SOCIALE EUROPEO 2014/2020

Energy modelling and optimization of PEM fuel cells power plants in view of shipping decarbonization

Settore scientifico-disciplinare: **ING-IND/09 SISTEMI PER L'ENERGIA E L'AMBIENTE**

DOTTORANDA
CHIARA DALL'ARMI

COORDINATORE
PROF. ALBERTO TESSAROLO

SUPERVISORE DI TESI
PROF. RODOLFO TACCANI

ANNO ACCADEMICO 2021/2022

Contents

List of Figures

List of Tables

Acronyms

CH_2 Compressed hydrogen

CO_2 carbon dioxide

LH_2 Liquefied hydrogen

NH_3 ammonia

NO_x nitrogen oxide

SO_x sulphur oxide

ABS American Bureau of Shipping

ABSC ABSorption Chiller

AC Alternating Current

AFC Alkaline Fuel Cells

AH Auxiliary Heater

BAU Business As Usual

BOG Boil Off Gas

BoP Balance of Plant

BtL Biomass to Liquid

BV Bureau Veritas

CAPEX CAPital EXpenditure

CC Compression Chiller

CcH2 Cryo-compressed hydrogen

CCHP Combined Cooling Heating and Power

CCS Carbon Capture and Storage

CDF Cumulative Distribution Function

CHP Combined Heat and Power

CNG Compressed Natural Gas

CO carbon monoxide

COP Coefficient Of Performance

D&O Design and Operation

DC Direct Current

DF Dual Fuel

DME DiMethyl Ether

DMFC Direct Methanol Fuel Cells

DNV-GL Det Norske Veritas - Germanischer Lloyd

DOD Depth Of Discharge

EEDI Energy Efficiency Design Index

EESS Electric Energy Storage System

EMS Energy Management Strategy

EoL End of Life

ETS European Trading System

EU European Union

FAME Fatty Acid Methyl Esters

FC Fuel Cells

FCHEA Fuel Cells and Hydrogen Energy Association

GB Gear Boxes

GHG GreenHouse Gas

GSA Global Sensitivity Analysis

HFO Heavy Fuel Oil

HP Heat Pump

HT High Temperature

HT-PEMFC High Temperature Polymer Electrolyte Membrane Fuel Cells

HTH High Temperature Heaters

HTHP High Temperature Heat Pump

HVO Hydrotreated Vegetable Oil

ICE Internal Combustion Engines

IGF International Code of Safety for Ships using Gases or other Low-flshpoint Fuels

IMO International Maritime Organization

KOH potassium hydroxide

KRS Korean Register of Shipping

KS Kolgmogorov-Smirnov

LFP Lithium Iron Phosphate

LHV Lower Heating Value

LIB Lithium-Ion Batteries

LiBr Lithium-Bromide

LNG Liquefied Natural Gas

LOHC Liquid Organic Hydorgen Carrier

LR Lloyd's Register

LT Low Temperature

LT-PEMFC Low Temperature Polymer Electrolyte Membrane Fuel Cells

LTH Low Temperature Heaters

LTO Lithium Titanate Oxide

LTTS Low Temperature Thermal Storage

MC Monte Carlo

MCF Monte Carlo Filtering

MCFC Molten Carbonate Fuel Cells

MDO Marine Diesel Oil

MeOH methanol

MEPCS Marine Environment Protection Committee

MGO Marine Gas Oil

MH Metal Hydride

MILP Mixed Integer Linear Programming

MT Medium Temperature

MTHP medium Temperature Heat Pump

MTTS Medium Temperature Thermal Storage

NG Natural Gas

NMC Nickel Manganese Cobalt

OPEX OPerational EXpenditure

OPS Onshore Power Supply

ORC Organic Rankine Cycle

PAFC Phosphoric Acid Fuel Cells

PBU Pressure Building Unit

PEMFC Polymer Electrolyte Membrane Fuel Cells

PM Particulate Matter

RoPax Roll-on Passenger

SC Super Capacitors

SCR Selective Catalytic Reduction

SEEMP Ship Energy Efficiency Management Plan

SEI Solid Electrolyte Interface

SMR Steam Methane Reforming

SOC State of Charge

SOFC Solid Oxide Fuel Cells

SOH State Of Health

TEG ThermoElectric Generator

TS Termal Storage

TTP Tank To Propeller

UC Uncertainty Characterization

WHR Waste Heat Recovery

Summary

The need to reduce pollutant and greenhouse gases emissions in the shipping sector is leading to a growing interest in fuel cells propulsion. In particular, Polymer Electrolyte Membrane Fuel Cells (PEMFC) based power systems have been addressed as a promising solution for zero-emission navigation, provided that green hydrogen, *i.e.* produced from renewable energy sources, is used as fuel. Nonetheless, the use of PEMFC in the maritime sector is still in its early stages, as several issues related to PEMFC and hydrogen use on board still need to be overcome. First of all, PEMFC and hydrogen technologies are still affected by high costs, which often undermine their economic competitiveness, when not their economic feasibility. From a technical point of view, also the lack of a solid infrastructure for hydrogen production, distribution and bunkering is hampering today the feasibility of numerous projects on the use of hydrogen fueled PEMFC in shipping. All these aspects are somewhat related to the still incomplete regulatory framework for the use of PEMFC and hydrogen in shipping, which is indeed among the greatest challenges to face in this context. A further aspect to consider is related to the dynamic performance of PEMFC. As widely demonstrated in the literature, the hybridization of PEMFC with Electric Energy Storage Systems (EESS) could sensibly improve the overall system dynamics and efficiency. However, the power allocation between PEMFC and EESS is a complex issue, which involves the performance degradation of both the energy units. Considering the whole degradation effects in the energy management of hybrid PEMFC systems to determine the best compromise between costs and plant lifetime is a challenging yet crucial aspect, rarely addressed in the literature. In addition, the low temperature of PEMFC waste heat (<70°C) makes Waste Heat Recovery (WHR) on board challenging. While this aspect may not influence the overall operation of PEMFC systems for small vessels, it could hamper future

installation of PEMFC power systems for larger vessels such as cruise ships, where WHR is essential for efficiently covering thermal demands onboard. Recent studies address PEMFC WHR for stationary systems, but it appears to be a lack of studies on PEMFC WHR for ship applications. To fill these gaps, the proposed thesis aims at developing a general methodology that allows to optimize the synthesis, design, and operation of PEMFC ship power plants while considering the power units degradation and the possibility to recover the PEMFC waste heat. The proposed optimization models have been developed following a Mixed-Integer Linear Programming (MILP) approach and have been applied to different case studies. A small size RoRo passenger was considered as case study for the application of a health-conscious energy management strategy for a hybrid PEMFC/Lithium Ion Batteries (LIB) propulsion system, where a multi-objective optimization was set to concurrently minimize the operation cost and the PEMFC/LIB degradation over the entire lifetime of the plant. Subsequently, an uncertainty analysis was carried out to analyze the impact of uncertainties in the input parameters on the optimization results. As for the analysis of WHR integration for PEMFC installed on board, a cruise ship was considered as case study, and a multi-objective optimization was set to concurrently minimize the fuel oil consumption of the ship and the total operating and investment costs. The proposed energy system for the cruise ship includes PEMFC to supply the auxiliary electrical power onboard, WHR solutions as high temperature heat pumps and absorption chillers to recover PEMFC heat, and internal combustion engines to supply the mechanical power. The synthesis, design and operation of the cruise ship's energy system are optimized to match the mechanical, electrical, heating, and cooling power demand while minimizing the marine diesel oil consumption of the ship and the investment and operation costs. The results show that the multi-objective optimization of the hybrid PEMFC/LIB power plant of the ferry can effectively improve the performance of hybrid PEMFC/LIB energy system over time, ensuring not only the most effective operation in terms of costs and efficiency, but also avoiding stressful events that would decrease the overall lifetime of the plant, hence increasing the costs. With the progressive ageing of PEMFC and LIB, the hybrid propulsion system modifies the energy management strategy to limit the increase of the daily operation cost. Comparing the optimization results at the beginning and at the end of the plant lifetime, the daily oper-

ation cost and hydrogen consumption results to increase, affecting the overall volume and weight of the plant. As for the cruise ship case study, the results show that the optimal plant configuration allows to cut the vessel's marine diesel oil consumption by about 53% with respect to the current ship energy system, highlighting the need to substitute also the main propulsion engines with PEMFC for achieving higher decarbonization rates. The thesis is organized as follows: Chapter 2 outlines the main strategies to cut emissions from shipping, focusing on the role of alternative fuels and power systems. Afterwards, Chapter 3 reports the literature review on hydrogen fuelled PEMFC based energy systems. The methodology proposed in the present thesis is then described in Chapter 4, while results are presented and discussed in Chapter 5. Lastly, conclusions are drawn in Chapter 6, where suggestions for further research on the topic are also proposed.

Sommario

La necessità di ridurre le emissioni di inquinanti e gas serra dovute al trasporto marittimo ha portato, nel tempo, ad un crescente interesse nei confronti della propulsione navale con celle a combustibile. In particolare, i sistemi energetici basati su celle a combustibile con membrana a elettrolita polimerico (PEMFC - Polymer Electrolyte Membrane Fuel Cells) sono considerati, ad oggi, tra le soluzioni più promettenti per la navigazione a emissioni zero - a condizione che come combustibile venga utilizzato idrogeno prodotto a partire da fonti di energia rinnovabile. L'utilizzo di sistemi PEMFC nel settore marittimo risente, tuttavia, di problematiche relative non solo all'utilizzo delle stesse PEMFC e dell'idrogeno a bordo, ma anche legate ad aspetti economici e logistici che ne ostacolano, ad oggi, un utilizzo su larga scala. Innanzitutto, le PEMFC - ed in generale le tecnologie a idrogeno - sono ancora affette da costi elevati, che spesso ne minano la competitività economica, quando non la fattibilità stessa dell'impianto. Da un punto di vista tecnico, inoltre, la mancanza di un'infrastruttura diffusa per la produzione, distribuzione e bunkeraggio dell'idrogeno rappresenta spesso un ostacolo per la realizzazione di progetti sull'uso di PEMFC alimentate a idrogeno nel settore navale. Tutto ciò è legato anche alla situazione normativa relativa all'impiego di PEMFC e idrogeno nel settore del trasporto marittimo. Infatti, nonostante i recenti miglioramenti, ci sono ancora molte lacune in ambito normativo, che comportano in genere un allungamento dei tempi previsti per la certificazione degli impianti ed un conseguente aumento dei costi. Un ulteriore aspetto da considerare è legato alle prestazioni dinamiche delle PEMFC. Come ampiamente dimostrato in letteratura, l'ibridazione delle PEMFC con sistemi di accumulo di energia elettrica (EESS - Electrical Energy Storage System) potrebbe migliorare sensibilmente le prestazioni dinamiche e l'efficienza complessiva del sistema. Tuttavia, la ripartizione dei flussi di potenza tra PEMFC e EESS è un problema comp-

lesso, che richiede anche un'attenta valutazione del degrado delle prestazioni di entrambe le unità energetiche nel tempo. Infatti, considerare gli effetti del degrado complessivo nella gestione energetica dei sistemi PEMFC/EESS per uso marittimo al fine di determinare il miglior compromesso tra costi e durata dell'impianto è un aspetto critico, che risulta tuttavia essere solo in parte affrontato in letteratura. In aggiunta, la bassa temperatura del calore di scarto delle PEMFC (<70°C) rende difficile il recupero del calore di scarto (WHR – Waste Heat Recovery) a bordo. Sebbene questo aspetto potrebbe non influire sul funzionamento complessivo dei sistemi PEMFC per piccole imbarcazioni, esso potrebbe ostacolare la futura installazione di sistemi energetici basati su PEMFC per imbarcazioni più grandi, come ad esempio le navi da crociera, dove il WHR è essenziale per soddisfare le richieste termiche di bordo. Studi recenti hanno affrontato il tema del WHR delle PEMFC per i sistemi stazionari, mentre solo pochi studi in letteratura analizzano il WHR dalle PEMFC per le applicazioni navali. Per colmare queste lacune, la tesi proposta mira a sviluppare una metodologia generale che consenta di ottimizzare la sintesi, la progettazione e il funzionamento dei sistemi energetici navali con PEMFC, tenendo conto del degrado delle unità di potenza nel tempo e della possibilità di recuperare il calore di scarto delle PEMFC. I modelli di ottimizzazione proposti sono stati sviluppati seguendo un approccio di programmazione MILP (Mixed-Integer Linear Programming) e sono stati applicati a diversi casi studio. Un traghetto RoRo di piccole dimensioni è stato considerato come caso studio per lo sviluppo e l'applicazione di una strategia di gestione energetica per un sistema di propulsione ibrido PEMFC/batterie al litio (LIB - Lithium-Ion Batteries) che tenga conto del degrado dei componenti nel tempo. In questo caso, l'ottimizzazione multi-obiettivo è stata impostata per minimizzare contemporaneamente il costo totale dell'impianto e il degrado di PEMFC e LIB nel tempo. Successivamente, è stata effettuata un'analisi dell'incertezza per analizzare l'impatto dei parametri di input incerti sui risultati dell'ottimizzazione. Per quanto riguarda l'analisi del WHR da PEMFC per uso marino, si è considerata come caso studio una nave da crociera. Il sistema energetico proposto comprende PEMFC per fornire l'energia elettrica ausiliaria a bordo, soluzioni WHR come pompe di calore ad alta temperatura e refrigeratori ad assorbimento per recuperare il calore della PEMFC, e motori a combustione interna per soddisfare la domanda di energia meccanica. Le

taglie dei componenti e il funzionamento del sistema energetico della nave da crociera nel suo complesso sono stati ottimizzati al fine di minimizzare contemporaneamente il consumo di gasolio marino della nave e i costi di investimento e funzionamento, garantendo la copertura delle richieste di energia meccanica, elettrica e termica di bordo. I risultati dimostrano che l'ottimizzazione multi-obiettivo dell'impianto ibrido PEMFC/LIB del traghetto può migliorare le prestazioni del sistema ibrido PEMFC/LIB nel tempo, garantendo non solo un design e un funzionamento più efficaci in termini di costi ed efficienza, ma anche evitando eventi stressanti nell'operazione di PEMFC e LIB che ne ridurrebbero la vita utile. Con il progressivo invecchiamento di PEMFC e LIB, la strategia di gestione dell'energia si modifica, adattandosi alle nuove caratteristiche dell'impianto al fine di limitare l'aumento dei costi di funzionamento giornalieri. Confrontando i risultati dell'ottimizzazione all'inizio e alla fine del ciclo di vita utile dell'impianto, il costo di funzionamento giornaliero e il consumo di idrogeno risultano in aumento, incidendo sul volume e sul peso complessivo dell'impianto. Per quanto riguarda il caso di studio della nave da crociera, i risultati mostrano che la configurazione ottimale dell'impianto consente di ridurre il consumo di gasolio marino della nave del 53% circa rispetto all'attuale sistema energetico della nave. La tesi è organizzata come segue: il Capitolo 2 delinea le principali strategie per ridurre le emissioni del trasporto marittimo, concentrandosi sul ruolo dei combustibili alternativi e dei sistemi energetici alternativi. Successivamente, il Capitolo 3 riporta la rassegna della letteratura sui sistemi energetici basati su Polymer Electrolyte Membrane Fuel Cells (PEMFC) alimentate da idrogeno. I Capitoli 4 e 5 riportano, rispettivamente, la metodologia proposta in questa tesi ed i risultati ottenuti. Infine, nel Capitolo 6 si traggono le conclusioni, suggerendo ulteriori approfondimenti sull'argomento.

Chapter 1

Research context and motivation

The driving motivation of the present thesis is the urge to reduce pollutant and GreenHouse Gas (GHG) emissions from the maritime transport, in order to curb the emission levels under the limits set by national and international initiatives (*e.g.* the European Green Deal). Such initiatives pose severe technical and economical challenges to the entire energy, industrial, mobility, and residential sectors. The maritime industry makes no exception, as new regulations on acceptable pollutant and GHG emission thresholds start to be set at national and international level (*e.g.* the International Maritime Organization (IMO) [1]). Hence, recent research is focusing on exploring possible actions and measures needed to achieve acceptable levels of emissions while ensuring the economical sustainability of shipping in the long term. As of today, the maritime transport is responsible of about 3% of global GHG emissions, with about 940 million tons of equivalent carbon dioxide (CO_2) emitted every year [1]. Such emission levels are expected to grow by more than 30% if no actions are taken, *i.e.* if the Business As Usual (BAU) scenario is kept [2]. This is the reason behind the establishment of ever more stringent regulations on both pollutant and GHG emissions from the maritime transport. As shown in Figure 1.1, the regulatory initiatives to reduce the emissions from the shipping sector started already in 2011, when the efficiency indicators Energy Efficiency Design Index (EEDI) and Ship Energy Efficiency Management Plan (SEEMP) were introduced with the Marine Environment Protection Committee (MEPCS) 62 Resolution (July 2011) [3]. In 2018 further restrictions on

GHG emissions were imposed, setting the challenging goal of cutting the annual shipping emissions by 50% with respect to the 2008 levels by the year 2050 [1]. Other initiatives and restrictions spread directly from national bodies and entities, as for example the resolution adopted by the Norwegian Parliament to halt GHG emissions from vessels navigating in Norwegian fjords by 2026 [4]. Figure 1.2 shows the cumulative CO_2 emissions of international shipping

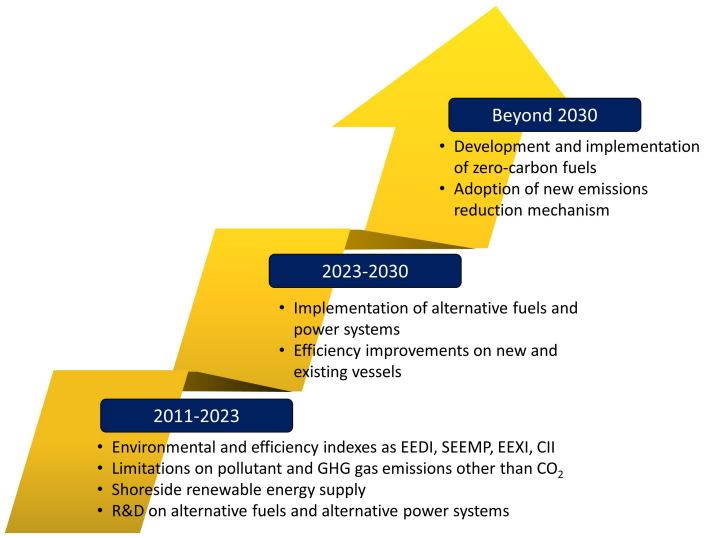

Figure 1.1: *Timeline of shipping emission reduction strategies and actions to achieve shipping decarbonization as outlined by IMO [1, 3].*

under the different scenarios, highlighting the positive impact that the new regulations could have in terms of CO_2 emissions reduction from shipping in the next years. Additionally, new stringent European Union (EU) regulations for shipping are expected in the forthcoming years, as a result of the launch of the *Fit for 55* package by the EU Commission on July 2021 [2, 5]. The general goal of the *Fit for 55* package is of cutting the EU emissions by 55% by 2030, and affects the entire industrial sector. There are, however, some specific proposals referred to the shipping industry, and in particular [5]:

- European Trading System (ETS) directive, which would imply the inclusion of maritime transport in the EU emission trading scheme;

- FuelEU Maritime Regulation, which would impose GHG intensity requirements on marine fuels;

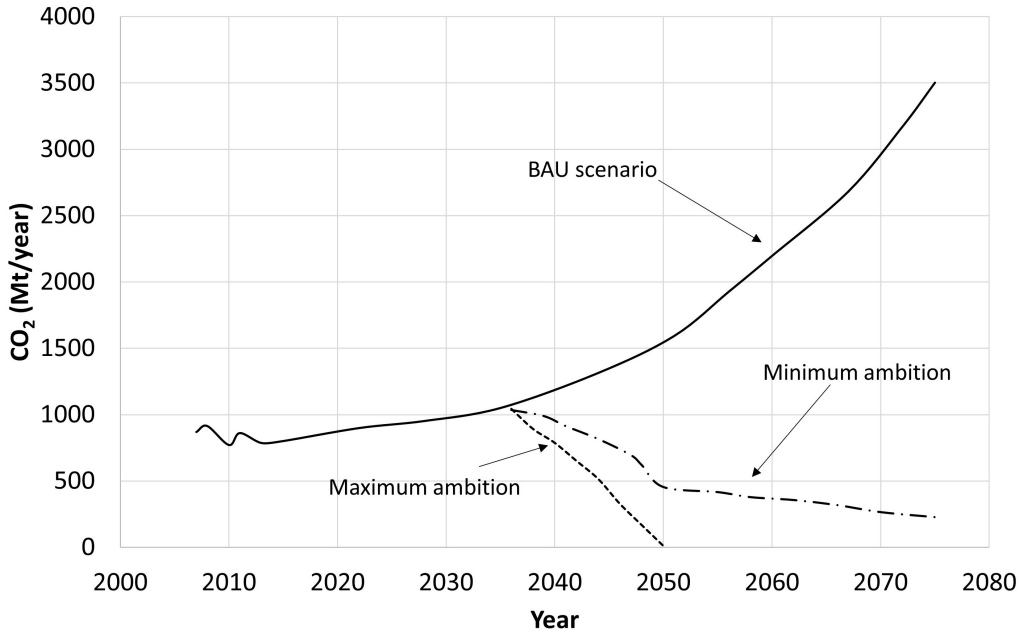

Figure 1.2: *Cumulative CO_2 emissions of international shipping under three scenarios: BAU, IMO's minimum and IMO's maximum ambitions. Elaborated from [1, 3].*

- Energy Taxation Directive revision, with the proposal of removing tax exemptions for fossil fuels used in maritime transport;

- Alternative FUel Infrastructre Regulation, which would entail the adoption of a new regulation for the realization of an infrastructure for alternative fuels.

Such new rules and regulations require the rethinking of the entire shipping industry to ensure not only the environmental sustainability of the sector over time, but also its economic competitiveness. For example, it has been estimated that the only application of the ETS on the Italian fleet of ferries would increase the energy costs by 27% [6]. In such a context, the ultimate goal of this thesis is to contribute to the analysis of alternative pathways and strategies that could guarantee the reduction of shipping emissions. Among the possible strategies proposed in the literature, that will be listed and described in the first part of the thesis, focus will be given here to the use of alternative fuels and alternative power systems, and particularly on hydrogen fueled PEMFC as they could guarantee the zero local emission navigation.

1.1 General approach of the thesis

Different approaches can be followed to analyze the possibility of using hydrogen PEMFC for ship propulsion. For instance, they can focus on the optimization of the operation of a single component of the energy system, or on the deep understanding and optimization of the electrochemical reactions happening in the fuel cells, or can be directed to the understanding and improvement of the safety aspects related to this type of systems, to mention a few. In this thesis it has been chosen to follow an approach typical of the energy system engineering: rather than focusing on single aspects and components of the energy system, the ship energy system is considered as a whole, and the analysis is carried out by accounting for the possible trade offs that could guarantee the optimal synthesis, design, and operation of such systems under an environmental as well as economical point of view.

1.1.1 Goal of the thesis and research questions

The primary goal of the present thesis is to contribute to the analysis of hydrogen PEMFC energy systems in view of shipping decarbonization. Following an approach typical of the energy systems engineering, this thesis aims to develop a general methodology for defining the optimal synthesis, design, and operation of hydrogen fueled PEMFC-based ship energy systems taking into account the power sources degradation over time and the possibility of recovering the waste heat of the PEMFC. As will emerge later in the literature review (Chapter 3), despite the key role that such aspects may have in the establishment of a widespread use of PEMFC systems in shipping, they have been only partially addressed in the available literature.

More in detail, the present thesis aims at answering the following research questions, divided into two groups for the sake of clarity:

1. **Group 1** Macro-research area: optimal synthesis, design, and operation of hydrogen fuelled PEMFC-based ship energy systems taking into account the degradation of the power sources over time

    - What is the best way to design and operate a maritime hydrogen PEMFC energy system to ensure optimal operation of the plant as a whole in terms of efficiency and costs?

- What is the influence of PEMFC and Lithium-Ion Batteries (LIB) degradation over time on the overall performance of a maritime hybrid PEMFC/LIB energy system in terms of costs and efficiency of the plant?
- What is the best way to design and operate a maritime hydrogen PEMFC energy system to ensure optimal operation of the plant as a whole in terms of efficiency and costs?
- What is the influence of PEMFC and LIB degradation over time on the overall performance of a maritime hybrid PEMFC/LIB energy system in terms of costs and efficiency of the plant?

2. **Group 2** Macro-research area: optimal synthesis, design, and operation of hydrogen fuelled PEMFC-based ship energy systems taking into account the the possibility of recovering the waste heat of the PEMFC

   - Is it possible to design an alternative ship energy system where PEMFC substitute the auxiliary Internal Combustion Engines (ICE) for on board auxiliary electric demand?
   - Can PEMFC's Waste Heat Recovery (WHR) guarantee the supply of heating demand on board?
   - Which WHR technologies could be implemented on board to ensure the thermal power supply to the ship, while limiting cost?
   - What would be the advantage of such energy system in terms of reduction of fossil fuel usage?

1.1.2 Modelling approach used in the thesis

Following the approach typical of the energy systems engineering for modelling and optimizing complex multi-energy systems, a Mixed Integer Linear Programming (MILP) approach has been adopted in this thesis for developing the optimization models. In fact, MILP models allow to account for large sets of design and operational variables without excessively increasing the computational effort required to solve the optimization problems. The analysis in this thesis has been developed in two phases. Firstly, MILP models have been developed for assessing the optimal design and operation of a hybrid

PEMFC/LIB energy system for the propulsion of a small size ferry. Both PEMFC and LIB performance degradation over time have been taken into account in determining the optimal energy management strategy of the vessel. Secondly, a cruise ship case study has been considered for applying the general methodology to assess the optimal synthesis, design, and operation of the whole ship energy system in which ICE for covering auxiliary electric loads are substituted by PEMFC. In this case, the analysis included of the possibility recovering the fuel cells waste heat onboard since the early design phases of the energy system.

1.2 Structure of the thesis

The thesis starts by outlining the main strategies to cut emissions from shipping, focusing on the role of alternative fuels and power systems, particularly fuel cells, in Chapter 2. Afterwards, the literature review on hydrogen fueled PEMFC based energy systems for shipping is presented in Chapter 3, starting from the overview of the main projects on the use of Fuel Cells (FC) in shipping. Chapter 4 outlines the methodology developed in the thesis to address the research questions, describing the case studies chosen for applying the methodology. Chapter 5 hence reports the results, while conclusions are drawn in Chapter 6.

Chapter 2

Introduction and background

This chapter outlines the main concepts that are necessary to understand the general framework in which the present thesis is developed. After a brief introduction on the conventional fuels and power systems used today in shipping in Section 2.1, the main strategies proposed in the literature and industry for the reduction of shipping emission are presented in Section 2.2. Particular attention is given to alternative fuels and fuel cell systems, the core object of the present thesis. More in detail, Section 2.3 outlines the main characteristics of the alternative fuels proposed for use in shipping, while Section 2.4 describes the main types of fuel cell systems that have been propose as possible alternative power systems on board of ships. Eventually, the thesis' object and delimitations are refined in Section 2.6.

2.1 Conventional marine fuels and power systems

Conventional marine fuels can generally be classified as distillate and residual fuels, with the last ones being produced from the residue of the refining process [7]. Currently, three main fuel oils are used in shipping:

- **Heavy Fuel Oil (HFO)**: residual fuel oil mostly used in larger vessels (*e.g.* tankers, bulk carriers), it is currently the most widely used fuel in shipping (47-66% of marine fuel mix); it has poor environmental performances, mainly due to its high sulfur content (about 2.7%); due to its high viscosity, it requires to be heated before being used to feed ICE [7];

- **Marine Diesel Oil (MDO)**: distillate fuel oil, lighter than HFO and with lower sulfur content (0.3-2.0 % m/m - *i.e.* % mass of sulfur per mass of fuel); generally used in small size vessels with medium/high speed four-strokes ICE, it is usually preferred for applications with relatively uniform speeds and high loads [7];
- **Marine Gas Oil (MGO)**: distillate fuel oil, similar to MDO in terms of sulfur content (0.10-1.50% m/m), is generally used for small to medium size ships with medium/high speed four stroke ICE;it is usually preferred to MDO in applications with frequently varying loads and speeds [7].

Table 2.1 reports a list of the main characteristics of current marine fuels.

Table 2.1: *Main properties of the most common fuels currently in use in shipping. Elaborated from [8].*

Fuel	**LHV (MJ/kg)**	**Flash point (°C)**	**Density @15°C (kg/m^3)**	**Sulfur content (% m/m)**
HFO	39	140-150	940-1010	2.7
MDO	43	60-75	840-860	0.3-2.00
MGO	43	60-75	840-860	0.1-1.5

As for power systems, ships mainly rely on ICE. Marine ICE are generally classified into three categories, according to the engine speed: (i) high speed, (ii) medium speed, and (iii) low speed ICE [8]. Each category differs from the others in terms of efficiency, dimensions, rated power, and other characteristics (*e.g.* cylinder number, bore, etc.). Table 2.2 reports a list of the main characteristics of the three categories of marine ICE [8]. It should be noticed the high efficiency that can be achieved by low speed two-stroke marine ICE. Such aspect, together with the high level of technological maturity of ICE, the well-known storage systems for fossil fuel oils on board of ships, and the solid know-how on fuel and ICE management on board, represents for sure a benchmark that is difficult to achieve in the short term by alternative marine fuels and power systems. Nonetheless, if no actions are taken, the conventional marine power systems cannot guarantee the compliance with the new and upcoming emission regulations, and is hence essential to explore different emission reduction strategies.

Table 2.2: *Main characteristics of marine ICE. Elaborated from [8].*

Engine type	**Rated speed (rpm)**	**Power (kW)**	**Stroke number (-)**	**Efficiency (%)**
High speed	$\geq$ 1400	$\leq$ 9000	4	$>$ 40
Medium speed	400-1200	$\leq$ 2000 per cylinder	4	$>$ 45
Low speed	$<$400	$\leq$ 7000 per cylinder	2	$\leq$ 50-54

2.2 Strategies to reduce shipping emissions

The reduction of pollutant and GHG emissions from the maritime transport is a complex issue, which involves various aspects of ship design, construction, operation, and disposal. In general, the maritime emission reduction strategies are classified into two macro-categories: (i) operational measures and (ii) technical measures [9, 10, 11], according to whether the measures address (i) the way the ship is operated (*e.g.* speed, route choice according to weather conditions, etc.) or (ii) the design and technical aspects of the ship (*e.g.* propulsion systems, hull design, emission abatement systems, fuel type, etc.). Each strategy comes at different costs and technological maturity, and can guarantee different levels of emission reduction. Moreover, it should be noticed that only some of the technical strategies can be applied to existing vessels, *i.e.* as retrofit measures, while others apply only to new-built ships. Differently, all the operational strategies can generally be applied independently to both existing and new-built vessels [10]. Table 2.3 reports a summary of the main technical and operational strategies that can be followed for reducing shipping emissions, specifying those that can be applied as retrofit measures to existing vessels [9, 10, 11].

Table 2.3: *Main emission reduction measures in shipping (• = applicable; ◦ = not applicable). Elaborated from [9, 10, 11].*

Category	Sub-category	Strategy	Retrofit
Technical strategies	Power and propulsion	ICE Advanced turbocharging	•
		ICE Water injection	•
		ICE Air humidification	•
		ICE hybridization	•
		Thrust efficiency improvement	◦
		Assisted propulsion with renewable sources	•
		Alternative power systems	◦
		Alternative fuels	•
		Onshore Power Supply (OPS)	•
	Emission abatement systems	Scrubber	•
		Selective Catalytic Reduction (SCR)	•
	Ship fluid dynamics	Hull resistance reduction	◦
		Air lubrication	•
		Aftbody and forebody optimization	•
		Ship sizing and weight optimization	◦
Operational strategies	Voyage optimization	Speed reduction	•
		Weather/routing optimization	•
		Ship speed optimization	•
		Just-in-time arrival	•
		Trim, draft, and ballast optimization	•
	Vessel maintenance	Hull roughness control	•
		Propeller roughness control	•

Continued on next page

Table 2.3 – continued from previous page

Category	Sub-category	Strategy	Retrofit
	Energy management	Onboard energy demand reduction	•
		Fuel quality control	•

With regard to the technical strategies, a first option is to act on the power and propulsion system. For example, some measures aim to reduce the fuel oil consumption by improving the efficiency of the ICE [12, 13], while others involve the humidification of the inlet air or the water injection to reduce the pollutant emission during the combustion [14, 15]. Other measures could be taken to hybridize the ICE with an Electric Energy Storage System (EESS) (*e.g.* batteries, supercapacitors) to improve the operating conditions of ICE [13, 12, 16, 17]. Alternatively, some studies [18, 19] propose to assist the propulsion by means of renewable energy sources, particularly solar and wind assisted propulsion, or to substitute the ICE systems with low emission power plants (*e.g.* fuel cells or batteries) [20]. Other papers and initiatives [21, 22, 23] propose the use of OPS to cut the emissions of ships at berth (often referred to as *cold ironing*). Another sub-category of technical measures is represented by those actions that aim to directly abate the pollutant and/or GHG emissions through the installation of emission abatement technologies on board (*e.g.* SCR or scrubbers), helping to curb the emission levels under the national and international thresholds [24]. However, the bulkiness and weight of emission abatement systems often hamper their installation onboard [25]. Lastly, other technical strategies involve the improvement of the ship performance in fluid dynamic terms. For example, it could be possible to reduce the fuel consumption and hence emissions from shipping by reducing the hull resistance in the ship design phase, or by installing air lubrication systems that reduce the hull resistance also in existing vessels [16, 13]. Also the way the ship is operated can sensibly help in reducing the fuel oil consumption, and hence emissions. For instance, recent studies are proposing new ship navigation management systems that optimize the route according to the weather and sea conditions [26, 27], or that optimize the ship operation while guaranteeing reduced navigation speed [23]. Lastly, also the control of the hull and propellers roughness to ensure adequate fluid dynamic performance over time, and the energy management onboard (*e.g.* by limiting the onboard energy demand) could help in reducing shipping emissions [10].

2.3 Alternative fuels in shipping

This section briefly outlines the main characteristics, strengths, and weaknesses of the main alternative fuels recently proposed for reducing pollutant and GHG emissions from shipping. The characteristics outlined hereafter refer in particular to the environmental and techno-economic aspects of using a new fuel in the shipping industry (*e.g.* emissions, fuel price, investment and operational cots, engine adaptation, fuel properties, storage, bunkering, etc.). However, it must be emphasized that also other aspects may play a key role in determining the suitability and/or convenience of a certain fuel over another, *e.g.* geopolitical aspects related to fuel availability, public opinion, politics. The analysis of such aspects is not reported here as it is out of the scope of this thesis, but interesting and useful insights on these points can be found in [28, 29, 30].

2.3.1 Natural gas

The use of Natural Gas (NG) as alternative fuel in shipping has seen a growing industrial interest in the last years and there are already several examples of ships fuelled by NG [31]. In terms of emission reduction, the use of NG has several advantages in comparison with the use of traditional liquid fuels. Indeed, thanks to NG's chemical properties, if used in ICE it can guarantee almost zero emission of sulphur oxide (SO_x) and Particulate Matter (PM). If used in spark ignited and Dual Fuel (DF) engines, nitrogen oxide (NO_x) emissions can be cut by approximately 85% [32, 33]. Lastly, also Tank To Propeller (TTP) CO_2 emission can be potentially cut by up to 30% if NG is used instead of HFO or MDO [8], even if such advantage can be reduced by the methane slip phenomenon [34]. In addition to its use in ICE, NG could also feed FC, after being properly reformed with even higher emission reduction potential [20, 35]. For example, the results of the analysis proposed in [35] show that Solid Oxide Fuel Cells (SOFC) fed by NG for shipping could guarantee a reduction in ship GHG emissions by up to 34% with respect to traditional propulsion system. Despite the numerous advantages of using NG as fuel for shipping, a major concern of its use on board that hampered the large-scale use of NG for several years is represented by the storage system. NG is in gaseous form at ambient conditions (1 bar, 25 °C), and needs to be either liquefied or compressed to achieve higher energy densities. If stored in liquid form, *i.e.* as Liquefied Natural Gas (LNG), cryogenic storage tanks are required to guarantee a temperature of -162°C at atmospheric pressure [36]. In such conditions, an energy density of about 6-7 kWh/l can be achieved [36]. Generally, for LNG fuelled ships other than LNG carriers, type C tanks are used, as this type of storage tank allows an easier management of the Boil

Off Gas (BOG) [32]. LNG as fuel is used for different kind of vessels. As of September 2022, there are 317 LNG fuelled ships in operation worldwide and 516 confirmed LNG fuelled ships new builds [37]. LNG fuel is currently used especially by car/passenger ferry (42 operating vessels) and tanker (41 chemical tankers in operation, 39 crude oil tankers in operation), while new orders mainly refer to container ships (176 confirmed new orders) and car carriers (95 confirmed orders). Another possibility is to store NG as Compressed Natural Gas (CNG), at ambient temperature and high pressure, usually in the range of 200-700 bar. In this way, the complications linked with the installation and operation of a cryogenic plant on board are avoided, although the lower energy densities achievable by CNG with respect to LNG makes CNG convenient only for ships that operate on short routes. Also for this reason, LNG is often preferred over CNG as fuel for shipping [32].
The bunkering infrastructure dedicated to LNG is improving quite rapidly, with 140 bunkering infrastructures (bunker vessel, tank to ship, truck loading, bunker vessel loading, local storage, and others considered) already in operation worldwide and 54 decided ones [37]. A crucial aspect of LNG is represented by the costs: while in the past the cost of LNG was competitive, with an average of about 30 €/MWh between 2014 and 2021, the last years have seen and increase by up to about 360%, with the actual cost being about 110 €/MWh [37]. While such scenario may change rapidly in the forthcoming years according to the evolution of the today geopolitical events, an accurate monitoring of such market evolution is necessary to evaluate the competitiveness feasibility of LNG fuelled ships in the long term. Lastly, concerning the regulatory aspects, NG fulled ships are today a market ready solution, and class rules are already available for NG storage on board of ships and for the bunkering phase (International Code of Safety for Ships using Gases or other Low-flshpoint Fuels (IGF) Code).

2.3.2 Ammonia

In recent years, ammonia (NH_3) gained interest as alternative fuel for shipping, as its use could have advantages in economical, environmental, and technical terms [38]. In economical terms, the use of NH_3 could initially guarantee lower costs than other alternative fuels if NH_3 is considered to be produced starting from fossil fuels. In fact, NH_3 is already produced and used on a large scale in different industrial sectors, particularly for the production of fertilizers. Nonetheless, the NH_3 production processes are today carbon intensive. While carbon-free processes for the production of green NH_3 are already available, the they are more expensive than the one of NH_3 produced in the traditional way [39, 40, 41]. Nonetheless, it should be noticed that NH_3 is traditionally produced staring from NG, and as such it is sensitive to the price fluctuations

of NG. As seen before for NG, the recent geopolitical events resulted in an increase by about 360% of NG, which resulted in an increase of the NH_3 fossil cost from an average of about 60 €/Mwh in the years 2014-2021 to about 200 €/MWh during last year. Hence, an accurate monitoring of such market evolution is necessary to evaluate the competitiveness feasibility of NH_3 fuelled ships in the long term. As far as the environmental aspect is concerned, the chemical structure of NH_3, with no carbon atoms, is intrinsically advantageous as it could avoid the emission of carbon related GHG gases (*i.e.* CO_2) and pollutants (*e.g.* carbon monoxide (CO)) [38, 42]. Nonetheless, the use of NH_3 as fuel would produce other pollutants, above all NO_x, and also GHG gases, *e.g.* N_2O which need to be removed to curb the emissions under acceptable levels [40]. From a technical point of view, thanks to the large volumes of NH_3 transported every year by ship, the use of NH_3 as marine fuel could benefit from an already established bunkering infrastructure, with bout 200 bunkering infrastructures already in operation worldwide [37]. Additionally, an advantage of using NH_3 as marine fuel is the possibility of using NH_3 to feed either ICE or FC. If used in ICE, a reduction by up to about 90% of GHG emissions can be achieved with respect to conventional HFO fuelled ships [42], while post-combustion devices would be needed to reduce NO_x emissions [43]. As for FC, NH_3 could either directly feed FC, *e.g.* SOFC as proposed in the ShipFC project [44], or feed PEMFC after a cracking process to obtain hydrogen from NH_3 [42]. While crackers are largely used in different industrial sectors, their use on board may be unpractical. Moreover, possible NH_3 residuals in the obtained hydrogen may poison the PEMFC [45]. Lastly, although the storage conditions of NH_3 are easier than for other fuels (about 10 bar and 20°C), the toxicity of NH_3 represents today the main drawback of NH_3 use onboard, and is hampering its inclusion in international standards as fuel for shipping [46].

2.3.3 Methanol

As seen for NH_3, another alternative fuel for shipping that could be used in both ICE and FC is methanol (MeOH) [43]. MeOH is already produced on a large scale for its use in industrial applications [47], is mainly produced from NG and coal, although it can also be produced from renewable feedstock (*e.g.* biomass, agricultural or municipal waste) [48, 49]. In general, MeOH cannot guarantee zero-local emission. Today MeOH is mainly produced from NG, with GHG emissions on the lifecycle that are comparable to those of NG [50]. Nonetheless, MeOH could also be produced from renewable feedstock,*i.e.* bio MeOH. Bio MeOH can potentially guarantee the reduction of lifecycle NO_x emissions by up to 45% and lifecycle SO_x emissions by up to 8% with respect to conventional fuels [51, 52]. Alternatively, onboard Carbon Capture and Storage (CCS) could be implemented to ensure the zero-local emission

navigation, although such technologies are still in their early stage for ship applications, and hence would increase the overall complexity and cost of the system [43, 49]. Similarly to NG, MeOH could also feed PEMFC, provided and external reforming unit for obtaining hydrogen to feed the PEMFC. As previously said for NH_3 cracking systems, also MeOH reformers are not yet available for shipping, and hence it will probably take some time before MeOH fuelled PEMFC are implemented onboard [53, 54]. As for bunkering, MeOH can benefit today from 117 operating bunkering infrastructure worldwide [37]. The cost depends on the way MeOH is produced, and amounts today to about 60 €/MWh for fossil MeOH, with an average value over the last eight years of about 45 €/MWh [37]. From a regulatory point of view. MeOH is not yet encompassed in the IGF code fo low flashpoint fuels, and as such it sis necessary to demonstrate an equivalent safety level through the *alternative design* process. Nonetheless, guidelines start to be available from the regulatory bodies, as for example [55].

2.3.4 Hydrogen

The large interest in the use of hydrogen as alternative fuel for shipping is mainly due to its possibility of guaranteeing the zero-emission navigation. Indeed, if hydrogen fuels PEMFC the only by-product would be water vapor, hence eliminating not only pollutant emissions, but also GHG emissions [36]. Hydrogen could also feed ICE, although in this case NO_x emissions woule be formed and hence the navigation would not be emission free [56]. Hydrogen storage system can be classified as (i) physical or (ii) chemical, according to whether hydrogen is stored in its pure form at different levels of pressure and storage (physical) or coupled with other chemical substances, often referred to as hydrogen carriers (chemical) [57]. Today, hydrogen is mainly stored either in compressed form in high pressure cylinders, *i.e.* Compressed hydrogen (CH_2), at ambient temperature and pressure in the range 200-1000 bar, or liquefied, *i.e.* Liquefied hydrogen (LH_2), in cryogenic tanks, at atmospheric pressure and at -253 °C [57, 58]. Today hydrogen is mainly produce via NG Steam Methane Reforming (SMR), *i.e.* the so-called grey hydrogen. Such process is carbon intensive, with about 9 to 11 kg_{CO2} emitted per kg of hydrogen produced [59]. For this reason, it is important to stress that, similarly to what previously said for NH_3 or MeOH, hydrogen can be considered to be a cleaner fuel for shipping only if produced via electrolysis powered by renewable energy sources, *i.e.* the so called green hydrogen [60]. The cost of green hydrogen is today still not competitive with the one of grey hydrogen, even though recent estimates predict a reduction in the cost of renewable-based hydrogen to as low as 1.3-4.5 $/kg_{H2}$ in the next few years [61].

2.3.5 Biofuels

Biofuels have also been proposed as possible marine alternative fuels, as they are biodegradable, nontoxic, and renewable substances that could help in reducing both pollutant and GHG emissions (at least in the whole life cycle of the fuel), even though their cost is still not competitive with the conventional diesel fuels [36]. As for bio-diesels, three main types can be distinguished [62]:

- **Fatty Acid Methyl Esters (FAME)**: long-chain methyl esters derived from biomass or biomass residual (*e.g.* soya, coconut, palm, cooking oils), esterificated with methanol as catalyst; the direct use of FAME in diesel engines is possible in principle, although FAME are generally blended with diesel fuel (up to 7% FAME content in the fuel blend). FAME have similar properties to diesel, but lower gravimetric energy density; also, FAME could have issues in operating in severe cold circumstances [63];
- **Hydrotreated Vegetable Oil (HVO)**: hydrocarbons produced from vegetable oils with a chemical composition almost identical to diesel, which makes them suitable for being used directly in diesel engines without the need to be blended with MGO; HVO also have high Lower Heating Value (LHV) with respect to other biofuels (about 34.4 MJ/l) and tend not to form debris in the fuel injection systems, hence requiring less maintenance than other fuels; also, differently from FAME, HVO can be used in cold circumstances [63]; the cost of HVO is highly dependent on the feedstock used for its production, and currently amounts to about 2000 €/ton [64];
- **Biomass to Liquid (BtL)**: synthetic liquid hydrocarbons produced from lignocellulosic biomass;similarly to HVO, they are compliant with normal diesel fuel specifications; however, they are still in their early stage development and far to be commercialized [65].

Also **ethanol (bio-ethanol)** and **DiMethyl Ether (DME) (bio-DME)** have been proposed as promising biofuels for use as marine fuels [66, 67]. The former can be either produced via fermentation of sugarcane or starch (the most widely used method today) or starting form lignocellulosic biomass (**e.g.** wood, grass), and has a LHV of about 21.2 MJ/l. Sustainability of sugarcane derived bio-ethanol is a trivial issue: while the overall balance of CO_2 absorbed and produced in the whole biomass-to-ethanol cycle could guarantee net zero emissions, the production of bio-ethanol from sugarcane is in conflict with the food production. Lignocellulosic ethanol could be better in this sense, even though the global production levels are still lower than the ones of sugarcane derived bio-ethanol [68]. As for DME, it can be easily used in diesel engines, and could be bio-produced from biomass. The production of bio-DME is still in its early stage, but promising results have already been obtained [69, 70].

2.4 Fuel cells systems for shipping

The different types of FC are generally distinguished according to the type of electrolyte (*i.e.* the material separating the fuel and air electrode)[71], and are classified into the following types:

- Low Temperature Polymer Electrolyte Membrane Fuel Cells (LT-PEMFC)
- High Temperature Polymer Electrolyte Membrane Fuel Cells (HT-PEMFC)
- SOFC
- Alkaline Fuel Cells (AFC)
- Phosphoric Acid Fuel Cells (PAFC)
- Direct Methanol Fuel Cells (DMFC)
- Molten Carbonate Fuel Cells (MCFC)

The electrolyte material of the different FC types also determines the different electrochemical reactions that happen in the FC, determining the different working temperature at which the electrochemical reaction occur, the resulting emissions, and the mobile ion moving between the electrodes [62]. A summary of the electrochemical reactions, operating temperatures and mobile ions of the different FC types is reported in Figure 2.1. As for maritime applications, LT-PEMFC, SOFC, and HT-PEMFC have been identified as the most promising alternatives [20].

2.4.1 LT-PEMFC

As the name suggest, LT-PEMFC use a polymer membrane as electrolyte. Such membrane needs to be kept hydrated to conduct protons (H^+) from the anode to the cathode, and hence the operating temperature of LT-PEMFC needs to be kept under 100°C, typically in te range 65-85°C [72]. Such low operating temperature facilitate on the one side the cold startup (in seconds) and the easiness for LT-PEMFC to follow the load. On the other side, such low functional temperature also means low quality waste heat, hampering the waste heat recovery on board [20]. Other aspects such as the complex water management, the performance degradation due to load cycling, and the low tolerance to impurities are also seen as drawbacks for an effective use of LT-PEMFC in marine applications [73, 20]. Nevertheless, LT-PEMFC are today the most mature FC technology, and have been already installed on board of ships [74]. Further details on LT-PEMFC can be found in Chapter 3.

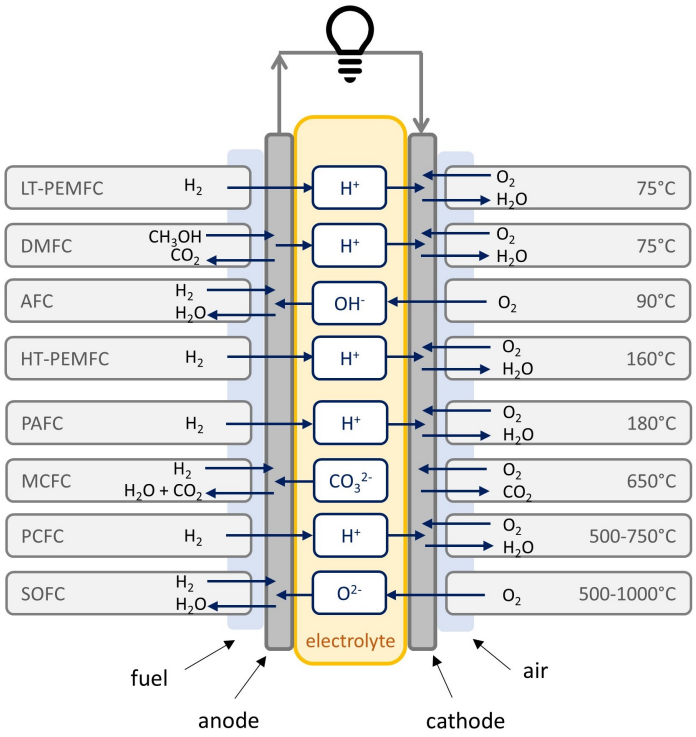

Figure 2.1: *Summary of the electrochemical reactions, mobile ions, and operating temperatures of the main FC types. Elaborated from [62].*

2.4.2 HT-PEMFC

To overcome the issues of LT-PEMFC linked to their low operating temperature, a high temperature variant has been developed: HT-PEMFC. HT-PEMFC generally use a phosphoric acid (H_3PO_4) doped polybenzimidazole polymer matrix as electrolyte [72]. Such material is able to guarantee the protonic conductivity at temperatures in the range of 140-180°C [72]. Such temperatures make HT-PEMFC less sensitive to fuel impurities than LT-PEMFC, and make waste heat recovery from HT-PEMFC easier, while limiting the size required by the cooling system. Nonetheless, HT-PEMFC have longer start-up and shut-down times when compared with LT-PEMFC, and need a more accurate heating and cooling management to ensure proper working conditions. In fact, thermal stress may accelerate the performance degradation of HT-PEMFC, hence limiting the lifetime. Such aspect, together with the higher costs of HT-PEMFC with respect to the one of LT-PEMFC, is currently hampering the large scale use of HT-PEMFC, for marine as well as land applications [62, 20].

2.4.3 SOFC

The electrolyte of SOFC are solid oxides, a ceramic membrane material through which the oxygen ions (O^{-2}) diffuse at temperatures in the range 500-1000 °C [72, 71, 62]. Such high operating temperature allow SOFC to use cheaper catalysts, such as nickel, and to tolerate higher levels of impurities in the inlet fuel [72]. In addition, such temperature make possible for SOFC to internally reformate NG and to crack NH_3, which can hence be used as fuel [42, 75]. A further advantage in using SOFC in the maritime industry is their high electrical efficiency (up to 60%) and, most importantly, the possibility to effectively recover the waste heat to cover also thermal power demand on board [62, 76]. Nevertheless, a drawback of using SOFC for maritime applications may be represented by their relatively low power densities (lower than LT-PEMFC), as SOFC require a large Balance of Plant (BoP) (*i.e.* auxiliary components needed for the operation), and a bulky insulation is needed to keep the high operating temperatures while minimizing the heat losses. Additionally, SOFC have generally poor performances in terms of cold start-ups and load following, given their high thermal mass [72, 62]. Lastly, SOFC market is still in its early stage, and hence SOFC costs are still relatively high (about 3000 €/kW) [77].

2.4.4 AFC

AFC are low temperature (< 100°C) hydrogen fuelled FC, which use an alkaline solution as electrolyte, generally potassium hydroxide (KOH) in watery dissolution, in which the hydroxyl ions (OH^-) move from the cathode to the anode [78]. Their low cost and good electrical efficiency (50-60% LHV-based) could constitute an advantage for their use in ship energy systems. However, AFC are highly sensitive to CO_2, and hence require to be fed with pure hydrogen and oxygen to prevent the CO_2 reaction with the electrolyte and the consequent reduction in the FC efficiency, possibly ending up in the cell blocking [78, 62, 73]. This is the main reason why AFC are not considered for possible use in shipping, although their use could become advantageous if NH_3 is considered as fuel thanks to the good tolerance of AFC to NH_3 impurities [62].

2.4.5 PAFC

PAFC use liquid phosphoric acid acid as electrolyte, through which protons (H^+) move from the anode to to the cathode side [78]. They operate at temperatures in the range 150-220 °C, which makes them less sensitive to fuel impurities, particularly CO, and also offers good possibilities of recovering the waste heat [78, 62, 79]. Indeed, their overall performance (electrical + heat)

can reach efficiencies of up to 85% [73]. A main drawback for PAFC use in shipping is represented by their bulkiness and weight, as they have relatively low power densities. Moreover, their high operating temperature implies lathe start up times and accelerated degradation of the components [62].

2.4.6 DMFC

Similarly to PEMFC, also DMFC use a polymer membrane electrolyte, although DMFC' electrodes containing platinum-rhutenium catalyst allow them to operate directly with MeOH, without the need of reforming MeOH to produce hydrogen [72, 62, 73]. A main drawback of DMFC is their poor efficiency, about 20%, mainly due to the MeOH crossover. As for the operating temperature, DMFC generally work at 50-120°C [20].

2.4.7 MCFC

MCFC use a mixture of molten alkali metal carbonates as electrolyte, where the carbonate ions (CO_3^{-2}) move from the cathode to the anode [72]. MCFC currently reach electrical efficiencies up about 50-60%, but their high operating temperature (around 650°C) makes them suitable also for co-generation plants, where they can achieve an overall efficiency of up to 85% [71]. MCFC have a good tolerance to fuel impurities, and can be fed by multiple fuels (*e.g.* NG, hydrogen). Nonetheless, major drawbacks such as slow start-up timing and low power density makes them less attractive than other FC technologies for maritime applications [73].

2.4.8 Summary and comparison

Table 2.4 reports a summary of the main characteristics of the different types of FC as briefly described in the previous sections. Overall, the types of FC that have been identified as promising for maritime applications are LT-PEMFC, HT-PEMFC, and SOFC, thanks to their high technological maturity and low relative cost (LT-PEMFC), high system efficiencies (SOFC, HT-PEMFC), or good tolerance to fuel impurities (SOFC, HT-PEMFC). In particular, LT-PEMFC could have a great impact in the near future as they could guarantee zero emission shipping. In addition, draft guidelines for their installation on board start to be available, also thanks to an increasing number of application on board. For these reasons, this thesis will particularly focus on hydrogen fuelled LT-PEMFC for maritime applications.

Table 2.4: *Main characteristics of the different types of FC. Elaborated from [62, 72, 20].*

FC type	**Main fuel options**	**Operating temperature (°C)**	**LHV based electrical efficiency (%)**	**Emissions**	**Relative cost (-)**	**Sensitivity to fuel impurities (-)**
LTPEMFC	Hydrogen	65-85	50-60	Water	Low	High
HTPEMFC	Hydrogen, NG, MeOH	140-180	40-45	Water	Medium	Medium
SOFC	NG, diesel, hydrogen, ammonia	500-1000	50-60*	Water + CO_2 if carbon contained in the used fuel	High	Low
AFC	Hydrogen, Ammonia	50-230	50-60	Water	Low	High
PAFC	NG, diesel, hydrogen	150-220	40*	Water + CO_2 if carbon contained in the used fuel	Medium	Medium
DMFC	MeOH	50-120	20**	20	Medium	Medium
MCFC	NG, diesel, hydrogen	600-700	45-55*	Water + CO_2 if carbon contained in the used fuel	High	Low
* based on NG; ** based on MeOH.						

2.5 Review of projects on the use of FC in shipping

To better define the object and delimitations of the present thesis, a detailed review of the available projects on the application of FC systems on board of ships (both sea and inland water vessels) has been performed. Indeed, by studying the available projects on the use of FC in shipping it is possible to retrieve useful information on this type of systems concerning the industrial

interest on this type of systems, as well as to understand the main barriers and bottlenecks regarding this type of applications. A first part of the projects review has been published in the paper [80], and has been further extended here.The projects overview has been conducted for 71 projects started after 2000 for which the information was freely available on the web. Both feasibility studies an projects for the development of real vessel or prototypes have been included in the analysis, but a distinction has been made between projects in which the vessel is currently in service/has navigated at least once (*operating* projects) or not (*non-operating* projects). All the projects have been cataloged in a database according to: project name, ship name, project country, start and end date, state of the vessel (operating and not operating), vessel type, FC type, logistic fuel, type of EESS, funding, project partners. The complete database is reported in A.1 in the Appendix A of this thesis. An infographic of the data reported in the project database is shown in Figure 2.2, which presents information about projects start date, vessel status, FC type, logistic fuel, and type of vessel application. Firstly, it should be noticed that not all information was available for each project, and hence each chart in Figure 2.2 reports the number of projects responding to each criterium, so that the reader can easily retrieve the number of projects considered for each information.

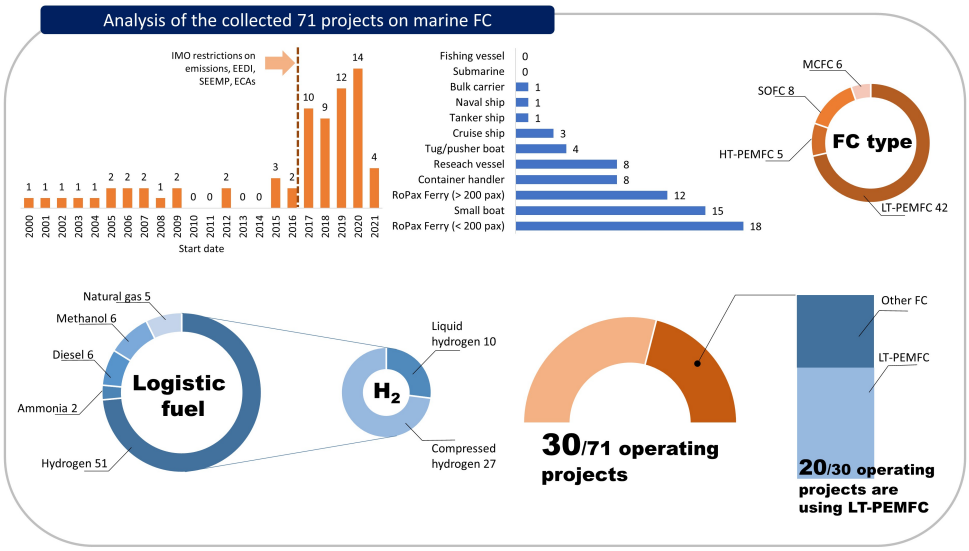

Figure 2.2: *Infographic reporting the analysis of the 71 collected projects available in the attached database (see Appendix A). Numbers indicate the number of projects according to the respective criterium. Operating projects refer to those where the vessel is currently in service/has navigated at least once.*

As for the start date, it can be retrieved from Figure 2.2 that last years have seen an increase in the development of projects in this field. This demonstrates the recent growing interests of shipowners and shipbuilders in the development

of vessels with FC fueled by low carbon fuel that will comply with the upcoming IMO restrictions [3]. With reference to the FC type, the analysis showed that 42 projects out of 58 for which information was available consider LT-PEMFC as FC, as this type is today the most mature one. It should be noticed that some projects investigated both the use of LT-PEMFC and other types of FC, *e.g.* MCFC. Among the 42 projects considering LT-PEMFC, 19 projects are *operating*. The second most investigated FC type is the Solid Oxide FC (SOFC), with 8 out of 58 projects involving this type of technology. Among these, the ShipFC project [44] is planning to fuel SOFC with ammonia. As for the logistic fuel category, reference is made here to the fuel stored onboard the vessel, used to fuel FC either directly in its pure form or as reformate fuel (*e.g.* NG is intended as logistic fuel in projects where it is reformed to produce hydrogen for feeding the FC). From the review it emerged that hydrogen is the most used logistic fuel (51 projects out of 70), mainly stored in compressed form (27 projects out of 37 for which data on the storage system is available). Lastly, the project review pointed out that most of projects focus on small to medium size ships, while projects focusing on larger ships often propose FC as auxiliary power units. Projects that imply FC propulsion mainly focus on small to medium size ships, with 33 to 71 projects considering small boats or Roll-on Passenger (RoPax) ferries with a capacity up to 200 passengers. Among these, the 67% proposes the use of LT-PEMFC and the 42% are operating and powered by LT-PEMFC. In all cases, LT-PEMFC are considered coupled with EESS, mainly batteries.

2.6 Thesis' object and delimitations

In the outlined research context, it has been decided to focus the present thesis on the use of alternative fuels and power systems for the reduction of shipping emissions. In particular, from the review of projects on the use of FC in shipping, it emerged that hydrogen fueled LT-PEMFC systems are today the most widely implemented for real-life applications aiming at reducing both pollutant and GHG emissions from shipping. Hence, hydrogen fueled LT-PEMFC systems for ship propulsion have been chosen as object of the present thesis. For the sake of simplicity, in the following chapters LT-PEMFC will be referred to as simply PEMFC. In the following Chapter 3 it is proposed the literature review on hydrogen fueled PEMFC-based energy systems for shipping, which has been conducted in order to identify the main research gaps. The whole analysis has been conducted by adopting an energy system engineering approach, and by considering the boundaries of the ship energy systems as delimitations of the study. Other aspects, such as the detailed modelling of the hydrogen bunkering process, the analysis of the chemical

and electrochemical reactions of PEMFC and batteries as well as the lifecycle analysis of the environmental and social impact of the technologies are not accounted for in this study.

Chapter 3

Literature review: hydrogen PEMFC energy systems for shipping

This chapter presents the literature review on the use of hydrogen fuelled PEMFC for maritime applications. Firstly, the main types of system architecture are presented in Section 3.1. Afterwards, in Section 3.2 are described the main alternatives available today for hydrogen storage on board of ships, while Section 3.3 describes and analyzes the main points regarding the correct design and operation of PEMFC, highlighting the main drawbacks for the installation of PEMFC on board. Section 3.4 analyzes the energy storage system, often coupled with PEMFC in hybrid propulsion systems. Being a key point for such systems the definition of the proper Energy Management Strategy (EMS), a dedicated literature review is proposed in Section 3.5. Lastly, a summary on the regulatory framework for the use of hydrogen and PEMFC on board of ships is proposed in Section 3.6. The chapter is concluded by listing the identified research gaps emerged from the literature review, that the present thesis aim to fill. It should be noticed that some of the content reported hereafter may not be original content, but reproduced and/or adapted from previously published papers of the author during the course of the PhD. When appropriate, specific reference to the original publication is given.

3.1 Typical architecture of PEMFC energy systems

There are mainly two possible uses of PEMFC on board of ships: (i) as auxiliary power system or (ii) as propulsion system. Clearly, if PEMFC are used as

main propulsion system, the ship will have an electrical propulsion, where an electrical generator (alternator) powers the propellers. Differently, if PEMFC are use as auxiliary power units, the ship can either have an electrical propulsion or a mechanical propulsion, where the shaft of the propulsion ICE is directly connected with the propellers.
When PEMFC are used in mobility applications, they are usually coupled with EESS into hybrid power-trains to improve the system response to load changes and to allow the PEMFC to operate in the best load conditions. This is valid also for shipping applications, and it is particularly the case of PEMFC used for propulsion [81]. Hybrid powertrains generally encompass a main power source (*e.g.* ICE, PEMFC) and a EESS (*e.g.* supercapacitors, battery). According to the way the power sources are connects to the EESS, hybrid powertrains can be classified as series, parallel, or series-parallel hybrid [82, 17]. Figure 3.1 reports the simplified schematics of the three hybrid configurations including both ICE and PEMFC. In Figure 3.1 all the electrical power units are connected to a Direct Current (DC) bus, as this type of connection allows an easier and more efficient power distribution between the power units operating in DC and the DC power loads [83, 84, 85]. Indeed, although today ships mainly rely on Alternating Current (AC) grids at fixed frequency, recent studies [83, 84, 85] demonstrated that the latest development in the power electronic technologies and highly stable DC systems could lead to a widespread use of onboard DC grid. As for the EESS, Figure 3.1 reports the general case where EESS is recharged by the main power source through a bidirectional power connection with the DC bus. Alternatively, EESS could be directly recharged with onshore electricity when the ship is mooring (*i.e.* plug-in hybrid) [86]. Although this solution would reduce ICE or PEMFC sizes and fuel consumption [87], it would require additional components to be installed on board, the development of an onshore infrastructure, and it might also imply longer stay at quay for ships at berth to ensure sufficiently long recharging time [21, 22].

3.2 Hydrogen storage

Given the peculiar physical characteristics of hydrogen, the hydrogen storage system plays a fundamental role in determining the technical and economical feasibility of hydrogen fuelled mobility applications. Marine applications make no exception, as the bulkiness of hydrogen storage system could imply significant reduction of the pay load on board, hence mining the economic competitiveness of the system. In this section, the main alternative currently available for storing hydrogen on board of ships are described and compared.

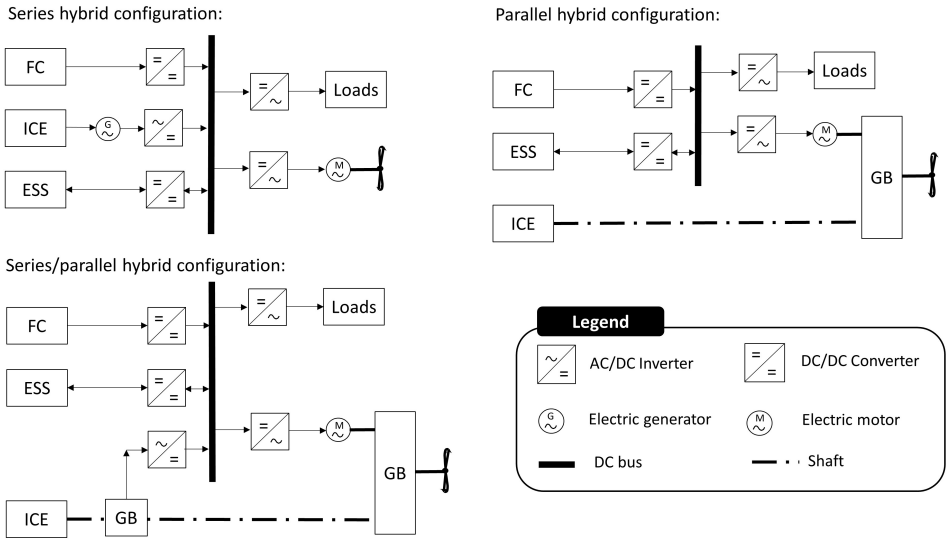

Figure 3.1: *Typical configurations of hybrid powertrains architectures including both FC and ICE. (GB = Gear Boxes). Elaborated from [82, 17].*

3.2.1 Compressed hydrogen

The most mature technology to store hydrogen for mobility applications is CH_2 [88]. Shipping applications make no exception, although in this case the large quantities of hydrogen needed for shipping may be challenging if CH_2 is considered. Indeed, CH_2 is generally characterized by low energy densities, which imply bulky storage system on board. As shown in Table 3.1, which reports the main categories of CH_2 cylinders classified according to the materials and storage pressures[88, 89, 57, 58, 90], energy density is particularly low for Type I and Type II cylinders. Nonetheless, Type I and Type II cylinders are also the cheapest ones, and hence are often preferred in maritime applications. Type III and Type IV cylinders, have higher energy densities, mainly related to the materials used for the cylinder's liner, but also linked to the higher pressure levels achievable (potentially up to 1000 bar for Type IV cylinders) . However, higher storage pressures also imply higher energy required by the hydrogen compressors of the bunkering stations, and hence higher costs [88]. Indeed, bunkering process and infrastructure have a key role in assessing the technical and economic feasibility of CH_2 fuelled ships. In general, the main components of a CH2 bunkering station are: compressors, chiller units, and pressure regulation valves. Chiller units are needed to keep the hydrogen temperature under the set limits, hence ensuring the right pressure levels and also avoiding material stresses due to high temperature in the CH_2 cylinders. A further issue that may arising during CH_2 bunkering process is the under-filling of the cylinders. In fact, hydrogen temperature increases also during expansion processes, hence resulting in lower density of the gas and a consequent under-

filling of the cylinders [91]. To avoid such issues, the bunkering speed needs to be accurately monitored to keep hydrogen temperatures in the desired range (usually under 85°C) [92]. To avoid the issues linked with the installation and management of such a bunkering infrastructure, some projects [93] proposed the use of swappable CH_2 cylinders that can be loaded/unloaded on/from the ship when needed [71]. Nonetheless, such solution may not be convenient for large ship as it would imply too long port calls [53].

Table 3.1: *Main characteristics of CH_2 storage cylinders [88, 89, 57, 58, 90].*

Type	Materials	Maximum pressure (bar)	Energy density (kWh/l)	Energy density (kWh/kg)	Cost (€/kgH2)	Technological maturity
I	All-metal, usually austenitic steels or aluminum alloys	≤ 300	0.3-0.5	0.3-0.6	83	++
II	Load-bearing metal liner hoop wrapped with resin-impregnated filament	≤ 700	0.4-0.5	0.5-0.8	86	+
III	Non-load-bearing metal liner axial and hoop wrapped with resin-impregnated filament	≤700	0.3-0.8	1.1-1.9	700	-
IV	Non-load-bearing non-metal liner axial and hoop wrapped with resin-impregnated filament	≤1000	0.3-0.7	1.4-2.7	600-700	–

3.2.2 Liquefied hydrogen

The storage of hydrogen in liquefied form, *i.e.* as LH_2, allows to overcome the problems linked to the bulkiness of hydrogen storage systems, as LH_2 itself has a density (at -253 °C and 1 bar) of 70.9 kg/m^3, three orders of magnitude higher than hydrogen at atmospheric conditions [94]. Figure 3.2 reports the volumetric and gravimetric energy densities of both CH_2 cylinders and LH_2 cryogenic tanks as emerged from the analysis of different commercial products in [80], highlighting the convenience of LH_2 over CH_2 in terms of space requirements on board. Nonetheless, the cryogenic storage conditions of LH_2 (at -253

°C) require the use of specific materials and of complex safety instrumentation and technologies [58]. Moreover, given the high levels of energy required for hydrogen liquefaction (about 12 kWh for kg of liquefied hydrogen),only few large plants today produce LH_2, and only recent projects [95] are investigating the possibility of exporting LH_2 by ship. Also for these reasons, time is still needed before LH_2 is available on a large scale for use as fuel in shipping. Similarly to what previously seen for CH_2, also for LH_2 the bunkering system plays a crucial part in assessing the economical and technical viability of a LH_2 fuelled ship. Several studies in the literature propose and analyze different configurations for LH_2 bunkering stations [96, 97]. For example, in [96] are proposed two methods for the LH_2 bunkering for the SF-BREEZE ferry concept. The first option involves the use of a Pressure Building Unit (PBU) to transfer LH_2 from the on land LH_2 storage system (either stationary or mobile on a truck/ship), while the second option envisages the use of a cryogenic pump. PBU are generally cheaper than cryogenic pumps, although the latter are less energy demanding and allow shorter bunkering times than PBU [98, 99, 100]. As of 2022, only few LH_2 bunkering station have been developed [101, 102]. As reported in [103], the lack of infrastructure is indeed one of the most critical bottlenecks in the large scale utilization of LH_2 in maritime transportation, and it is hence expected that a transition towards LH_2 use in shipping would imply high cost also due to the development or retrofit of the necessary infrastructure.

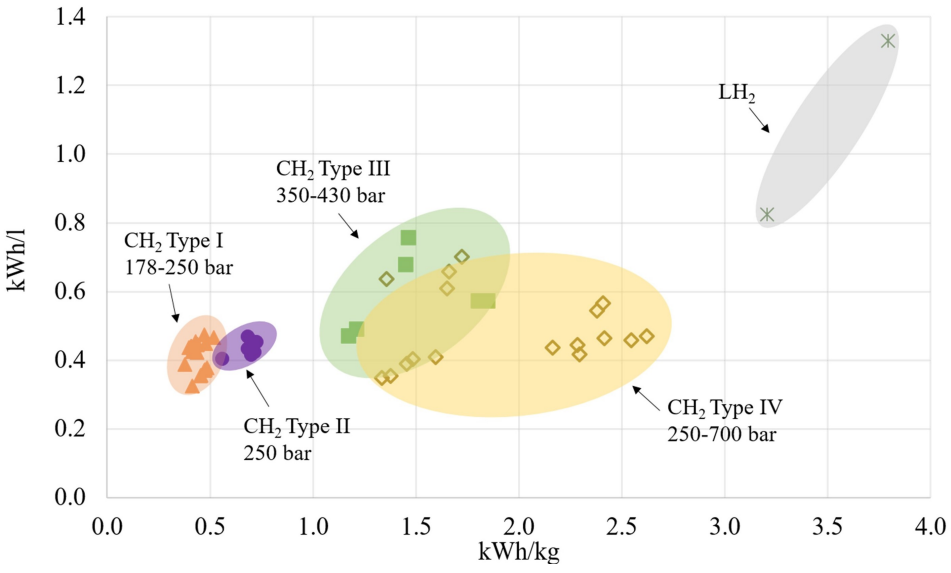

Figure 3.2: *Volumetric and gravimetric energy densities of CH_2 cylinders and LH_2 cryogenic tanks as emerged from the analysis of different commercial products. Retrieved from a previous study by the author [80].*

3.2.3 Other hydrogen storage methods

Although still far from a large scale commercialization, **Cryo-compressed hydrogen (CcH2)** could be a promising solution for storing hydrogen for mobility applications [54, 104, 105, 106, 107]. As the name suggests, CcH2 consists in compressed hydrogen at low temperatures, typically below 75 K but that could be as low as 20 K if the CcH2 tanks are filled directly with LH_2. CcH2 can reach densities up to 81 kg_{H2}/m^3 (at 21 K and 240 bar) [106]. A further option that has seen a growing interest in recent year for hydrogen storage in mobility applications is the use of **Metal Hydride (MH)**, and recent studies [108, 109, 110] also proposed the use of MH in shipping. In MH, hydrogen is stored chemically as metallic or inter-metallic alloy into a parent hydride [108]. Different materials have been proposed as potential MH, such as powders that absorb/desorb hydrogen according to changes in the temperature or water concentration [111, 112, 113] or metallic structures working as hydrogen sponges [114, 115]. A main drawback of MH is the need of thermal energy for the dehydrogenation process, *i.e.* the process of extracting hydrogen from the hydride. Hence, some studies [116, 117] demonstrated that the thermal energy demand for dehydrogenation can be efficiently recovered by the waste heat of FC. To this extent, magnesium based MH, inter-metallic compounds, and alanates may be advantageous as these types of MH are characterized by low dehydrogenation temperatures [118, 119, 120, 121]. Another challenging related to MH is their high weight, even though for shipping applications this issue can be solved by properly positioning the tanks on the vessel [122].
Alternatively, hydrogen could also be chemically stored in **hydrogen carriers**. In particular, NG, NH_3, MeOH, and Liquid Organic Hydorgen Carrier (LOHC) are often addressed as potential hydrogen carriers for FC applications, as they have easier storage conditions than CH_2 or LH_2 and are already transported by ship [123, 28, 124]. NH_3, NG, and MeOH have been already presented as alternative fuels in shipping in Section 2.3. Nonetheless, if considered as hydrogen carriers, other aspects need to be considered, and in particular their hydrogen content and the possibility to obtain hydrogen at adequate purity levels for use in FC [45]. NH_3 has a high hydrogen content of approximately 18%wt, and can be cracked at high temperatures to obtain hydrogen, although in this case specific purification processes would e needed to ensure adequate hydrogen purity levels if hydrogen is to be used in PEMFC [42]. In addition, the cracking process would decrease the overall energy efficiency of the power plant. Similarly to NH_3, also LNG (hydrogen content about 25%wt) and MeOH (hydrogen content 12%wt)could be used as hydrogen carriers provided an adequate reforming process and hydrogen purification to obtain adequately pure hydrogen [53]. In both cases, however, the reforming process would worsen the overall efficiency of the system.

Lastly, hydrogen could also be stored in LOHC, *i.e.* organic substances liquid at ambient conditions consisting of homocyclic or heterocyclic aromatic with hydrogen content typically in the range of about 6-7%wt [125]. here are different types of LOHC, which differ one from the other not only in terms of hydrogen content, but also in terms of technical and economic requirements for the hydrogenation and dehydrogenation processes, *i.e.* the processes of enriching the organic substances with hydrogen (hydrogenation) and to extract hydrogen from the organic carrier (dehydrogenation) [126]. Despite the low technological maturity of LOHC systems for shipping, toluene, N-ethyl carbazole, and dibenzyltoluene have been addressed as the most suitable LOHC for shipping applications [126, 127, 128, 129, 125, 130, 131]. However, it should be noticed that the membranes currently in use for dehydrogenation cannot meet the requirements on hydrogen purity for all the FC (*e.g.* PEMFC), and hence catalyst poisoning issues may occur [132, 133].

3.2.4 Summary and comparison

Table 3.2 reports the main characteristics of the different alternatives for storing hydrogen in mobility applications, with particular reference to shipping applications. As for fuel costs, reference is made here to January 2022, so that to avoid the recent market fluctuations.

Table 3.2: *Main characteristics of the available hydrogen storage methods. Lower and upper limits of cost ranges for physical hydrogen storage and metal hydride refer to grey and green production methods, respectively (i.e. hydrogen produced from methane via steam reforming or from water via electrolysis powered by renewable energy sources). (T = temperature).*

Type	**P (bar)**	**T (K)**	**H2 content (%wt)**	**Cost (€/kgH2)**	**Remarks**	**Refs.**
CH_2	200-1000	293	100	0.9-8.4	About 10% of the H_2 LHV required for the compression process. Limited energy density, suitable only for short-range shipping.	[58, 57]

Continued on next page

Table 3.2 – continued from previous page

Type	P (bar)	T (K)	H2 content (%wt)	Cost (€/kgH2)	Remarks	Refs.
LH_2	1-12	20	100	2.4-9.9	Up to 40% of the H_2 LHV required for the liquefaction process. Limited availability. Suitable for medium-long range shipping. Boil off management required.	[53, 58]
CcH_2	150-350	20-80	100	2.4-9.9	Require strict insulation. Suitable for medium-long range shipping.	[58]
MH	20-150	260-425	>8	0.5-8*	Requires thermal management. Could be coupled with heat recovery from PEMFC.	[58]
LOHC	1	293	6-7	<1**	Highly endo/exothermal processes. Large volumes required onboard. PEMFC poisoning with current technology for dehydrogenation.	[125]
NH_3	10-17	293	17.6	0.7-0.8**	Suitable for medium-long distance shipping. Requires cracking process to obtain hydrogen for feeding PEMFC. Typical cracker efficiency 75%. Main issues: toxic substance, possible poisoning of PEMFC if no adequate hydrogen purification.	[42]
LNG	1-1.2	111	25	0.4-0.5**	Reforming process required for obtaining hydrogen to feed PEMFC. Typical reformer efficiency 75%. Main issues: zero emission is not guaranteed, methane slip, PEMFC CO poisoning.	[33]
MeOH	1-81	293	12	0.4-1.2	Possible to use directly in HT-PEMFC. For the use in LT-PEMFC reforming is required (efficiency 75%). No zero emissions, PEMFC CO poisoning.	[124]

*cost per kg of hydrogen without taking into account the hydrogenation costs, which depends on the used technologies;**kg of stored fuel.

3.3 PEMFC

Starting from a brief overview on the working principle of PEMFC, this section describes the main characteristics of PEMFC that may be relevant for marine applications. A particular focus will be given in Section 3.3.2 to degradation phenomena of PEMFC and in Section 3.3.3 to WHR solutions.

3.3.1 PEMFC working principle

Figure 3.3 shows a simplified schematic of the PEMFC working principle, representing the operation of a single cell. Hydrogen enters the FC at the anode side, while oxygen enters the cell at the cathode side. Anode and cathode are separated by a polymer electrolyte (*i.e.* the proton exchange membrane), usually Nafion® [134], that allows only protons (H^+) to pass through. At the anode side hydrogen is ionized thanks to a platinum-based catalyst. At this point, the protons migrate through the polymer electrolyte membrane towards the cathode, while the electrons, blocked by the membrane, pass through a wire connection to an electrical load (*e.g.* a DC motor or an electric accumulator) and eventually reach the cathode. The cathode, supplied with (atmospheric) oxygen, receives the hydrogen protons through the electrolyte and the electrons through the electrical circuit, and thanks to a platinum-based catalyst a chemical reaction that produces pure water is triggered.

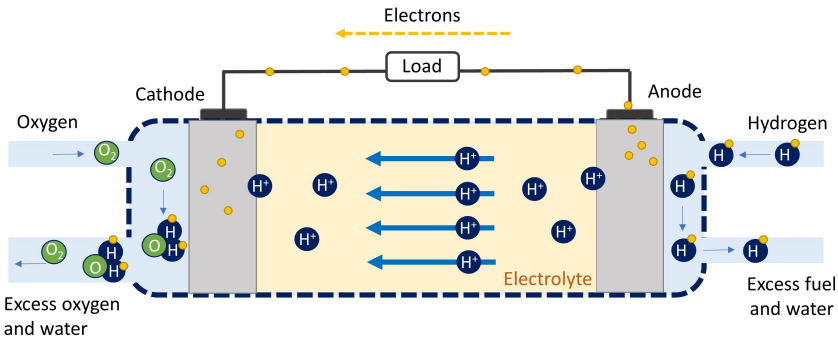

Figure 3.3: *PEMFC working principle. Elaborated from [71].*

PEMFC are modular power units, in which single cells can be grouped together to make a module. Several modules together make up a PEMFC stack, which can eventually be coupled with other stacks to meet the power and voltage required by the specific applications. As of today, marine PEMFC applications that successfully operated the vessels at least once have not exceeded few hundred kW in the installed power on board. While recent projects aim to reach MW-scale power plants (see for instance [135, 136, 137]), it is important

to analyze the reason behind such power limitation. Firstly, MW-scale PEMFC would imply larger hydrogen consumption and hence bulkier and heavier storage systems. Secondly, MW-scale PEMFC plants would also entail a larger and more complex BoP, *i.e.* the set of auxiliary components needed to run the system. For PEMFC systems, the BoP can be generally divided into three main subsystems:(i) fuel processing and fuel/air supply lines, (ii) cooling circuit, (iii) power conditioning, control and monitoring. Figure 3.4 shows a simplified schematic of the typical structure of a liquid cooled PEMFC's BoP.The fuel processing and fuel/air supply lines subsystem ensures the appropriate conditions of fuel and air at the PEMFC inlet. In addition to the basic components shown in Figure 3.4, the fuel processing line could also encompass a reformer to obtain hydrogen from hydrogen carriers, hydrogen evaporator if LH_2 is considered, hydrogen humidifier to ensure the correct hydrogen humidity at the PEMFC inlet, a condensate collector to remove liquid water from the circuit, and a hydrogen re-circulation pump. As for the air processing line, in addition to the air filter, blower, humidifier, and water separator shown in Figure 3.4, it is important to notice that for maritime PEMFC application it may be necessary to remove sodium chloride vapor from the inlet air in order to prevent the degradation of the PEMFC's membrane due to the exposure to sea-air conditions [53, 138]. The role of the cooling circuit is to keep the operating temperature of the PEMFC's stack in the range of 65-70°C [139]. Liquid cooling system is often preferred for PEMFC in mobility applications, thanks to its large cooling capability and good efficiency [140]. Demineralized water or mixtures of demineralized water and ethylene glycol are typically used as refrigerants [140]. Other types of cooling may be edge cooling, air cooling, and phase change cooling [141]. As shown in Figure 3.4, the cooling circuit subsystem typically encompasses a re-circulation pump, a refrigerant reservoir, and a heat exchanger. In addition, a deionizer might be included in the system to keep the refrigerant's conductivity in the desired range, avoiding PEMFC short circuits. Lastly, all the instrumentation and components necessary for acquiring data and monitoring the system operation are part of the power conditioning, control, and monitoring system. Example of components included in the power conditioning, control, and monitoring system are: safety valves, pressure transducers, temperature transducers, power inverter/converter, remote control system. Table 3.3 reports a summary of the main components of a PEMFC's BoP and their role in a PEMFC system.

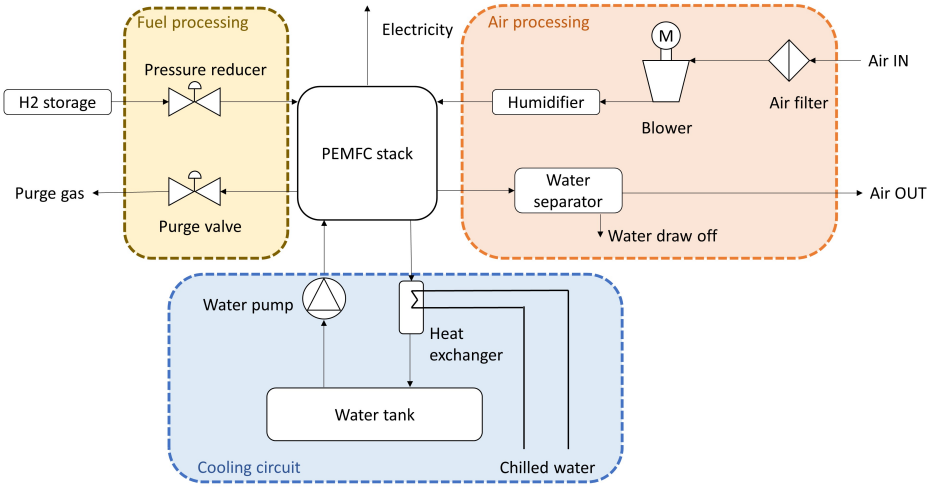

Figure 3.4: *Simplified schematic of a PEMFC BoP, divided into the three main subsystems. The power conditioning, control, and monitoring system is not represented here for the sake of image clarity. Elaborated from [140].*

Table 3.3: *Main components of each subsystem of the BoP of a PEMFC system [140, 142, 143, 144].*

BoP subsystem	**BoP component**	**Role**	**Typical requirements and additional remarks**
Fuel processing and fuel/air supply lines	Fuel reformer + purification units	When hydrogen is not stored in its pure form, chemical and/or physical reactions are triggered in the fuel reformer, which convert fuel (e.g. LOHC, NH3, and NG) into pure hydrogen for feeding PEMFC. Reformers are usually followed by a purifier that guarantees the absence of pollutants in the hydrogen fuel that may poison the PEMFC stack (e.g. CO and NH3).	ISO 14687 and SAE J2719 limits: Max CO: 0.2 ppm. Max NH3:0.1 ppm.
	Hydrogen evaporator	When hydrogen is stored in liquid form, the evaporator is needed to obtain gaseous hydrogen at the PEMFC inlet.	-
	Hydrogen pressure reducers	Guarantee the right pressure of hydrogen fuel entering the fuel cells.	Hydrogen pressure at PEMFC inlet: 3-6 bara.

Continued on next page

Table 3.3 – continued from previous page

BoP subsystem	BoP component	Role	Typical requirements and additional remarks
	Hydrogen humidifier	Guarantees the right level of humidity in the hydrogen fuel to maintain good performances of the polymer electrolyte membrane.	-
	Condensate collector	Prevents residual water in liquid form in hydrogen inlet stream that enters the PEMFC stacks.	-
	Hydrogen recirculation pump	Allows the recirculation of residual hydrogen in the system.	-
	Sodium chloride removal pretreatment	Prevents the degradation of the polymer electrolyte membrane due to the exposure to sea-air conditions. It is usually implemented in marine PEMFC applications.	-
	Inlet air blower	Pressurizes the atmospheric air that enters the stack, maintains a sufficient air flow to the stack and potentially allows the reduction of stack sizes by increasing the inlet air density.	-
	Inlet air filter	Prevents pollutant in the inlet air stream to enter the PEMFC.	-
	Inlet air humidifier	Guarantees the right level of humidity in the inlet air to maintain good performances of the polymer electrolyte membrane.	-
	Inlet air condensate collector	Prevents residual liquid water in air inlet stream from entering the PEMFC stacks.	-
	Outlet air condenser and condensate collector	Partially recovers steam residuals in the air outlet stream to reuse them in the humidifiers.-	

Continued on next page

Table 3.3 – continued from previous page

BoP subsystem	BoP component	Role	Typical requirements and additional remarks
Cooling circuit (liquid cooling case)	Refrigerant circulating pump	Guarantees a sufficient refrigerant flow rate to the stack to keep the stack temperature in the desired range.	PEMFC desired temperature range: 50-70°C Typical coolant pressure range at PEMFC inlet 1.5-2 bara.
	Refrigerant reservoir	In case of liquid cooling refrigerant, ensures that the coolant flow rate remains in the recommended range.	Coolant flowrate dependent on FC stack characteristics and cooling circuit geometry.
	Heat exchanger	Dissipate the waste heat of the stack to the surrounding environment or to the heat recovery system.	-
	Deionizer	Usually connected to a conductivity meter, allows to keep the refrigerant conductivity under the set limits to prevent the short circuit of the stack.	Electrical conductivity usually limited to values <100µS/cm.
Power conditioning, control and monitoring	Safety valves	Ensure the system operation under safe conditions.	Usually required to comply with ATEX directives.
	Measuring instrumentation	Ensures the correct monitoring of the system and the data acquisition needed by the control system. Common instrumentation includes pressure transducers, temperature transducers, flow meters.	-
	Control system	Ensures the correct operation of the stack to guarantee the compliance with safety regulations and power demands of the load. The control system also provides for emergency shutdown procedures.	-
	Power inverters/converters	Ensure the correct connection of the PEMFC with the electric load.	-

3.3.2 PEMFC degradation

A major drawback of PEMFC systems is their performance degradation over time, which generally results in a voltage drop that prevents the PEMFC to work properly. In the literature, the following main sources of PEMFC degradation are identified: operation at low or high current, galvanostatic decay, load cycling, and start/stop phases [145]. More in detail, PEMFC operation at low current might result in high cathode voltage, electrodes oxidation, and change in the polymer decomposition mechanism [146, 147]. Differently, when PEMFC are subject to high current, they may incur increased membrane temperature and possibly overcurrent that cause local hot spots if the cooling capabilities are exceeded. Additionally, high current operation may also results in fuel starvation [148, 149, 150]. Also when operating at constant current, the PEMFC is subject to degradation, mainly due to the galvanostatic decay. Nonetheless, galvanostatic decay is often neglected as it is the the degradation cause with the lowest impact on the overall PEMFC degradation rate [151]. As for load cycling, it is considered the first cause of electrode oxidation, platinum dissolution and corrosion of carbon support, as it increases the cathode potential hand hence accelerates its dissolution [152, 153]. Start/stop phases, instead, results in a non-uniform distribution of the reactant gas due to the decrease of the active surface area caused by the carbon oxidation of the anode [153, 154]. All these causes generally concur in determining the overall degradation of the cell, although load cycling and frequent start/stop phases are generally the greatest causes of degradation [145].
PEMFC stack ageing is usually modeled through three approaches: impedance estimation (based on electrochemical impedance spectrometry), remaining useful life estimation, and a stack voltage degradation model. Stack voltage degradation model are often used to limit the computational effort required in solving complex energy system models, although such modelling approach is less accurate with respect to other degradation models and strongly depends on experimental data [155].

3.3.3 Waste heat recovery

Despite the relatively high electrical efficiency of PEMFC (30-55% depending on the power load), a main drawback of such systems is represented by the difficulties in recovering the waste heat, which is generally low quality heat, at temperature in the range 60-80 °C [156]. Such aspect makes WHR particularly challenging for PEMFC, and consequently limits the overall energy efficiency of a PEMFC system as large part of the waste heat generally goes unused. This aspect is fundamental for all PEMFC applications, but results to be particularly critical for maritime PEMFC installed on board of large ships.

In fact, large ships can currently count on the large amount of high quality ICE's waste heat to supply the heat demand from the ship utilities [8]. If ICE are to be substituted with the zero emission alternative PEMFC, there would be a challenging part in determining how the heat demand on board is supplied. In the literature there are several studies addressing the WHR from PEMFC in residential applications, and comprehensive reviews on the WHR from PEMFC are available at [141] and [156]. Among the different possibilities for recovering the waste heat from the PEMFC, the following emerged from the literature reviews:

- Heat use in the hydrogen storage – PEMFC system, either to preheat the reactants or to facilitate the hydrogen release from MH when this type of storage is considered;
- Provide heat in Combined Heat and Power (CHP) systems; given the low quality of the waste heat, papers in the literature often refer to the case of systems that encompass also a fuel reforming unit, as in this way it is possible to recover the heat coming also from the reformer, at higher temperature;
- Drive absorption or adsorption chillers to supply cooling power in Combined Cooling Heating and Power (CCHP) systems;
- Provide electricity by means of Organic Rankine Cycle (ORC) or ThermoElectric Generator (TEG).

Nonetheless, only few studies in the literature address the WHR from PEMFC when considering shipping applications. Among these, some consider the WHR from PEMFC to heat the reactants or to enhance the hydrogen release from MH, while others consider the WHR by means of ORC for power generation on board [157]. Differently, it appears to be a lack of studies that consider the use of PEMFC waste heat in CHP or CCHP systems on board of ships, considering the possibility of recovering the waste heat from PEMFC since the design phases of a system. However, this could indeed lead to more accurate evaluations on the technical and economical convenience of such systems. For this reason, in the present thesis it will be analyzed the possibility of recovering the low grade waste heat from the PEMFC since the early design phase of the ship energy system. (See Chapter 4 for the proposed methodology and case study).

3.4 The electric energy storage system

The roles of the EESS in future marine power plant are diverse, and include: (i) guaranteeing the operation of the main engine in the optimal efficiency condi-

tions, (ii) buffering the load changes, (iii) guaranteeing backup and additional power when needed, and (iv) storing surplus energy coming from renewable power plats on board [158]. In the case of marine PEMFC power plant, the EESS is particularly important in managing the power load of PEMFC, and could potentially guarantee longer PEMFC lifetimes. Different types of EESS are available today for marine use, each of them with peculiar features (*e.g.* costs, efficiency, safety aspects, energy and power density). Among the different types of EESS, LIB and Super Capacitors (SC) are addressed in the literature as the most promising technologies thanks to their good performances in terms of energy density (LIB) and power densities (SC) [158]. In this section, the main characteristics of SC and LIB will be briefly outlined, with particular reference to their use in PEMFC marine applications.

3.4.1 Super Capacitors

SC are mainly used for applications that do not require high energy capacities and that need high power densities, *e.g.* for peak shaving applications [158, 159]. Moreover, SC have longer lifetimes than batteries (> 500,000 charging/discharging cycles) [160]. Figure 3.5 shows the general working principle of SC. In general, a SC cell encompasses two electrodes, separated by a selective separator soaked in electrolyte. The separator material is ion-permeable, while it prevents the electric contact of the two electrodes. During the charging phase, the electric current flows from the anode towards the cathode, negatively polarizing the anode. When discharging, the previously accumulated anions and cations are released and can move freely in the electrolyte, while electrons flow from the anode towards the cathode through the electric load.

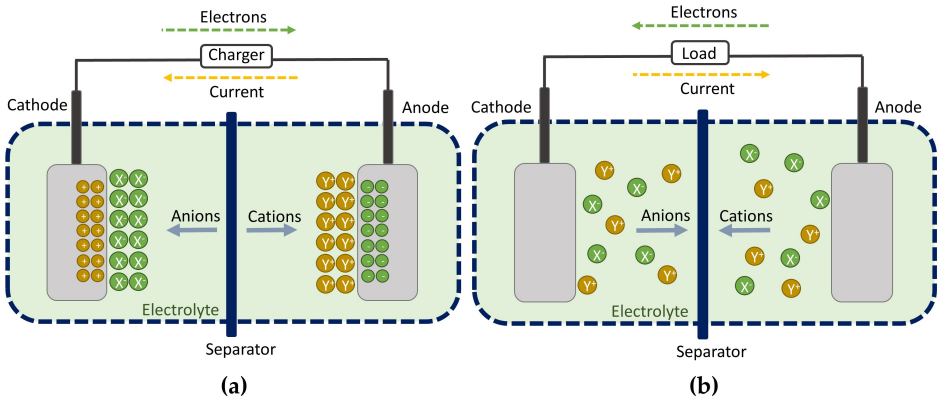

Figure 3.5: *General working principle of a (a) charged SC and (b) discharged SC. Elaborated from [158].*

3.4.2 Lithium-ion batteries

LIB are, today, the most widely used type of battery for shipping applications, mainly because they have higher specific energy than other types of batteries [158, 161]. Figure 3.6 shows the general working principle of LIB. The lithium is stored in the electrodes, which are soaked in the electrolyte and separated by a separator. The role of the separator is to isolate the electrodes (i.e. avoiding short circuit) while leaving lithium-ions (Li+) to pass through. When LIB is discharging, the Li+ flow from the anode to the cathode through the separator, leaving free electrons in the anode which can hence flow through the electric load towards the cathode. While charging, the Li+ are released by the cathode and flow towards the anode.

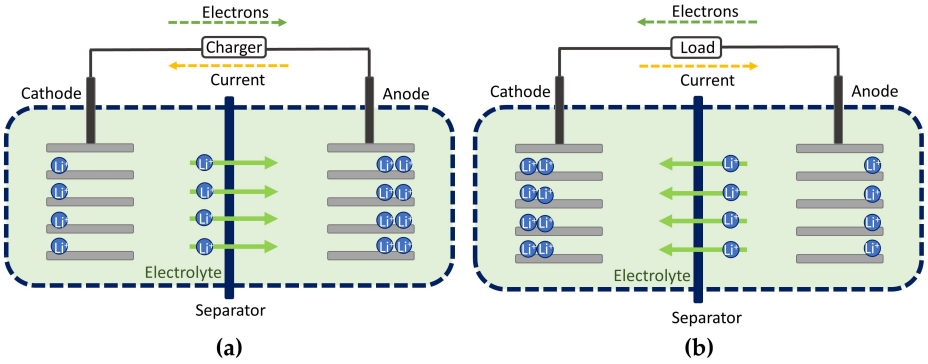

Figure 3.6: *General working principle of LIB during (a) charging and (b) discharging phase. Elaborated from [158].*

Different LIB chemistries are available today, which differ one from the others according to the materials they are composed by, and are hence characterized by different efficiency, energy and power density, and cost. The main LIB chemistries used for shipping are: Nickel Manganese Cobalt (NMC), Lithium Iron Phosphate (LFP), and Lithium Titanate Oxide (LTO) [158, 161]. Among these, NMC and LFP are today the most widely used LIB chemistries in shipping. The former have a relatively high energy density, low cost, and are characterized by high flexibility in terms of energy and power performances. The latter are characterized by relatively low energy densities, but are generally highly resilient to temperature fluctuations, have good safety performances, and can reach good levels of power density if the cathode is appropriately doped [162]. Nonetheless, given the limited cycling lifetime of both NMC and LFP, LTO are usually preferred for applications that require a large amount of cycling. LTO, at a higher investment cost than other LIB chemistries, provide good levels of overall battery safety and relatively high power density. Furthermore, it is pointed out in the literature that their high investment costs can be mitigated by their high life expectancy [158].

Table 3.4 summarizes the main characteristics of the main EESS available for use in ship power plants. When available, cost data reported in Table 3.4 specifically refer to marine applications, *i.e.* including the additional costs usually entailed for the *marinization* of batteries.

Table 3.4: *Characteristics of the main EESSs for ship applications.*

EESS	Chemistry (-)	Energy density (Wh/kg)	Power density (W/kg)	Cost (€/KWh)	Life (cycles)	Marine applications (-)	Refs.
LIB	**NMC**	150-220	520	500-1,000	1,000-1,2000	Currently the most largely used type of LIB in shipping, especially thanks to adjustable power and energy density.	[158, 163, 164, 165]
	LFP	90-120	200	500-1,000	1,000-12,000	Relatively low specific energy but good safety feature and resiliency to temperature characteristics; together with NMC is among the most largely used LIB in shipping.	[158, 164]
	LTO	50-80	70	1000-2000	600-20000	Suitable especially for applications where high power or large number of cycles are required.	[158, 164, 166]
SC	-	0.01-15	500-5000	100-500*	>500,000	Suitable for applications where high power density is needed but low energy capacity is required, *e.g.* offshore drilling unit.	[158, 167, 164]

Continued on next page

Table 3.4 – continued from previous page

EESS Chemistry (-)	Energy density (Wh/kg)	Power density (W/kg)	Cost (€/KWh)	Life (cycles)	Marine applications (-)	Refs.

*Cost related to land application. Cost of marine SC is likely to be at least five times higher (estimation on in accordance with cost difference between LIB for land and marine use).

3.4.3 EESS degradation

Similarly to PEMFC, also SC and LIB are prone to cycle ageing. However, both SC and LIB are also subject to calendar ageing when at resting conditions. As for SC, the performance degradation over time mostly results in the decrease of the electrodes pores accessibility and increase in the internal pressure [168]. Such phenomenon is mainly due to the cycle ageing and it is caused by the SC operation at high charge/discharge current levels, high temperature conditions, and over-voltage conditions [169, 170]. The calendar ageing of SC usually has a limited impact on the overall SC degradation rate, and is usually related with voltage and temperature conditions [171]. The ultimate result of the overall SC cycle and calendar ageing is the increase in the equivalent resistance of the system and the consequent decrease of the energy storage capacity and of the deliverable power [171, 172, 173].
As seen for PEMFC, also for SC there are different approaches to model degradation, which can be mainly classified as electrochemical/equivalent circuit methods and empirical/semi-empirical methods. The choice of the appropriate model should provide a compromise between accuracy and computational effort required, with empirical and semi-empirical models performing better in this last point [168, 172].
The degradation of LIB is a complex phenomenon linked with both cycle and calendar ageing. The former takes place during the charge/discharge cycles of the LIB, and depends mainly on the State of Charge (SOC), C-rate (*i.e.* the power/capacity ratio), temperature, number of performed equivalent cycles, and Depth Of Discharge (DOD). Conversely, calendar ageing takes place when no current flows through the LIB, and is mostly dependent on SOC and temperature [174, 175]. It should also be noticed that the LIB degradation phenomena also depends on theLIB chemistry. In general, however, it is possible to identify degradation mechanisms common to different LIB chemistries that occur at the anode, cathode, and electrolyte. Specifically, LIB degradation results at the anode in structural disordering, graphite exfoliation, lithium plating, growth of a solid layer (Solid Electrolyte Interface (SEI)), binder de-

composition, corrosion of current collectors, electrode particle cracking, and contact loss. At the cathode, degradation results in the dissolution of species, cracking of particle, structural disordering, passivation layer, corrosion of collector, and contact loss. Finally, at the electrolyte, separator dissolution and decomposition generally occurs . Such phenomena mainly result in the LIB voltage decay (mainly related to the increase of the cell inner impedance) and capacity fade (mainly linked with the loss of conductivity, loss of lithium inventory, and loss of active materials) [153, 176, 177, 178].
Different degradation modelling approaches have been proposed in the literature, either based on electrochemical and equivalent circuit models (*e.g.* SEI thickness modelling, internal resistance models), or on empirical/semi-empirical methods (*e.g.*capacity fade models) [155]. Electrochemical and equivalent circuit models are usually more accurate than empirical/semi-empirical ones, but they are often unpractical due to the computational effort required for their solution. Conversely, empirical and semi-empirical models can take advantage from experimental data to limit the overall complexity of the model and thus limit its solving time [155, 179].

3.5 Energy Management Strategy

The need to define an efficient EMS arises whenever an energy system involves the use of more than one energy source to supply a certain energy demand [180, 181]. When it comes to ship energy systems, the definition of a proper EMS is even more important, as ship energy systems are by definition isolated energy systems not connected to the grid, and as such the optimal integration and management of the power units is required not only for an efficient operation of the plant, but also for a safe operation. The EMS is aimed at allocating the power flows in the whole energy system, *i.e.* between the power units (*e.g.* ICE, FC), the storage units (*e.g.* EESS such as SC and LIB, but also thermal storage units), the WHR units (*e.g.* heat pumps, adsorption chillers), and the final users. The definition of a proper EMS is crucial for the optimal and efficient operation of PEMFC systems, as through the definition of an appropriate EMS it is possible (i) to ensure a safe and prolonged operation of the power plant, (ii) to match the power supply and demand of the ship, (iii) to guarantee the operation of power units in their best efficiency conditions, and possibly (iv) to avoid stressful operating conditions that may favorite the premature ageing of the components [182]. Generally, approaches for the definition of the EMS can be categorized as (i) rule-based or (ii) optimization-based. The former involves the definition of a set of rules on the basis of which the power flows are allocated among the units. Such approach is simple and practical to

use, but the rules may not guarantee the optimal operation of the plant as they might be biased by the human knowledge on the topic. Rule-based approaches are generally more common in simple systems, and are generally based either on the definition of rules based on look-up tables [80, 183, 184, 185, 186] or on the use of fuzzy logic techniques [187]. Differently, the optimization-based approach determines the power flow allocation by solving optimization problems based on mathematical models describing the system operation. Generally, optimization-based EMSs can be either global optimization EMSs or real-time optimization EMSs. The former require the definition in advance of the operating profile of the vessel (or in general the power demand) to subsequently perform a global optimization on the overall power demand profile [188, 189, 190, 191, 192, 193, 194, 195, 196, 197]. Differently, real-time EMSs do not require to know in advance the power demand profile, as they define instantaneous objective function(s) over time which are continuously updated according to the vessel operating conditions [198, 199, 200, 201]. In general, for each application, the choice between global and real-time optimization approaches for defining the EMS is made according to the availability of datasets for training and testing the real-time algorithms and according to the global degree of complexity deemed acceptable for the given application. Lastly, given the peculiar characteristics of FC and EESS, recent studies [189, 183, 188] in the literature propose the so-called *health-conscious* EMSs, which account for the power units degradation over time and aim at allocating the power flows in the system to minimize the occurrence of stressing events that may favorite the premature ageing of the components. Health-conscious EMSs are usually proposed for hybrid powertrains used in transport applications, and represent today a hot research topic not only for maritime applications, but also for land transport applications [155, 202].

3.6 The regulatory framework

The regulatory framework for hydrogen fuelled maritime PEMFC systems is still incomplete, with only some guidelines and draft regulations available for their installation on board. Hence, the compliance to classification safety standards must be proved for each application by means of an *alternative design* process [203]. However, the *alternative design* process sensibly increases the time and the cost required for class rules approval of a new PEMFC installation on board, and hence still represents one of the main obstacles to overcome for a large scale implementation of these systems. Indeed, although regulations are already available for land applications (*e.g.* for automotive applications or stationary systems), maritime applications need to comply with safety requirements that are specific for the maritime case (*e.g.* to ensure the safe return to

port). Guidelines and draft regulations in this sense start to be available for PEMFC maritime installations, while guidelines and rules are already available for batteries installations. Table 3.5 reports the list of guidelines and rules available for PEMFC and EESS on board of ships. Concerning PEMFC, guidelines are available today by American Bureau of Shipping (ABS), Bureau Veritas (BV), Det Norske Veritas - Germanischer Lloyd (DNV-GL), and Korean Register of Shipping (KRS) [204, 205, 206]. Recently, also IMO approved the *Interim guidelines for the safety of ships using fuel cell power installations* [207]. Regarding EESS, rules and guidelines are available by ABS, BV, DNV-GL, and Lloyd's Register (LR) [208, 206, 209].
In addition to these guidelines, however, key knowledge for hydrogen fuelled maritime PEMFC systems might also b retrieved by the available regulations for land transportation and stationary applications, as such rules may facilitate the obtainment of the alternative design approval[71, 158]. To this extent, a list of international standards for hydrogen PEMFC and for EESS systems for applications other than shipping is reported in Table 3.6. Additional and updated information on hydrogen and FC regulations can be retrieved in the HyLaw online database [210], or in the Fuel Cells and Hydrogen Energy Association (FCHEA) website [211], or in [212].

Table 3.5: *Class rules regulations and standards available for the use of fuel cell and batteries on board of ships as of September 2022.*

Institution	Document	Year	Notes	Refs.
Fuel cells				
ABS	Guide for fuel cell power systems for marine and offshore applications	2019	-	[204]
BV	Ships using fuel cells	2022	-	[205]
DNV-GL	Rules for classification of ships	2019	Pt. 6 Ch. 2 Sec. 3, Fuel cell installation	[206]
KRS	Guidance for fuel cell systems on board of ships	2015	-	[213]
IMO	Interim Guidelines for the safety of ships using fuel cell power installations	2022	-	[207]
Batteries and EESS				
ABS	Guide for the use of lithium-ion batteries in the marine and offshore industries	2022	-	[214]

Continued on next page

Table 3.5 – continued from previous page

Institution	Document	Year	Notes	Refs.
BV	Rules for classification of steel ships	2021	Pt. F Ch. 11 Sec. 22, Electric hybrid	[208]
DNV-GL	Rules for classification of ships	2019	Pt. 6, Ch. 2 Sec. 1, Battery power	[206]
LR	Large battery installation	2015	-	[209]

Table 3.6: *International standards on PEMFC, hydrogen technologies, and batteries available for both shipping applications and sectors other than shipping that could be relevant for the use in maritime applications. (u.d. = under development; n.a. not applicable; amd. = amendment).*

Standard number/series	Title	Year	Notes
PEMFC and hydrogen technologies			
ISO/TC 197	Hydrogen technologies	n.a.	Cover hydrogen production, storage, transportation, measurement, and use. Not yet used in the maritime sector, but packages under development (19885 series) on hydrogen fueling could be used for bunkering of maritime vessels. Packages of ISO/TC 197 considered particularly relevant also for maritime applications are reported in the following lines.
ISO 19880	Gaseous hydrogen - fueling stations	2020 (Pt.1) 2018 (Pt.3) 2019 (Pt.5) u.d. (Pt.6) 2019 (Pt. 8)	Part of ISO/TC 197. Part 1 (General requirements). Part 3 (Valves). Part 5 (Dispenser hoses and hose assemblies). Part 6 (Fittings). Part 8 (Fuel quality control).
ISO 16110	Hydrogen generators using fuel processing technologies	2007 (Pt.1) 2010 (Pt.2)	Part of ISO/TC 197. Part 1 (Safety). Part 2 (Test methods for performance).

Continued on next page

Table 3.6 – continued from previous page

Standard number/series	Title	Year	Notes
ISO/TR 15916	Basic considerations for the safety of hydrogen systems	2018	Part of ISO/TC 197. Includes considerations on hydrogen embrittlement, material compatibility, low-temperature hydrogen effects on materials.
ISO 26142	Hydrogen detection apparatus - Stationary applications.	2010	Part of ISO/TC 197. Standard intended to be used for certification purposes. Covers hydrogen detection apparatus, useful for the requirements in terms of hydrogen leaks detection.
ISO 14687	Hydrogen fuel – product specification	2019	Part of ISO/TC 197. Part 3 (Proton exchange membrane (PEM) fuel cell applications for stationary appliances).
ISO 19881	Gaseous hydrogen – Land vehicle fuel containers	2018	Part of ISO/TC 197. Referred to compressed hydrogen cylinders for land vehicles. Volume up to 1000 l and pressure up to 70 MPa. Only cylinders permanently attached to the vehicles are addressed.
ISO 19882	Gaseous hydrogen – Thermally activated pressure relief devices for compressed hydrogen vehicle fuel containers	2018	Part of ISO/TC 197. Minimum requirements for pressure relief devices of hydrogen vehicles compliant with ISO 19881, IEC 62282-4-101, ANSI HGV 2, CSA B51 Part 2, EC79/EU406, SAE J2579, or the UN GTR No. 13.
ISO 19884	Gaseous hydrogen – Cylinders and tubes for stationary storage	u.d.	Part of ISO/TC 197. Information can also e found at the previously available ISO 15399:2012 – "Gaseous hydrogen. Cylinders and tubes for stationary storage" for cylinders and tubes up to 110 MPa, 10000 l.

Continued on next page

Table 3.6 – continued from previous page

Standard number/series	Title	Year	Notes
IEC 62282	Fuel cell technologies	n.a.	IEC 62282-2-100:2020 "Fuel cell modules - Safety";IEC 62282-3-100:2019 "Stationary fuel cell power systems - Safety";IEC 62282-3-200:2015 "Stationary fuel cell power systems – Performance test methods";IEC 62282-3-300:2012 "Stationary fuel cell power systems – Installations"; IEC 62282-3-400:2016 "Small stationary fuel cell power systems with combined heat and power output"; IEC 62282-7-1:2017 "Single cell test methods for polymer electrolyte fuel cell (PEFC)"; IEC 62282-8-101:2020 "Energy storage systems using fuel cell modules in reverse mode"
IEC 60050-485	International Electrochemical Vocabulary (IEV) – Part 485: Fuel cell technologies.	2020	Replaces the withdrawn IEC 62282-1:2013 "Terminology".
ISO/TC 220	Cryogenic vessels	n.a.	Land-based cryogenic vessels (vacuum or non-vacuum). Could be useful for the maritime as it addresses also design and safety of the cryogenic vessels, gas/materials compatibility, insulation, operational requirements. Packages of ISO/TC 220 considered particularly relevant also for maritime applications are reported in the following lines.
ISO 20421	Cryogenic vessels – Large transportable vacuum-insulated vessels	2019 (Pt.1) 2017 (Pt.2)	Part of ISO/TC 220. Part 1 (Design, fabrication, inspection and testing). Part 2 (Operational requirements). Static vessels regulation available in ISO 21009.
ISO 21011	Cryogenic vessels – Valves for cryogenic service	2008	Part of ISO/TC 220. Manufacturing and tests of valves for rated temperatures <-40°C.
ISO 21029	Cryogenic vessels – Transportable vacuum insulated vessels of not more than 1000 l volume	2018 (Pt. 1) 2015 (Pt. 2)	Part of ISO/TC 220. Part 1 (Design, fabrication, inspection and tests). Part 2 (Operational requirements).

Continued on next page

Table 3.6 – continued from previous page

Standard number/series	Title	Year	Notes
ISO 24490	Cryogenic vessels – Pumps for cryogenic service.	2016	Applicable to centrifugal pumps, but could be applied also to other types of cryogenic pumps, e.g. reciprocating pumps.
ISO/TC 58	Gas cylinders	n.a.	Technical committee for the standardization of gas cylinders. Of relevance for hydrogen cylinders is the package ISO 11114.
ISO 15649	Petroleum and Natural gas industry	2001	Often used as a guidance in hydrogen piping systems.
UNI EN 13480	Industrial metallic piping	2020	Specifies design and calculation methods for industrial piping systems and relative supports.
ISO 23273	Fuel cell road vehicles — Safety specifications — Protection against hydrogen hazards for vehicles fuelled with compressed hydrogen	2013	Part 2 (Protection against hydrogen hazards for vehicles fuelled with compressed hydrogen). Part 3 (Protection of persons against electric shock, etc.).
NFPA 2	Hydrogen Technologies Code	2016	Fundamentals for generation, installation, storage, piping, use, and handling of compressed and cryogenic hydrogen.
NFPA 55	Compressed Gases and Cryogenic Fluids Code	2020	Guidelines for protection against physiological, explosive, over-pressurization, and flammability hazards associated with compressed and cryogenic gases.
NFPA 221	Standard for High Challenge Fire Walls, Fire Walls, and Fire Barrier Walls	2021	Prescriptions for design and construction of fire protection structures for use in protecting life and property from fire.
NFPA 853	Standard for the Installation of Stationary Fuel Cell Power Systems	2020	Related to stationary systems, provides fire prevention and proception measures for the safeguarding of life and buildings.

Continued on next page

Table 3.6 – continued from previous page

Standard number/series	Title	Year	Notes
SAE J2578	Recommended Practice for General Fuel Cell Vehicle Safety	2014	Related to the design, construction, operation and maintenance of fuel cell vehicles.
SAE J2579	Standard for Fuel Systems in Fuel Cell and Other Hydrogen Vehicles	2018	Design, construction, operational, and maintenance requirements of hydrogen fuel storage and handling systems (road vehicles).
SAE J2600	Compressed Hydrogen Surface Vehicle Fueling Connection Devices	2015	Design and testing of fueling connectors, nozzles, and receptacles.
SAE J2601/2	Fuelling Protocol for Gaseous Hydrogen Powered Heay Duty Vehicles	2014	Independent document from SAE J2601 related to light-duty vehicles. Provides performance requirements for hydrogen dispensing systems for heavy-duty vehicles with hydrogen storage pressures up to 35 MPa.
EN 1626	Cryogenic vessels – Valves for cryogenic service	2008	Design, fabrication, and testing of valves for cryogenic use. Valid for valves diameters up to DN150.
EN 60079	Explosive atmosphere	n.a.	Regulation series for explosive atmospheres (ATEX).
Batteries and ESS			
EN 50110	Operation of electrical installations	2013	Part 1 – General requirements (documentation for batteries and electrical testing).
IEC 61508	Functional safety of electrical/-electronic/programmable electronic safety-related systems	2010	-
IEC 61511	Safety instrumented systems for the process industry sector	2016 (2017 amd.)	Amendment 1: 2017. Prescription on requirements for specification, design, installation, operation, and maintenance of Safety Instrumented Systems (SIS).

Continued on next page

Table 3.6 – continued from previous page

Standard number/series	Title	Year	Notes
IEEE 45	Recommended practice for electrical installation on shipboard	2017 (Pt.1) 2020 (Pt.2)	Part 1 (Design of electrical power generation, distribution, propulsion, loafs systems, and equipment on merchant, commercial, and naval vessels). Part 2 (Controls, control applications, control apparatus, automation on shipboards).
IEC 62619	Secondary cells and batteries containing alkaline or other non-acid electrolytes - Safety requirements for secondary lithium cells and batteries, for use in industrial applications	2017	Requirements and tests or safe operation of secondary lithium cells and batteries in industrial applications, including marine applications.
IEC 62620	Secondary cells and batteries containing alkaline or other non-acid electrolytes – Secondary lithium cells and batteries for use in industrial applications	2014	Marking, tests, and requirements of secondary lithium cells and batteries in industrial applications, including marine applications.
DOT/UN 38.3	UN Manual of tests and criteria, Transport of Dangerous goods	209	Chapter on lithium metal and lithium-ion batteries.
IEC 62281	Safety of primary and secondary lithium cells and batteries during transport	2019 (2021 amd.)	Test methods and requirements for batteries (rechargeable and non-rechargeable) for safety during transport.
UL 9540	Energy storage systems and equipment	2020	Safety standard for grid connected or standalone ESS (battery system safety, fire detection and suppression, environmental performance, etc.).

Continued on next page

Table 3.6 – continued from previous page

Standard number/series	Title	Year	Notes
IEC 60529	Degrees of protection provided by enclosures (IP Code)	2020	-
IEC 60092	Electrical installations in ships	2022	Part 504: Special features – control and instrumentation.
IEC 62061	Safety of machinery - Functional safety of safety-related control systems.	2021	2021 version still not harmonized. The harmonized version is still the one of 2015.

3.7 Challenges and research gaps identified

The literature review on PEMFC-based ship propulsion systems fuelled by hydrogen here presented allowed to identify the challenges and research gaps that need to be addressed to allow a widespread use of such technologies in the maritime sector in the upcoming years. Firstly, the definition of an internationally accepted and harmonized set of rules for the safe installation and operation of fuel cell systems on board, and for the safe hydrogen handling and bunkering procedure is essential for the commercialization of such systems on a large scale. It must be noted that the last years have seen a remarkable progress in this context, and further advancements are expected in the forthcoming years thanks to the research on hydrogen system safety. Also the limited availability of hydrogen bunkering infrastructure and in general of the infrastructure needed for the hydrogen distribution constitutes a bottleneck for the large scale use of hydrogen as marine fuel. This is also related to the high costs of hydrogen technologies today (including fuel cells), which is indeed a limiting factor for the deployment of hydrogen use not only in shipping but also in other applications. In this sense, future research studies both in hydrogen economics and electrochemistry as well as material science could help in solving this challenges. From an energy system engineering point of view, however, the following research gaps appear to be interesting, and will hence be addressed in this thesis:

- **Degradation over time of PEMFC and EESS**. The limited lifetime of both PEMFC and EESS is a major drawback of this type of system,

which could hamper the economic competitiveness of such systems in the long run. Hence, the evaluation of the ageing mechanism and their impact in terms of cost and energy efficiency of the entire energy system is becoming a hot research topic, as well as the definition of the so-called health conscious EMSs that allow to operate the systems while limiting the components' degradation. In this regard, the main research gap appears to be the analysis of the energy systems performance over time due to the progressive degradation of PEMFC and EESS.

- **PEMFC waste heat recovery**. The low quality of the PEMFC's waste heat, usually available at a temperature of 60-70°C, represents a challenge for the efficient use of PEMFC in shipping, as it is difficult to recover. While this aspect may not influence the overall operation of PEMFC propulsion systems for small vessels, it could hamper future installation of PEMFC power systems for larger vessels as cruise ships, where WHR is essential for efficiently covering heating and cooling demands onboard. Recent studies address PEMFC WHR for stationary systems (*e.g.* residential applications), but it appears to be a lack of studies on PEMFC WHR for ship applications.

Chapter 4

Methodology

This section presents the general methodology developed to address the research gaps identified after the literature review on PEMFC based systems for shipping. While the developed methodology is general, it is here proposed its specific application to two case studies, in order to analyze in deep (i) the health-conscious EMS of a hybrid ship propulsion system over the entire plant lifetime and (ii) the optimal design and operation of a multi-energy system for a cruise ship taking into account PEMFC WHR. Starting from the definition of the power demand profile of the vessels, this Chapter outlines the rationale behind the two optimization problems, and the set of equations describing the dynamic behaviour of all the energy systems' components. It should be noticed that some of the content reported hereafter may not be original content, but reproduced and/or adapted from previously published papers by the author during the PhD. In particular, part of the contents in this section may have been reproduced or adapted from the following publications:

- **Dall'Armi, C.**, Micheli, D., Taccani, R. (2021). Comparison of different plant layouts and fuel storage solutions for fuel cells utilization on a small ferry. International Journal of Hydrogen Energy 46, 13878-13897. doi.org/10.1016/j.ijhydene.2021.02.138.

- Pivetta, D., **Dall'Armi, C.**., Taccani, R. (2021). Multi-objective optimization of hybrid PEMFC/Li-ion battery propulsion systems for small and medium size ferries. International Journal of Hydrogen Energy 46(72), 35949-35960. doi.org/10.1016/j.ijhydene.2021.02.124.

- **Dall'Armi, C.**, Pivetta, D., Taccani, R. (2021). Health-conscious optimization of long-term operation for hybrid PEMFC ship propulsion systems. Energies 14, no. 13:1813. https://doi.org/10.3390/en14133813.

- **Dall'Armi, C.**, Pivetta, D., Taccani, R. (2022). Uncertainty analysis of the optimal health-conscious operation of a hybrid PEMFC coastal

ferry. International Journal of Hydrogen Energy 47(21), 11428-11440. doi.org/10.1016/j.ijhydene.2021.10.271.

- **Dall'Armi, C.**, Pivetta, D., Taccani, R. (2022). On optimal integration of PEMFC and low temperature waste heat recovery in a cruise ship energy system, ECOS 2022 - Proceedings of the 35th International Conference on Efficiency, Cost, Optimization, Simulation and Environmental Impact of Energy System, Copenhagen 3-7 July 2022, Denmark.

4.1 Hybrid PEMFC/LIB ferry: health-conscious energy management strategy

This section presents the methodology proposed to analyze how to manage a hybrid PEMFC/LIB ship propulsion system taking into account the power sources degradation. Firstly, the main characteristics and power demands of the ferry chosen as case study are outlined. Afterwards, it is presented the energy system's layout proposed in this study, and the set of equations describing the optimization problem.

4.1.1 Main characteristics of the ship chosen as case study

A typical small size RoPax ferry operating in coastal areas has been chosen as case study, similar to the one represented in Figure 4.1. Table 4.1 reports the main characteristics of the vessel.

Figure 4.1: *Typical RO-Pax small size ferry [189].*

Power system volume and weight in Table 4.1 have been elaborated from data available on diesel storage on board and diesel-electric generator for marine propulsion, scaled by the installed power of the ferry. The choice of small

size RoPax ferry operating in coastal areas as case study was made as hybrid PEMFC/EESS power systems could be particularly advantageous for this type of vessels. On the one hand, hydrogen fuelled hybrid PEMFC system would guarantee the navigation at zero local emissions, decreasing the environmental impact of the vessel on the surrounding coastal environment. On the other hand, the typical operating profiles of this type of vessels, with short and frequent voyages during the day, require long navigation range and often do not guarantee enough time at the harbor for recharging batteries with onshore power.

Table 4.1: *Main characteristics of the RoRo passenger ferry chosen as case study [80].*

Parameter	**Value**
Length x width	40m x 9m
Design speed	8-9 knots
Gross tonnage	282 t
Propulsion engines	2 x 206 kW
Auxiliary engines	2 x 28 kW
Yearly MDO consumption	27 t
Power system volume	15.5 m^3
Power system weight	7,185 kg

Power demand profile

Figure 4.2 shows the power demand profile of the ferry over a typical day of operation, used as input data of the optimization problem. The power demand at each time step has been evaluated as function of typical speed data available online [215].

Cubic polynomial fits have been used to approximate the speed-power relationship of each vessel, as proposed for example in [216]. Auxiliaries power demand have been estimated in accordance with typical values for each ferry. Each electrical demand has been evaluated for 1-min intervals. At each time step, the energy system shall fulfill the entire energy demand of the ferries.

The proposed energy system

Figure 4.3 shows the simplified schematic of the proposed ferry energy system. Hydrogen has been assumed to be stored in liquid form in a cryogenic tank, with the aim of reducing the volume and weight for the storage system in comparison to other type of hydrogen storage systems (*e.g.* compressed hydrogen tanks) [80]. It has been set that the ferry has enough fuel for a daily

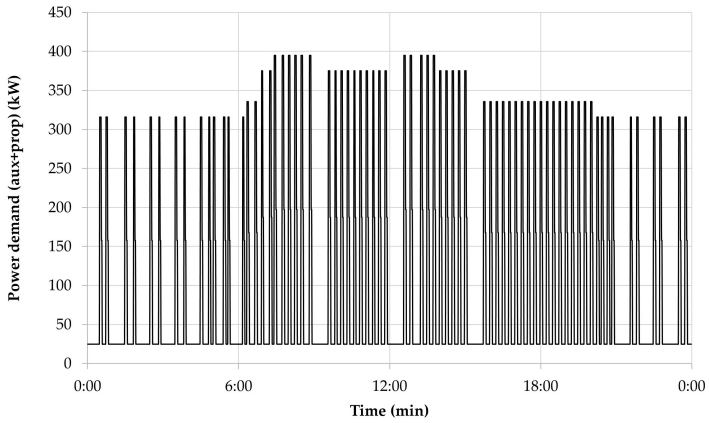

Figure 4.2: *Power demand profile of the ferry chosen as case study for developing the health-conscious EMS of a hybrid PEMFC ship propulsion system. Reproduced from [80].*

operation. After evaporation, hydrogen feeds the PEMFC stacks, which are coupled with a LIB. The entire system fulfills the power demand of the ferry, both propulsion and auxiliary power demand, at each time step. As will be explained in the next sections, the sizes of both PEMFC and LIB are determined by solving a dedicated design and operation optimization over a typical day of operation. On the basis of the optimal design, the optimal EMS that accounts for both PEMFC and LIB degradation over time is then determined by solving an iterative optimization problem.

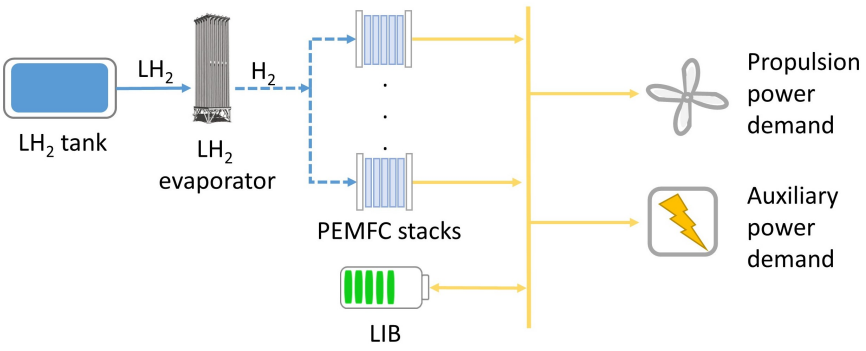

Figure 4.3: *Simplified schematic of the proposed hybrid PEMFC/LIB energy system for covering the ferry's propulsion and auxiliary power demands.*

4.1.2 The optimization problem

As widely recognized, the MILP approach is appropriate for the optimization of complex energy system as it allows to reduce the computational effort with

respect to other optimization techniques [217, 218, 219]. Therefore, it has been chosen to adopt a MILP approach to develop and solve the optimization problems proposed hereafter. In general, all the optimization problems are hence set as:
Find the optimal value of $x^*(t)$ and $\delta^*(t)$ that maximize or minimize the objective function(s) Z (Equation 4.1) subject to the equality constraints $g(t)$ and inequality constraints $h(t)$ (Equations 4.2 and 4.3), on which the model of the energy system of the considered ship is based. The continuous variables (x) and binary variables (δ) are the decision variables of the optimization problem. In particular, binary variables have been used to decide about on/off status of each energy unit during operation. All the models have been developed in Python programming language [220] and solved with Gurobi Optimizer [221].

$$Z = f(x^*(t), \delta^*(t)) \tag{4.1}$$

$$g(x^*(t), \delta^*(t)) = 0 \tag{4.2}$$

$$h(x^*(t), \delta^*(t)) \leq 0 \tag{4.3}$$

The methodology has then been developed in three different optimization phases. Firstly, a deterministic design and operation optimization has been run in order to determine the optimal sizes of the energy conversion and storage units of the energy system and their optimal operation over a typical day (Figure 4.2), following the approach described in [190]. Afterwards, a further design and operation optimization has been developed, taking into account explicitly the performance degradation over time not only of PEMFC but also of LIB, as described in [189]. Lastly, the third phase optimization considers uncertain cost parameters as input to the optimization problems, in order to obtain risk-aware information on the optimal management of the plant as well as the cost over the entire lifetime, as reported in [191].
In the followings, the three methodology phases (*i.e.* the three optimization problems) are described, with particular reference to the objective function(s) of the problems, the main constraints describing the components operation, and the ones setting the energy system power balances and limits on the overall weight and volume.

Phase 1: design and operation optimization over a typical operating day

The first phase of the optimization is aimed at determining the optimal size of the energy conversion and storage units. Concurrently, also the operation of the entire system is optimized over a typical day of operation of the ferry (Figure 4.2). A multi-objective optimization has been set to define the optimal Design and Operation (D&O) of the hybrid PEMFC/LIB ferry propulsion

system that allows to concurrently minimize the operation and investment costs and the PEMFC degradation. Following the general approach outlined in Equations 4.1, 4.2, and 4.3, two objective functions have hence been specified in this first phase of the methodology: the operation and investment cost (f_1 in Equation 4.4) and the PEMFC performance degradation expressed in terms of voltage decay (f_2 in Equation 4.5). In Equation 4.4, $F_{FC,i}(t)$ defines the hydrogen consumption at time t of the i-th PEMFC stack, c_H2 is the hydrogen fuel cost, $E_{LIB,max}$ is the LIB capacity, c_{LIB} is the cost of LIB, n_{FC} is the number of PEMFC stacks of rated power $P_{FC,max}$ and cost c_{FC} installed in the system. dV_i in Equation 4.5 is the total voltage decay of the i-th PEMFC stack. The multi-objective optimization has been developed following a *hierarchical objective* method, where different priorities are fixed for each objective function. A higher priority has been set in this case for the f_2 objective function, which is hence optimized first. Afterwards, f_1 is minimized by the solver, and solutions are chosen in order to ensure that the optimal value of the primary objective function f_2 is not worsen more than a certain relative tolerance, fixed in this case at 1% (see [221] for further information about the solver algorithm).

$$f_1 = \sum_i (\int_t (F_{FC,i}(t)dt) \cdot c_{H2}) + E_{LIB,max} \cdot c_{LIB} + n_{FC} \cdot P_{FC,max} \cdot c_{FC} \quad (4.4)$$

$$f_2 = \sum_i (\int_t (dV_i(t)dt) \quad (4.5)$$

MILP Equations 4.6 to 4.24 describe the behavior of conversion and storage units, *i.e.* PEMFC stacks and LIB, at each time step t. The innovative approach developed allows to include the performance degradation model for PEMFC stacks in the D&O optimization for one day of operation of the ferry, while limiting also the LIB performance degradation.
Equations 4.6, 4.7,4.8, and 4.9 describe i-th PEMFC stack operation. The design decision variable of PEMFC is the number of stacks installed in the system n_{FC}, each with an installed power ($P_{FC,max}$). A typical performance characteristic curve, *i.e.* PEMFC efficiency at varying PEMFC power load, has been elaborated on the basis of commercial products [222, 223, 224, 225]. In order to simplify the overall mathematical structure of the optimization problem, it has been decided to represent the PEMFC characteristic curve in terms of fuel consumption per power output. The fuel consumption has been expressed in kW, and is defined as the ratio between the PEMFC power output and the PEMFC efficiency.

$$F_{FC,i}(t) = k_{1FC} \cdot P_{FC,i}(t) + k_{2FC} \cdot \delta_{FC,i}(t) + \delta_{st-up,i} \cdot F_{start} \cdot P_{FC,max} \quad (4.6)$$

$$load_{FC,min} \cdot P_{FC}^{MAX} \cdot \Delta_{FC,i} \leq P_{FC,i}(t) \leq load_{FC,max} \cdot P_{FC}^{MAX} \cdot \Delta_{FC,i} \quad (4.7)$$

$$\Delta_{load,FC} \geq |P_{FC,i}(t) - P_{F,i}(t-1)| \quad (4.8)$$

$$n_{FC} = \sum_{i} \Delta_{FC,i} \tag{4.9}$$

Equation 4.6 defines the hydrogen consumption at time t of the i-th PEMFC stack $F_{FC,i}$ as function of the the PEMFC stack power output $P_{FC,i}$ by means of the linearization coefficients k_{1FC} and k_{2FC}. $\delta_{FC,i}$ and $\delta_{st-up,i}$ are binary variables that describe the on/off status of the i-th PEMFC stack and the happening of a start-up of the i-th stack, respectively. F_{start} is an additional hydrogen consumption due to the start-up of the i-th PEMFC stack. Equation 4.7 limits the power generated by the $i-th$ PEMFC stack in order not to exceed the minimum ($load_{FC,min}$) and maximum ($load_{FC,max}$) power load, expressed as percentage of the rated power of the stack P_{FC}^{MAX}. At each time step, the load variation cannot exceed the maximum value $\Delta_{load,FC}$, as reported in Equation 4.8. The binary variable $\Delta_{FC,i}$ in Equations 4.7 and 4.9 expresses the inclusion/exclusion of the i-th stack in the optimal system configuration. The sum of such variables $\Delta_{FC,i}$ defines the number of PEMFC stacks n_{FC} that should be included in the system (Equation 4.9).
Equations 4.10 to 4.14 describe the performance degradation of PEMFC stacks, which is defined as the voltage reduction of a single cell at equal current output, assuming that the behaviour of a single cell can approximate the one of the entire PEMFC stack [226, 148, 188]. The loss of power depends on: load variation (defined in Equation 4.10), start/stop cycles (defined in Equation 4.11), and power levels of the i-th PEMFC stack (defined in Equation 4.12). For each time interval t, Equation 4.14 defines the total loss of voltage in the single cell, which has been set to be linearly depending on the operation variables of the i-th stack (see Equations 4.12 and 4.13).

$$dV_{load,i}(t+1) = |P_{FC,i}(t) - P_{FC,i}(t+1)| * \Delta\nu_{load} \tag{4.10}$$

$$dV_{st-up,i}(t) = \delta_{st-up,i}(t) \cdot \Delta\nu_{st-up} \tag{4.11}$$

$$dV_{P,FC,i}(t) = k_{1,deg} \cdot I_{FC,i}(t) + k_{2,deg} \tag{4.12}$$

$$I_{FC,i}(t) = k_{1,I} \cdot P_{FC,I}(t) + k_{2,I} \cdot \delta_{FC,I}(t) \tag{4.13}$$

$$dV_i(t) = dV_{load,i} + dV_{st-up,i} + dV_{P,FC,i} \tag{4.14}$$

In Equation 4.10, $dV_{load,i}$ is the voltage reduction due to the load variations of the i-th single cell, proportional to the load variation by means of the coefficient $\Delta\nu_{load}$. Similarly, Equation 4.11 expresses the voltage reduction due to the start-up of the i-th cell $dV_{st-up,i}$ as a constant value of voltage reduction $\Delta\nu_{st-up}$ according to the binary variable $\delta_{st-up,i}$, which defines the happening of a start-up phase. As for the voltage reduction due to power level $dV_{P,FC,i}$, Equation 4.12 expresses it as linear function of the current of the i-th stack $I_{FC,i}$ by means of the linearization coefficients $k_{1,dv}$ and $k_{2,dv}$. The current $I_{FC,i}$ itself is defined as linear function of the i-th stack power level $P_{FC,I}$ by means of the

linearization coefficients $k_{1,I}$ and $k_{2,I}$ as reported in Equation 4.13. The total voltage reduction dV_i is then calculated as the sum of the three contributes as shown in Equation 4.14.
As for the LIB, Equations 4.15 to 4.17 define its operation at each time step t. More in detail, Equation 4.15 defines the energy stored in the LIB E_{LIB} at each time step t as function of the charging/discharging energy efficiency η_{LIB}, the output power of the LIB P^{+}_{LIB} and the input power of the LIB P^{-}_{LIB}. To limit the overall complexity of the optimization model, the charging/discharging efficiency η_{LIB} is set to be constant at varying of the C-rate (*i.e.* the ratio between the power input/output and the battery capacity $E_{LIB,max}$). At each time step, the energy store in the battery cannot exceed the limits set on the minimum and maximum SOC, *i.e.* the ratio between the energy stored at time t and the battery capacity $E_{LIB,max}$, as expressed in Equation 4.16. Lastly, Equation 4.17 sets the constraint to ensure that the energy stored in the battery at the first and last time step of the simulation is the same.

$$E_{LIB}(t) = E_{LIB}(t-1) + (\eta_{LIB} \cdot P^{-}_{LIB}(t) - (1/\eta_{LIB}) \cdot P^{+}_{LIB}(t)) \tag{4.15}$$

$$SOC_{min} \cdot E_{LIB,max} \leq E_{LIB}(t) \leq SOC_{max} \cdot E_{LIB,max} \tag{4.16}$$

$$E_{LIB}(0) = E_{LIB}(T_{end}) \tag{4.17}$$

Although this first phase of the optimization is aimed at minimizing the PEMFC degradation, a simplified constraint is set to limit also the LIB degradation, following the procedure proposed in [227, 228]. In this way, it is possible to take into account the necessary oversizing of the LIB to limit stressful events, while limiting the computational effort required by the system. A detailed LIB degradation model will then be introduced in the second phase of the optimization outlined in the next section. Firstly, the LIB capacity is oversized to ensure the required energy storage at the End of Life (EoL) of the LIB, as shown in Equation 4.18.

$$E_{LIB,os} = E_{LIB,max}/E_{EoL} \tag{4.18}$$

Where $E_{LIB,os}$ is the oversized capacity and E_{EoL} is the share of battery capacity at the EoL. Afterwards, assuming that the battery degrades linearly over its lifetime, an averaged LIB capacity $E_{LIB,avg}$ is calculated as shown in Equation 4.19.

$$E_{LIB,avg} = (E_{EoL} + 1)/2 \cdot E_{LIB,os} \tag{4.19}$$

A constraint is therefore included in the optimization model, defined as in Equation 4.20, where LT_{LIB} is the LIB lifetime and $E_{LIB,tp}$ is the energy throughput of the LIB over its lifetime.

$$LT_{LIB} \cdot \sum_{t} P^{+}_{LIB}(t) \leq E_{LIB,tp} \tag{4.20}$$

The energy throughput of the battery $E_{LIB,tp}$ is the total amount of energy that a battery can store and deliver over its lifetime, and it is calculated as reported in Equation 4.21, where

$$E_{LIB,tp} = \eta_{LIB} \cdot N_{cycle,max} \cdot E_{LIB,avg} \cdot DOD \tag{4.21}$$

Where $N_{cycle,max}$ is the maximum number of equivalent cycles of theLIB and DOD is the depth of discharge of the LIB. To ensure that the energy system fulfills the power demand of the ferry P_{demand} at each time step, the power balance of Equation 4.22 is set as constraint in the optimization.

$$\sum_i P_{FC,i}(t) + P^+_{LIB}(t) = P_{demand}(t) + P^-_{LIB}(t) \tag{4.22}$$

Moreover, two additional constraints have been set in Equations 4.23 and 4.24 to ensure that the alternative power system optimal design identified by solving the optimization model does not exceed the weight W_max and volume V_max of the currently installed power system (see data in Table 4.1) increased by an acceptable correction factor c_{ov} to take into account the current limited development state of FC systems. More in detail, Equation 4.23 expresses the weight constraint, where w_{H2} is the specific weight of hydrogen storage system, w_{LIB} is the specific weight of the LIB, and w_{FC} is the specific weight of the PEMFC stacks. Similarly, in Equation 4.24, v_{H2} is the specific volume of hydrogen storage system, v_{LIB} is the specific volume of the LIB, and v_{FC} is the specific volume of the PEMFC stacks.

$$\sum_i (\int_t (F_{FC,i}(t)dt) \cdot w_{H2}) + E_{LIB,max} \cdot w_{LIB} + n \cdot P_{FC,max} \cdot w_{FC} \leq W_max \cdot (1 + c_{ov}) \tag{4.23}$$

$$\sum_i (\int_t (F_{FC,i}(t)dt) \cdot v_{H2}) + E_{LIB,max} \cdot v_{LIB} + n \cdot P_{FC,max} \cdot v_{FC} \leq V_max \cdot (1 + c_{ov}) \tag{4.24}$$

Phase 2: health-conscious operation optimization over the entire plant lifetime

The optimal sizes of PEMFC and LIB resulting from the first phase optimization outlined in the previous section have been taken as input parameters of the new optimization approach for the long-term operation, further referred to as second phase optimization. Figure 4.4 reports a simplified schematic of the methodology approach of the second phase optimization here proposed. Starting from time $t_j = 0$, corresponding to a novel installation of both PEMFC and LIB, consecutive optimizations have been run in a loop until either PEMFC or LIB reached the end of their life. In order to limit the computational effort, it has been assumed that the first day of the month j is representative for the operation of all the days of the month (assuming all months have 30 days).

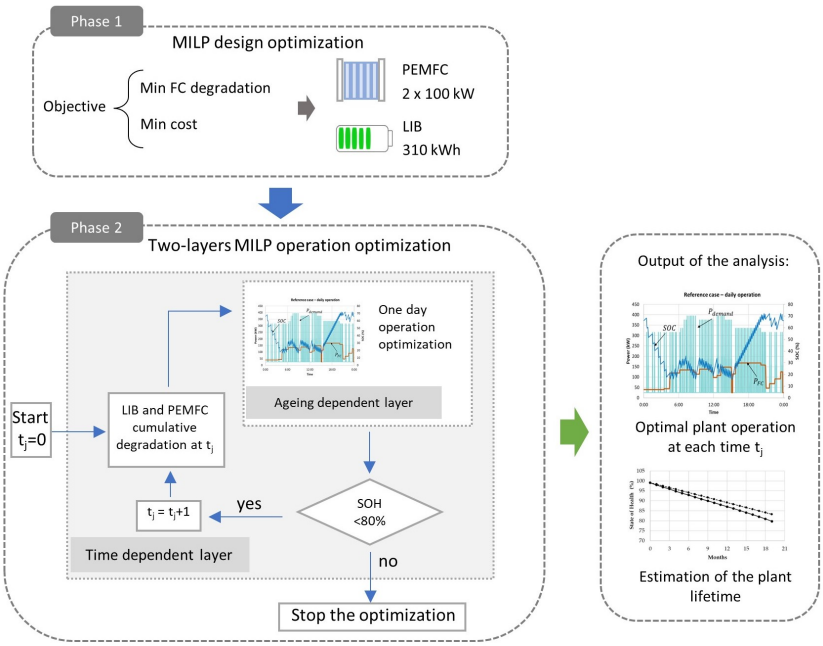

Figure 4.4: *Simplified schematic of the second phase of the proposed methodology for the health-conscious optimization of the hybrid PEMFC/LIB energy system operation over the entire plant lifetime. In the schematic, SOH indicates the State Of Health of either PEMFC or LIB.*

Operation optimization has been performed for the day representative of the entire month j. The cumulative degradation of PEMFC and LIB calculated at the end of month j has been taken as an input parameter for the operation optimization of month $j+1$. In this case a multi-objective optimization has been set to find the optimal long-term operation of the proposed PEMFC/LIB hybrid system that allows to minimize the fuel consumption, the degradation of PEMFC, and the degradation of LIB over their lifetime. Three objective functions have been specified, namely fuel consumption (f_1 in Equation 4.25), PEMFC performance degradation (f_2 in Equation 4.26), and LIB performance degradation (f_3 in Equation 4.27). For the multi-objective optimization, a *blended objectives* method has been adopted, considering a linear combination of the objective functions, each with a fixed weight [221]. In this case, a cost related weight has been assumed for each objective function. The weight of f_1 (w_1 in Equation 4.29) depends on the cost of hydrogen. Weights of f_2 and f_3 (w_2 and w_3 in Equations 4.30 and 4.31) derive from the cost of the components and their lifetime. The multi-objective optimization has been performed by minimizing the linear combination of the three objective functions, defined as f_MO (Equation 4.28). A 1% deviation from the optimal value of the f_{MO} function has been allowed.

$$f_1 = \sum_i \int_t F_{FC,i}(t)dt \tag{4.25}$$

$$f_2 = \sum_i \int_t dV_i(t)dt \tag{4.26}$$

$$f_3 = \int_t Q_{LIB,loss}(t)dt \tag{4.27}$$

$$f_{MO} = minimize(w_1 \cdot f_1 + w_2 \cdot f_2 + w_3 \cdot f_3) \tag{4.28}$$

$$w_1 = c_{H2} \tag{4.29}$$

$$w_2 = c_{FC} \cdot P_{FC,max}/V_0 \tag{4.30}$$

$$w_3 = c_{LIB} \cdot E_{LIB,max}/Q_{LIB,loss,max} \tag{4.31}$$

In Equations 4.29 to 4.31, c_{H2} is the cost of hydrogen fuel, c_{FC} is the cost of a PEMFC stack, V_0 is the total voltage loss allowed for a single cell of the PEMFC stack (set equal to 20% of the reference value $V_{ref,FC}$), c_{LIB} is the cost of the LIB, and $Q_{LIB,loss,max}$ is the maximum capacity fade of the battery (set equal to 20% of the LIB capacity). The final output of this second phase optimization is the estimation of the total plant lifetime and the definition of the optimal operation that allows to minimize not only the fuel consumption and the PEMFC degradation, but also the LIB degradation for the entire lifetime of the plant. By fixing the design according to the results of the phase 1 optimization, it is possible to limit the computational effort required by the

system, and hence to perform the analysis on a wider time frame and considering a larger amount of variable concerning the power units degradation.
As seen for the phase 1 optimization, also in this case the optimization model encompasses a power balance constraint, and the constraints on the maximum weight and volume of the proposed plant (see Equations 4.22, 4.23 and 4.24). Similarly, the previously seen Equations 4.6 to 4.14 remain valid for the definition of the PEMFC operation and degradation at each time step. In addition, in this case also the cumulative voltage degradation of the i-th stack $dV_{TOT,i}$ is calculated at the end of each j month as shown in Equation 4.32. In fact, the cumulative voltage degradation evaluated for the single cell modifies the characteristic curves of the entire stack. In particular, the relation between voltage loss and power has been approximated by a linear curve, which relates voltage loss to the angular coefficient of the power curve ($k_{1,P}$), as described in Equation 4.33. The State Of Health (SOH) for PEMFC i-th stack ($SOH_{PEMFC,i}$) has been defined in Equation 4.34.

$$dV_{TOT,i} = \int dV_{FC,i}(t)dt \tag{4.32}$$

$$k_{1,P} = k_{1,deg} \cdot dV_{TOT,i} + k_{2,deg} \tag{4.33}$$

$$SOH_{PEMFC,j} = (V_{ref,FC} - dV_{TOT,i})/V_{ref,FC} \tag{4.34}$$

In Equations 4.32 to 4.34 $dV_{TOT,i}$ is the cumulative loss of voltage, $k_{1,deg}$ and $k_{2,deg}$ are the linearization coefficients, $V_{ref,FC}$ is the reference maximum voltage for a novel single cell (voltage at the minimum current density $I_{FC,min}$). It has been assumed that k_{1FC} and k_{2FC} (see Equation 4.6) are not affected by the stack degradation $dV_{TOT,i}$. Therefore, when the power loss caused by degradation increases, the efficiency of the stack η_{FC} results to decrease. The stack efficiency is hence not included as a decision variable of the optimization problem, but it is evaluated as a result of the problem as in Equation 4.35.

$$\eta_{FC} = P_{FC,i}/F_{FC,i} \tag{4.35}$$

As for LIB operation, Equation 4.15 remains valid for the definition of the energy stored in the LIB at each time step according to the charging/discharging power $P^{\pm}_{LIB}$ and the relative efficiency η_{LIB}. The SOC of the battery is then calculated as the ratio between E_{LIB} and the energy capacity of the battery $E_{LIB,max}$ (Equation 4.36). The battery C-rate is determined as the ratio between the charging/discharging power of the battery and the battery capacity (Equation 4.37), and is set not to exceed the LIB manufacturer's limits (Equation 4.38). A constraint has been set on the SOC in the first time step of the day t_0 to make it correspond to the SOC at the end of the day T_{end} (Equation 4.39).

$$SOC(t) = E_{LIB}(t)/E_{LIB,max} \tag{4.36}$$

$$Crate^{\pm} = P^{\pm}_{LIB}(t)/E_{LIB,max} \tag{4.37}$$

$$|Crate^{\pm}| \leq Crate_{max} \tag{4.38}$$

$$SOC(t_0) = SOC(T_{end}) \tag{4.39}$$

As for LIB degradation, the most dominant ageing phenomenon of LIB is the formation of a SEI at the electrode/electrolyte interface. The thickness of SEI increases over time, leading to a progressive increase in the impedance of the battery and a consequent decrease in the battery capacity. Different degradation models are available in the literature, based either on electrochemical/equivalent circuit methods (*e.g.* SEI film thickness models and internal resistance models), or on empirical/semi-empirical methods (*e.g.* capacity fade models) [155] (see also Section 3.4.3 for further references on EESS degradation). In this thesis, it has been chosen to model the battery degradation over time with a capacity fade model, as such approach allows to limit the overall computational burden with respect to electrochemical models, allowing a comprehensive analysis of the entire system. As seen in Section 3.4 in the previous Chapter, battery ageing is commonly classified into two categories: calendar ageing and cycle ageing. Calendar ageing occurs when the battery is at rest condition, *i.e.* when no current is flowing through the battery. Calendar degradation rates depends on SOC and temperature. Cycle ageing occurs when the battery is charged or discharged, and depends on battery C-rate, SOC, temperature, number of performed equivalent cycles, and DOD [175, 174]. Here, the hybrid propulsion system has been considered to power a small-size ferry for public transport, which operates 24 hours, seven days a week (see power profile in Figure 4.2). Therefore, it is reasonable to assume that only cycle ageing occurs on the LIB. Nevertheless, to prevent an excessive calendar ageing of the battery in case of a prolonged stop of the vessel it has been decided to put a constraint on the SOC at the end of each day of operation (Equation 4.40). In this case, temperature does not exceed 30°C and hence the effect on calendar ageing is negligible. The reference SOC_{cal} has been set equal to 60%, according to data available in the literature [229].

$$SOC(T_{end}) = SOC_{cal} \tag{4.40}$$

Cycle ageing has been evaluated following the experimental studies available in [175] for a single cell. More in detail, in this case LFP chemistry has been chosen for LIB. Among different LIB chemistries, NMC and LFP batteries are addressed as the most mature technologies, but LFP are slightly better in terms of safety onboard [158]. As done for PEMFC, also in this case it has been considered the degradation of a single cell, representative for the whole battery. At each time step t of an operative day, T_{LIB} is expressed as linear function of $Crate$, with linearization coefficients $a_{1T,x}$ and $a_{2T,x}$ that depend on the ambient temperature (Equations 4.41 and 4.42). The capacity fade of

battery $Q_{LIB,loss}$ is then calculated as linear function of battery temperature T_{LIB} (Equation 4.43).

$$T_{LIB}(t) = a_{1T,x} \cdot Crate(t) + a_{2T,x} \tag{4.41}$$

$$a_{1T,x} = f(T_{amb,x}) a_{2T,x} = f(T_a mb, x) \tag{4.42}$$

$$Q_{LIB,loss}(t) = a_{1QT,j} \cdot T_{LIB}(t) + a_{2QT,j} \tag{4.43}$$

The time dependency of $Q_{LIB,loss}$ in the long-term operation has been taken into account by determining the linearization coefficients $a_{1QT,j}$ and $a_{2QT,j}$ in Equations 4.43 and 4.45 at each j month of the plant lifetime. In particular,$a_{1QT,j}$ and $a_{2QT,j}$ at the month j are evaluated as function of the energy throughput Ah_j at month j as reported in Equation 4.44.

$$a_{1QT,j} = k_{11,Ah} \cdot Ah_j^2 + k_{21,Ah} \cdot Ah_j + k_{31,Ah} \tag{4.44}$$

$$a_{2QT,j} = k_{12,Ah} \cdot Ah_j^2 + k_{22,Ah} \cdot Ah_j + k_{32,Ah} \tag{4.45}$$

Note that Equation 4.44 has not been formulated as MILP equation, since it is evaluated before starting the MILP optimization. The energy throughput Ah_j at month j is calculated as in Equation 4.46.

$$Ah_j = n_{days} \cdot N_{cycle,(j-1)} \cdot DOD \cdot Ah_{cell} \tag{4.46}$$

Where n_{days} is the number of days per month (assuming that all months have 30 days), $N_{cycle,(j-1)}$is the number of equivalent cycles performed by the battery during one day of operation, representative for the month $(j-1)$. N_{cycle} is determined via a rainflow algorithm. Ah_{cell} indicates the capacity of the single battery cell. DOD effect on the capacity fade has not been directly taken into account in the evaluation of $Q_{LIB,loss}$, since its effect on the capacity fade is negligible if compared to the cycling effect [175]. As for SOC effect, a constraint has been set (Equation 4.47) to limit the SOC-window of operation and hence further limit the degradation, as proposed for example in [230].

$$SOC_{min} \leq SOC(t) \leq SOC_{max} \tag{4.47}$$

At the end of each month j, it is determined the SOH of battery ($SOH_{LIB,j}$ in Equation 4.48).

$$SOH_{LIB,j} = (E_{LIB,max} - Q_{LIB,loss,j})/E_{LIB,max} \tag{4.48}$$

Phase 3: Uncertainty analysis of the optimal health-conscious operation of the hybrid PEMFC coastal ferry

A simplified schematic of the methodology is shown in Figure 4.5.

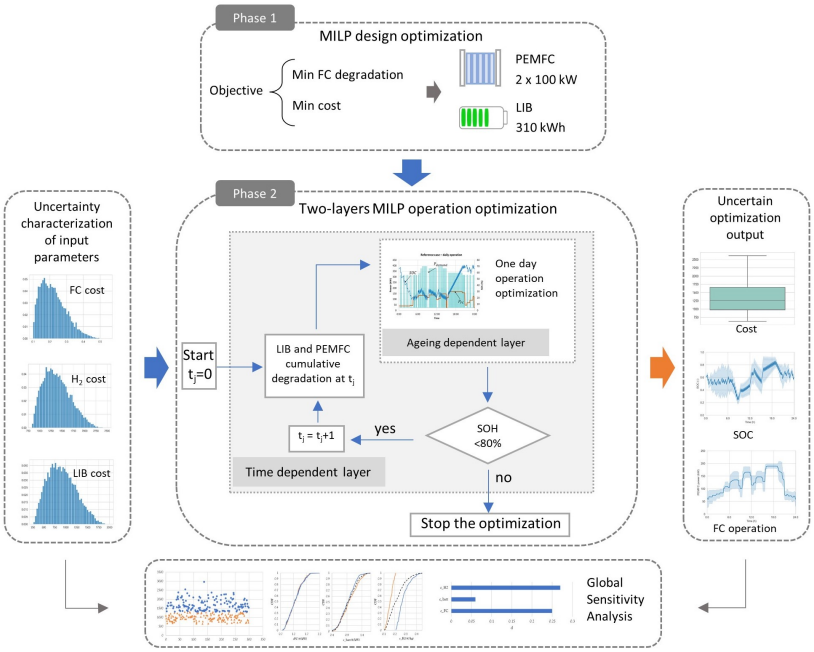

Figure 4.5: *Simplified schematic of the proposed methodology for the uncertainty analysis of the long term health-conscious operation of a hybrid PEMFC/LIB ferry. Retrieved from [191].*

Firstly, uncertainty characterization has been performed for the input parameters of the model, namely the cost of hydrogen fuel (c_{H2}), cost of LIB (c_{batt}) and cost of PEMFC (c_{FC}). Afterwards, multi-objective optimizations have been performed to find the optimal daily operation of the proposed hybrid ferry, following the two-layer optimization approach outlined in phase 2: an internal layer ("Ageing dependent layer") for the health-conscious operation optimization of one day representative of a specific month, and an external layer ("Time dependent layer") to evaluate the progressive degradation of PEMFC and LIB over the plant lifetime. Once either PEMFC or LIB have reached the EoL, the optimization is stopped. For each month, optimization results have provided information about (i) plant lifetime estimation, (ii) operation cost, and (iii) power flows in the representative days. Lastly, a sensitivity analysis has been conducted on the optimization outputs to identify the most influent input parameters. Uncertainty Characterization (UC) has been carried out to identify the uncertain parameters and to determine the probability associated with each value of the uncertain parameters [231]. For the specific case of maritime PEMFC/LIB powertrains fueled by hydrogen, three main uncertainties have been proposed, related to: cost of hydrogen fuel (c_{H2}), cost of LIB (c_{LIB}) and cost of PEMFC (c_{FC}). The uncertainties on the proposed input parameters have been evaluated by analyzing data avail-

able in the literature. Once the range of values that can be assumed by the input parameters has been determined, the data have been analyzed through a PERT distribution to assess the probability linked to each value. Among different probability functions, the PERT distribution has been chosen since it is often used to model experts' opinion [232], such for example data from technical reports, datasheets or research papers, and has already been used in similar analyses, as for instance in [233]. In fact, differently from uniform or triangular distribution, the shape of the PERT distribution is more similar to a normal distribution, with a smoother shape around the mode. PERT distribution has been defined for the three uncertain parameters by using the algorithm `pertdist` implemented in Python [220]. Such algorithm requires in input the lower and higher values assumed by the uncertain parameters, and the mode. Table 4.2 reports such values for the selected parameters, namely the hydrogen cost c_{H2}, the PEMFC stack cost c_{FC}, and the LIB cost c_{LIB}. The relative probability distributions of the parameters are shown in Figure 4.6. Both Table 4.2 and Figure 4.6 show a high variability of the parameters, demonstrating the importance of the analysis proposed in the study.

Table 4.2: *Characterization of uncertain parameters entering as input in the optimization model [191].*

Parameter	Unit	min	max	mode	mean	Refs.
c_{H2}	\$/kWh	0.12	0.55	0.20	0.25	[36, 234, 235, 236]
c_{FC}	\$/kW	830	2500	1000	1222	[20, 188, 212, 237, 238]
c_{LIB}	\$/kWh	400	2000	950	933	[158, 188, 164, 239, 240, 241]

The influence of uncertain input parameters on the optimization results has been evaluated by performing a Monte Carlo (MC) analysis over the energy system lifetime. At each MC iteration, uncertain parameters enter the optimization model as random numbers sampled among the ones that fall into the probability distributions linked to each parameter (see Figure 4.6). By increasing the number of the MC iterations, it is possible to cover as many combinations of uncertain parameters as desired, without the *a priori* definition of different scenarios. Once all the MC iterations have been completed, the results of the MILP optimization can be extrapolated with the relative degree of uncertainty, *i.e.* it can be evaluated the confidence through which it is possible to define the optimal operation of the plant. Considering the overall complexity of the optimization model, the number of MC iterations (n_{MC}) has been set equal to 300 for each month of the plant lifetime. The value of n_{MC}

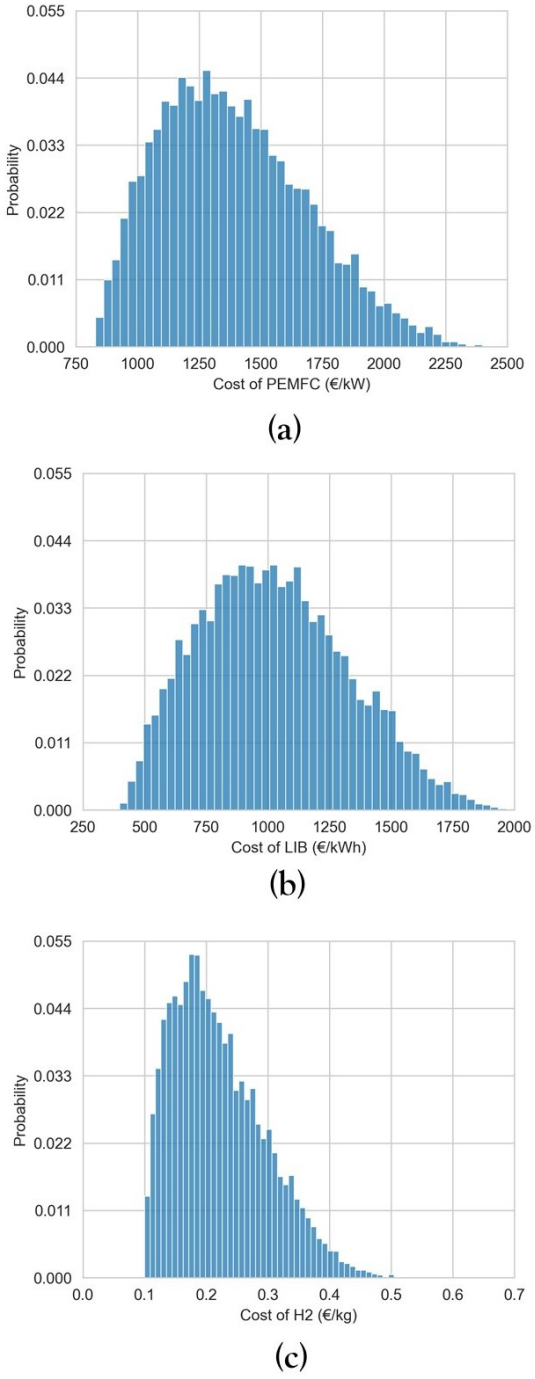

Figure 4.6: *PERT distributions of the uncertain parameters: (a) PEMFC cost (c_{FC}), (b) LIB cost (c_{LIB}), and (c) H_2 cost (c_{H2}).*

has been chosen to find a good compromise between the time required to solve the optimization problem and the convergence of results. This last aspect is dealt within the Appendix B.
As seen in the previous sections, the PEMFC rated power and the LIB capacity are fixed input parameters in the second phase optimization, according to the results of the phase 1 D&O optimization. Starting from these results, the MC iterations of the phase 2 optimization are run, considering the cost parameters in Equations 4.29, 4.30, and 4.31 as uncertain parameters. The objective functions of the optimization problems are still the ones defined for the phase 2 optimization (Equations 4.25, 4.26, and 4.27), linearly combined in a single-objective function (f_{MO} in Equation 4.28).
Once obtained the results of the MC iterations, a sensitivity analysis has been conducted to obtain an estimation of the parameters that mostly influence the optimization problem. Four methods are normally used to perform the sensitivity analysis: (i) local methods, (ii) regression-based methods, (iii) screening methods, and (iv) variance-based methods (or global methods) [242]. In this case, it has been chosen to perform a Global Sensitivity Analysis (GSA), as it allows to take into account the information linked to the stochasticity of input parameters. A Monte Carlo Filtering (MCF) has been performed through the application of the two-sample Kolgmogorov-Smirnov (KS) test. Such an approach has often been used for this type of problems as it allows to quantify how much a parameter influences the output of the problem [15,39]. The optimization results have been divided into two subsets: a behavioral subset B for the objective function results under the median, and a non-behavioral subset $\bar{B}$ for the objective function results above the median. Once obtained the B and $\bar{B}$ subsets of the MC results, each sample of the n_MC input parameters has been split into two subsets according to the associated B or $\bar{B}$ result , and the relative Cumulative Distribution Function (CDF) have been built and compared. The goal of this phase is to demonstrate or confute the null hypothesis formulated as: "Do the CDFs of the B and $\bar{B}$ subsets belong to the same distribution of the input parameter i?". Whenever the null hypothesis is demonstrated, the CDFs of the B and $\bar{B}$ subsets will appear similar, and the parameter will be flagged as non-influent for the model: each value of $x^{(i)}$ could equally result in B or $\bar{B}$ model output. On the contrary, if the CDFs of the B and $\bar{B}$ subsets are different, *i.e.* the null hypothesis is confuted, the parameter $x^(i))$ will be flagged as influent for the model, as some values of $x^{(i)}$ are more likely to return B outputs and others $\bar{B}$. To quantify the similarity between the twoCDFs, the KS-test requires the calculation of the parameter k, defined as in Equation 4.49.

$$k = max|F(x^{(i)})|B - F(x^{(i)})|\bar{B}| \tag{4.49}$$

Where $F(x^{(i)})|B$ and $F(x^{(i)})|\bar{B}$ are the CDFs of the B and $\bar{B}$ subsets, re-

spectively. Afterwards, the parameter k has been compared with the critical parameter D, defined as in Equation 4.50.

$$D = c(\alpha) \cdot \sqrt{(n_B + n_{\bar{B}})/(n_B n_{\bar{B}})} \tag{4.50}$$

Where n_B and $n_{\bar{B}}$ are the number of elements in the B and $\bar{B}$ subsets of the parameter $x^{(i)}$, and the constant $c(\alpha)$ is defined according to the significance level α as reported in [243]. Table 4.3 reports the values of D at different significance levels α.

Table 4.3: *Values of the critical parameter D for different significance levels α. The chosen values for the proposed GSA are reported in bold. [191].*

α	D
0.10	0.14
0.05	0.16
0.02	0.17
0.01	**0.19**

Whenever the parameter k is lower than or equal to D the parameter is defined as non-influent, while if k is higher than D the parameter is flagged as influent. In this study, the significance level α has been set to 0.01 to avoid incorrect estimations of the influent parameters, as suggested by [244]. Hence, the reference value of the critical parameter D to be considered in the GSA is 0.19.

4.2 On optimal integration of PEMFC and low temperature waste heat recovery in a cruise ship energy system

This section presents the methodology proposed to analyze how to integrate fuel cells in a complex ship energy system considering also PEMFC WHR. Firstly, the main characteristics and power demands of the cruise ship chosen as case study are outlined. Afterwards, it is presented the energy system layout proposed in this study, and the set of equations describing the optimization problem.

4.2.1 Main characteristics of the ship chosen as case study

The ship chosen as case study is a cruise ship operating in the Baltic Sea, similar to the one reported in Figure 4.7. The main characteristics of the ships, and the power demand data (mechanical, heating, electrical, and cooling power demand) for three typical days of different seasons have been retrieved from [245, 246]. Table 4.4 reports the main characteristics of the ship.

Figure 4.7: *Typical cruise ship similar to the one considered as case study. Image retrieved from [247].*

Table 4.4: *Main characteristics of the cruise ship chosen as case study. Data retrieved from [246, 245]*

Parameter	Value
Length x width	177m x 28m
Design speed	21 knots
N° of passengers	1800
Propulsion engines	4 x Wärtsilä 6L46 (7200 kW each)
Auxiliary engines	4 x Wärtsilä 6L32 (3480 kW each)
Yearly MDO consumption	9000 t

Power demand profile

The heating power demand retrieved from [246, 245] has been divided into three different temperature levels: Low Temperature (LT), Medium Temperature (MT), and High Temperature (HT). Table 4.5 reports the shares of the

heating power demand at the three temperature levels in the three seasonal conditions. The different shares have been determined in accordance with the typical energy requirements on board. Charts of the daily power demands are shown in Figure 4.8, while yearly power demands are obtained considering 182 winter days, 62 summer days, and 121 mid-season days (spring/fall) [245].

Table 4.5: *Typical shares of thermal power demand at the different temperature levels assumed for the simulations.*

Temperature level	Spring/fall	Winter	Summer
LT	60%	70%	50%
MT	32%	25%	40%
LT	8%	5%	10%

The proposed energy system

Figure 4.9 reports a simplified schematic of the base case layout of the ship energy system as proposed in [246], while a simplified schematic of the proposed ship energy system is represented in Figure 4.10. Base case layout includes ICE to cover the mechanical power demand (coupled with Gear Boxes (GB)), Compression Chiller (CC) the cooling demand, and High Temperature Heaters (HTH) the HT thermal demand. In Figure 4.10, components already included in the base case layout are represented with black boxes. New components modelled in this paper are represented with grey boxes and include: PEMFC for power and LT heat generation, LIB for storing electric energy, Low Temperature Heaters (LTH) to supply LT thermal power, Low Temperature Thermal Storage (LTTS) and Medium Temperature Thermal Storage (MTTS), AB-Sorption Chiller (ABSC) for supplying cooling power, medium Temperature Heat Pump (MTHP) to supply MT thermal power, and High Temperature Heat Pump (HTHP) for supplying HT thermal power. As for the HTH (*i.e.* boilers for the production of steam at 120°C), although they were already included in the base case layout, it has been considered here the possibility of substituting them with smaller HTH or with HTHP, and are hence represented here in grey.

4.2.2 The optimization problem

As previously seen, the MILP approach is appropriate for the optimization of complex energy systems [217, 218, 219], and hence it has been chosen to adopt such approach to develop and solve the optimization problem proposed

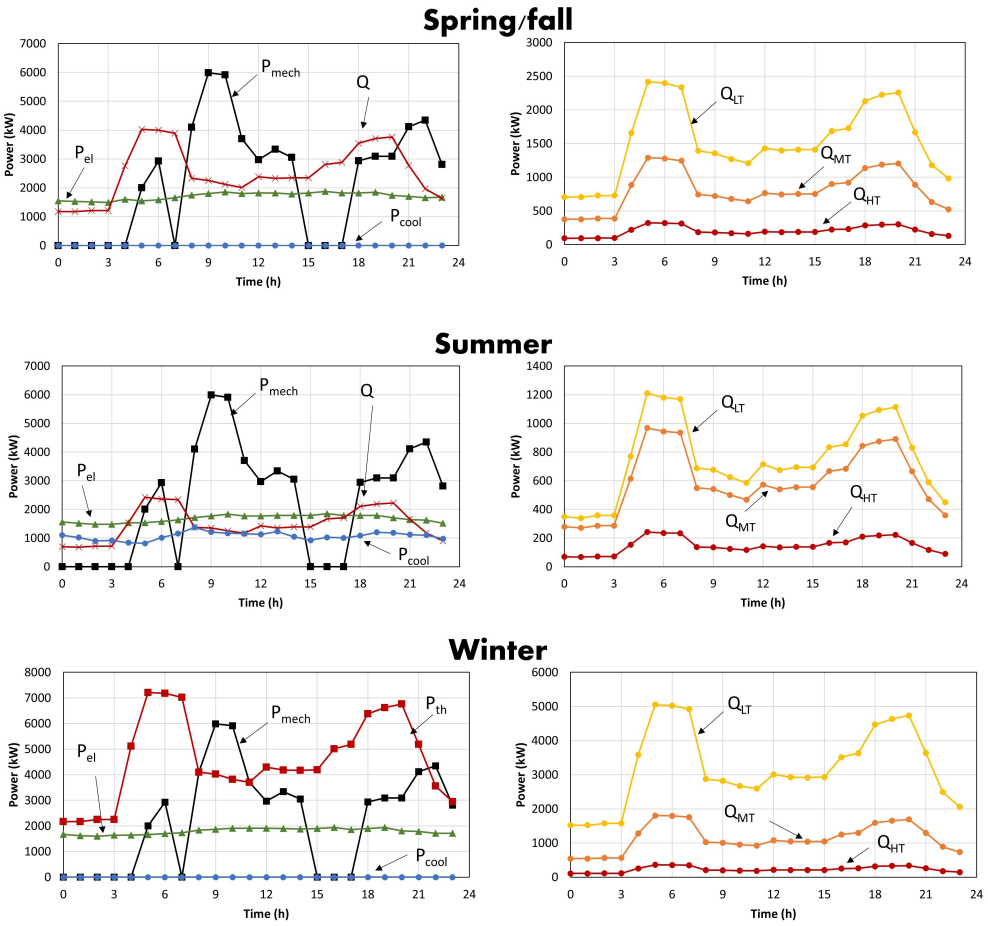

Figure 4.8: *Power demand profiles of the typical operating days in the different seasons. Charts on the left side report the mechanical (P_{mech}), the electrical (P_{el}), the cooling (P_{cool}), and the total heating (Q) power demands. The charts on the right side report the heating power demand divided into the three temperature levels: low temperature (Q_{LT}), medium temperature (Q_{MT}), and high temperature thermal power demand (Q_{HT}). Elaborated from [246, 245].*

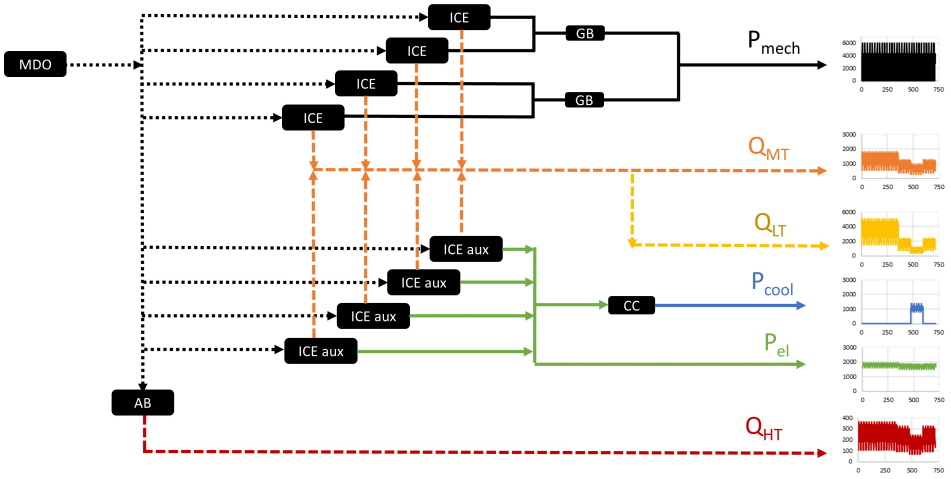

Figure 4.9: *Base case layout of the cruise ship energy system. Elaborated from [246].*

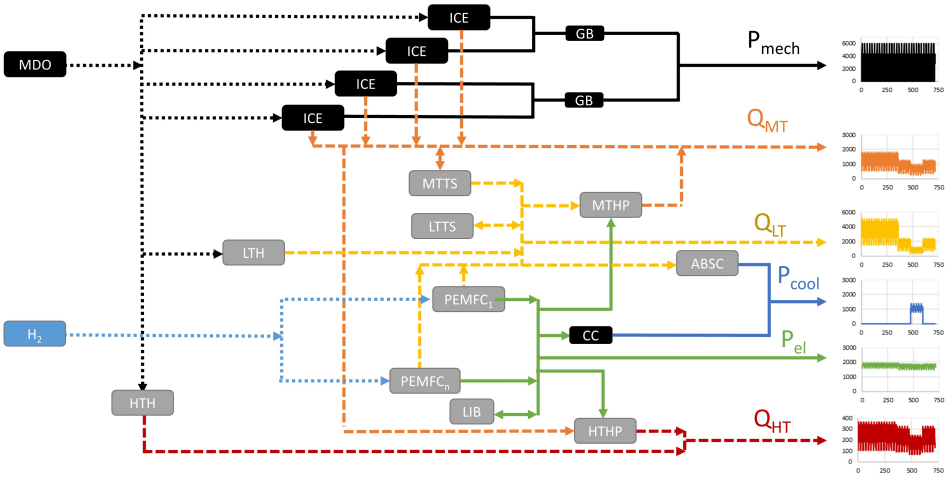

Figure 4.10: *Simplified schematic of the proposed ship energy system. Black boxes indicate the components that were already encompassed in the base case layout of the ship energy system reported in [246]. Grey boxes indicate the components that may be added to the system, according to the optimization results.*

hereafter. As previously seen in Equations 4.1 to 4.3 (reported here below for the sake of clarity in Equations 4.51, 4.52, and 4.53), the MILP optimization problem aims to find the optimum values of the continuous variables $x^*(t)$ and binary variables $\delta^*(t)$ that maximize or minimize the objective function Z (Equation 4.51). The variables are limited by equality constraints $g(t)$ (Equation 4.52 and inequality constraints $h(t)$ (Equation 4.53), which make up the model of the ship energy system. As for optimization models in Section 4.1.2, also in this case the models have been developed in Python programming language [220] and solved with Gurobi Optimizer [221].

$$Z = f(x^*(t), \delta^*(t)) \tag{4.51}$$

$$g(x^*(t), \delta^*(t)) = 0 \tag{4.52}$$

$$h(x^*(t), \delta^*(t)) \leq 0 \tag{4.53}$$

Objective functions

The optimization model has been set as a multi-objective optimization for the concurrent minimization of both MDO consumption (f_1 in Equation 4.54) and investment and operation cost (f_2 in Equation 4.55).

$$f_1 = \int_t F_{ICE}(t)dt + \int_t F_{AH}(t)dt \tag{4.54}$$

$$\begin{aligned} f_2 = (\int_t (F_{ICE}(t)dt) + \int_t F_{AH}(t) \cdot dt) \cdot c_{MDO} + (\int_t (F_{FC}(t)dt)) \cdot c_{H2} + \\ (\int_t (P_{comp,\alpha}(t)dt)) \cdot c_{comp,\alpha} + D_{comp,\beta} \cdot c_{comp,\beta,capex} \end{aligned} \tag{4.55}$$

In Equation 4.55, $P_{comp,\alpha}$ is the power output (electrical, mechanical, heating or cooling) of the generic component α, multiplied by the maintenance cost $c_{comp,\alpha}$. $D_{comp,\beta}$ is the optimal size of the generic new component β, multiplied the relative investment cost $c_{comp,\beta,capex}$. As for the phase 1 optimization of Section 4.1.2, also in this case the multi-objective optimization problem has been solved adopting a *hierarchical objective* approach, with different priorities assigned to each objective function. Here, the highest priority has been assigned to f_1 in Equation 4.54, which is hence optimized first. Secondly, the Gurobi [221] solver optimizes the objective function f_2, choosing among the solutions that do not degrade the objective f_1 more than a certain relative tolerance, fixed here at 3%.

Main engines for mechanical propulsion

The entire mechanical power demand of the ship for propulsion is assumed to be supplied by four ICE, *i.e.* keeping the ICE currently installed onboard the ship (4× Wärtsilä 6L46 [248]). Based on the performance data of the

ICE [248, 246], MILP equations describing fuel consumption, heat and power production of each i-th ICE in different load conditions have been defined as reported in Equations 4.56 to 4.58.

$$F_{ICE,i}(t) = k_{1ICE} \cdot P_{ICE,i} + k_{2ICE} \cdot \delta_{ICE,i}(t) \tag{4.56}$$

$$Q_{ICE,i}(t) = k_{3ICE} \cdot P_{ICE,i} + k_{4ICE} \cdot \delta_{ICE,i}(t) \tag{4.57}$$

$$load_{ICE,min} \cdot P_{ICE}^{MAX} \leq P_{ICE,i}(t) \leq load_{ICE,max} \cdot P_{ICE}^{MAX} \tag{4.58}$$

Equation 4.56 expresses the fuel consumption $F_{ICE,i}$ of the i-th ICE as linear function of the mechanical power output level $P_{ICE,i}$ according to the linearization coefficients k_{1ICE} and k_{2ICE}. Equation 4.57 expresses the thermal power output $Q_{ICE,i}$ of the i-th ICE according to the mechanical power output $P_{ICE,i}$. It is assumed that $Q_{ICE,i}$ can be directly used to supply MT heat (see Figure 4.10). In both equations, $\delta_{ICE,i}$ is the binary variable that defines the on/off status of the i-th ICE. It should be noticed that the four ICEs are all included because already installed onboard, and hence no binary variable appears in Equation 4.58. At each time step, the power output of the i-th ICE is constrained not to exceed the maximum and minimum ICE power load $load_{ICE,max}$ and $load_{ICE,min}$, expressed as percentages of the rated power P_{ICE}^{MAX}.

PEMFC for auxiliary electric power

In the proposed configuration it is assumed that the four auxiliary ICE of the base-case configuration of the ship (4 x Wärtsilä 6L32 [249]) are substituted by PEMFC, which provide electrical power to the ship auxiliaries and from which heat can be partially recovered for supplying thermal power to the LT heat circuit of the ship. As in the case of ICE, PEMFC design and operation are described by MILP equations starting from the characteristic curve of a PEMFC stack efficiency at different loads [222]. n_{FC} groups of PEMFC stacks can be installed onboard considering that each group allows the separate power generation as typically required as safety measure for onboard ship installation. It has been assumed that all the PEMFC stacks of each group work under the same load conditions. Equations4.59 to 4.62 report the MILP equations describing the performance of each i-th group of PEMFC stacks.

$$F_{FC,i}(t) = k_{1FC} \cdot P_{FC,i} + k_{2FC} \cdot \delta_{FC,i}(t) \tag{4.59}$$

$$Q_{FC,i}(t) = k_{3FC} \cdot P_{FC,i} + k_{4FC} \cdot \delta_{FC,i}(t) \tag{4.60}$$

$$load_{FC,min} \cdot P_{FC}^{MAX} \leq P_{FC,i}(t) \leq load_{FC,max} \cdot P_{FC}^{MAX} \tag{4.61}$$

$$n_{FC} = \sum_{i} \Delta_{FC,i} \tag{4.62}$$

Hydrogen consumption at time t for the i-th group of PEMFC stacks is expressed by $F_{FC,i}$ in Equation 4.59 as linear function of the power output $P_{FC,i}$ by using the linearization coefficients k_{1FC} and k_{1FC}. Similarly, the low temperature waste heat from te PEMFC $Q_{FC,i}$ is expressed in Equation 4.60 as a linear function of the PEMFC power $P_{FC,i}$ by means of the linearization coefficients k_{3FC} and k_{4FC}. Inequality constraints in Equation 4.61 are set to limit the power generated by the i-th group from the minimum $load_{FC,min}$ to the maximum $load_{FC,max}$ power load expressed as percentage of the rated power P_{FC}^{MAX}. $\delta_{FC,i}$ in Equation 4.59 is the binary variable that defines the on/off status of the PEMFC stacks in the i-th group, while $\Delta_{FC,i}$ in Equation4.61 is the binary variable defining the inclusion/exclusion of the i-th group. The sum of the binary variables $\Delta_{FC,i}$ is the optimal number of PEMFC groups to install onboard (Equation 4.62). It should be noticed that in this case degradation of PEMFC was not taken into account to avoid excessive computational effort.

Compression chiller

A CC is included in the system for supplying the cooling power demand of the ship over the year. Equations 4.63 and 4.64 report the MILP equations describing the design and operation of the CC at each time step.

$$F_{CC,i}(t) = k_{1CC} \cdot P_{CC,i} + k_{2CC} \cdot \delta_{CC}(t) \tag{4.63}$$

$$CC_{min} \cdot P_{CC}^{MAX} \cdot \Delta_{CC} \leq P_{CC,i}(t) \leq CC_{max} \cdot P_{CC}^{MAX} \cdot \Delta_{CC} \tag{4.64}$$

Where $F_{CC,i}$ and $P_{CC,i}$ are the power input to run the CC (power required by the compressor) and the cooling power output, respectively. k_{1CC} and k_{2CC} are the linearization coefficients, evaluated on the basis of the CC characteristic curve [246]. At each time step, $P_{CC,i}$ is constrained not to exceed the minimum and maximum power load, as shown in Equation 4.64, where CC_{min} and CC_{max} are the minimum and maximum load limits of the CC, and P_{CC}^{MAX} is the maximum installed power of the CC. It should be noticed that despite the base case layout already encompasses a CC, it is here chosen to include a binary variable Δ_{CC} that allows the optimization model to decide whether to include the CC or not. In this way, it is possible to evaluate whether it is more convenient to substitute the CC with an ABSC. Equations describing the design and operation of the ABSC are reported in the next section.

Absorption chiller

It is considered the possibility to include an ABSC to recover the LT waste heat and use it to generate cooling power. A Lithium-Bromide (LiBr) ABSC has been considered, as this technology is already available for its use in ship

applications [250]. Equations 4.65 and 4.66 describe the design and operation of the ABSC.

$$F_{ABSC}(t) = COP_{ABSC} \cdot P_{ABSC}(t) \cdot \delta_{ABSC}(t) \tag{4.65}$$

$$ABSC_{min} \cdot P_{ABSC}^{MAX} \cdot \Delta_{ABSC} \leq P_{ABSC}(t) \leq ABSC_{max} \cdot P_{ABSC}^{MAX} \cdot \Delta_{ABSC} \tag{4.66}$$

Where F_{ABSC} is the LT power input to run the ABSC, COP_{ABSC} is the coefficient of performance of the ABSC, P_{ABSC} is the cooling power output of the ABSC, and δ_{ABSC} is the binary variable describing the on/off status of the ABSC. COP_{ABSC} has been evaluated as function of the temperature of the available heat source, *i.e.* the temperature of the LT thermal power circuit in this case, according to the data available in [250]. As for the other components, also for ABSC the power output is constrained according to the minimum and maximum power load $ABSC_{min}$ and $ABSC_{max}$, expressed as function of the total installed power P_{ABSC}^{MAX} of the ABSC. Lastly, Δ_{ABSC} is the binary variable that identifies the inclusion or not of the ABSC in the system.

Thermal energy storage

Two Termal Storage (TS)s can be encompassed in the system: a LTTS and a MTTS. The former can receive heat from the LT thermal power circuit, to which it can later release heat when needed. The latter can receive heat from the MT thermal power circuit, and can release it both to LT thermal power circuit and to the MT thermal power circuit. Both LTTS and MTTS consist in thermocline tanks in which hot and cold water are stored in the upper and lower part, respectively. As suggested by [219], the thermal energy contained in a TS unit has been expressed as the total volume of hot water stored assuming constant values of the higher and lower water temperatures in the tank ($T_{TS,hot}$ and $T_{TS,cold}$, respectively), density (ρ_{TS}), and specific heat ($c_{p,TS}$). Equations4.67 to4.72report the constraints of the optimization model that describe the behaviour of the LTTS and MTTS.

$$\begin{aligned} V_{LTTS}(t) = V_{LTTS}(t-1) + 1/(\rho_{TS} \cdot c_{p_{TS}} \cdot (T_{LTTS,hot} - T_{LTTS,cold})) \\ \cdot(\eta_{TS} \cdot F_{LTTS}(t) - (Q_{LTTS}(t))/\eta_{TS}) \end{aligned} \tag{4.67}$$

$$TS_{min} \cdot V_{LTTS}^{max} \leq V_{LTTS}(t) \leq TS_{max} \cdot V_{LTTS}^{max} \tag{4.68}$$

$$V_{LTTS}(0) = V_{LTTS}(T) \tag{4.69}$$

$$\begin{aligned} V_{MTTS}(t) = V_{MTTS}(t-1) + 1/(\rho_{TS} \cdot c_{p_{TS}} \cdot (T_{MTTS,hot} - T_{MTTS,cold})) \\ \cdot(\eta_{TS} \cdot F_{MTTS}(t) - (Q_{MTTS}(t))/\eta_{TS}) \end{aligned} \tag{4.70}$$

$$TS_{min} \cdot V_{MTTS}^{max} \leq V_{MTTS}(t) \leq TS_{max} \cdot V_{MTTS}^{max} \tag{4.71}$$

$$V_{MTTS}(0) = V_{MTTS}(T) \tag{4.72}$$

More in detail, Equations 4.67 and 4.70 express the volume of water stored in the LTTS and MTTS at each time step t. A sort of thermal efficiency η_{TS} has been included to account for possible heat losses in the process. F_{TS} (with subscripts LTTS or MTTS depending on which TS is considered) is the thermal power entering the TS, while Q_{TS} is the thermal power output of the storage. It can be noticed in Equation 4.70 that both LT and MT thermal power can be drawn from the MTTS, namely $Q_{MTTS,LT}$ and $Q_{MTTS,MT}$. In both LTTS and MTTS, the volume of stored water is constrained not to exceed the upper and lower limit of the possible storage volume of the tank, expressed as percentage TS_{min} and TS_{max} of the total tank volume V_{LTTS}^{max} and V_{MTTS}^{max} (Equations 4.68 and 4.71). Lastly, a constraint (Equation 4.69 and 4.72) is set to ensure that the water volume stored at the first time step (time 0) is equal to the water volume at the last time step (time T).

Lithium-ion battery

PEMFC are considered to be coupled with EESS, which allow to limit the installed capacity of PEMFC onboard and also guarantee that PEMFC operate in optimal load conditions [81]. As previously seen in Chapter 3, LIB have higher energy densities in comparison with other types of batteries, and allow to store larger energy capacities with respect to, for example, supercapacitors [158], and are hence considered in the present study. The design and operation of LIB is described by Equations 4.73, 4.74, and 4.75.

$$E_{LIB}(t) = E_{LIB}(t-1) - (F_{LIB}(t))/(\eta_{LIB}) + P_{LIB}(t) \cdot \eta_{LIB} \tag{4.73}$$

$$SOC_{min} \cdot E_{LIB}^{MAX} \leq E_{LIB}(t) \leq SOC_{max} \cdot E_{LIB}^{MAX} \tag{4.74}$$

$$E_{LIB}(0) = E_{LIB}(T) \tag{4.75}$$

Where E_{LIB} is the electrical energy stored in the LIB at each time step, F_{LIB} is the discharge power, P_{LIB} is the charge power, η_{LIB} is the charging/discharging efficiency, SOC_{min} is the minimum SOC of the LIB, SOC_{max} is the maximum SOC, and E_{LIB}^{MAX} is the installed of the LIB. As done for TSs, also for LIB it is set that the energy stored at the first time step (time 0) is equal to the one at the last time step (time T) (Equation 4.75). As seen for PEMFC, also for LIB the degradation was not taken into account in the model to avoid excessive computational effort.

Water-water heat pumps

Two types of water-water heat pumps are considered: (i) a MTHP that operates between the LT thermal power circuit and the MT thermal power circuit, and (ii) a HTHP operating between the MT and the HT thermal power circuits. For both MTHP and HTHP the operation at each time step has been

described by the constraints reported in Equations 4.76 to 4.78 with the reference to a generic heat pump (subscript Heat Pump (HP)).

$$F_{HP}(t) = COP_{HP} \cdot P_{HP}(t) \cdot \delta_{HP}(t) \tag{4.76}$$

$$Q_{HP}(t) = (COP_{HP} - 1)/COP_{HP} \cdot P_{HP}(t) \cdot \delta_{HP}(t) \tag{4.77}$$

$$HP_{min} \cdot P_{HP}^{MAX} \cdot \Delta_{HP} \leq P_{HP}(t) \leq HP_{max} \cdot P_{HP}^{MAX} \cdot \Delta_{HP} \tag{4.78}$$

Where F_{HP} is the input electric power at the compressor of the HP, COP_{HP} is the Coefficient Of Performance (COP) of the HP, set in accordance with datasheets of available products and literature models [251, 252, 253], P_{HP} is the thermal power output at the condenser of the HP (MT thermal power for the MTHP and HT for the HTHP), δ_{HP} is the binary variable determining the on/off status of the HP, and Q_{HP} (Equation 4.77) is the thermal power input at the HP evaporator (LT thermal power for the MTHP and MT for the HTHP). In Equation 4.78 HP_{min} and HP_{max} are the minimum and maximum load percentages of the HP rated power P_{HP}^{MAX}, respectively. The inclusion or the exclusion of the HP is expressed by the binary variable Δ_{HP}.

Auxiliary heaters

From the simulation model standpoint, two types of Auxiliary Heater (AH)s can be encompassed in the system: HTH (*i.e.* boilers, here referred to as heaters for the sake of simplicity) and LTH. While the former are already encompassed in the base case layout and supply heat to the HT thermal power circuit, the latter can been included in the system in case the heat recovered from the PEMFC at LT is not sufficient/not convenient (*e.g.* would imply too large hydrogen consumption). The operation of both HTH and LTH is described as reported in Equations 4.79 and 4.80, where a generic subscript AH is reported.

$$F_{AH}(t) = k_{1AH} \cdot P_{AH}(t) + k_{2AH} \cdot \delta_{AH}(t) \tag{4.79}$$

$$AH_{min} \cdot P_{AH}^{MAX} \cdot \Delta_{AH} \leq P_{AH}(t) \leq AH_{max} \cdot P_{AH}^{MAX} \cdot \Delta_{AH} \tag{4.80}$$

F_{AH} is the fuel consumption of the AH, determined as linear function of the thermal power output P_{AH} according to the linearization coefficients k_{1AH} and k_{2AH}, and δ_{AH} is the binary variable describing the on/off status of the AH. k_{1AH} and k_{2AH} have been determined according to the performance characteristic available in [246]. In Equation 4.80, AH_{min} and AH_{min} are the minimum and maximum power load of the AH, P_{AH}^{MAX} is the AH installed power, and Δ_{AH} is the binary variable for the inclusion/exclusion of the AH from the system.

Power balances and volume constraint

In the following, the five power balances are reported in Equations4.81 to 4.86. More in detail, Equation 4.81 reports the mechanical power balance, Equation 4.82 reports the electrical power balance, Equation 4.83 reports the cooling power balance, Equations 4.84, 4.85, and 4.86 report the LT, MT, and HT thermal power balance, respectively.

$$P_{mech}(t) = \eta_{GB} \cdot \eta_{shaft} \cdot \sum_i P_{ICE,i}(t) \cdot \delta_{ICE,i}(t) \tag{4.81}$$

$$\begin{aligned} P_{el}(t) + P_{LIB}(t) + F_{CC}(t) \cdot \delta_{CC}(t) + F_{MTHP}(t) \cdot \delta_{MTHP}(t) + \\ F_{HTHP}(t) \cdot \delta_{HTHP}(t) = F_{LIB}(t) + \eta_{freqconv} \cdot \eta_{el} \cdot \sum_i P_{FC,i}(t) \cdot \delta_{FC,i} \end{aligned} \tag{4.82}$$

$$P_{cool}(t) = P_{CC}(t) \cdot \delta_{CC}(t) + P_{ABSC}(t) \cdot \delta_{ABSC}(t) \tag{4.83}$$

$$\begin{aligned} Q_{LT}(t) + F_{ABSC}(t) \cdot \delta_{ABSC}(t) + Q_{HTHP}(t) \cdot \delta_{MTHP}(t) + F_{LTTS} = \\ = \sum_i Q_{FC,i}(t) \cdot \delta_{FC,i}(t) + Q_{LTTS}(t) + P_{LTH}(t) \cdot \delta_{LTH}(t) + Q_{MTTS,LT}(t) \end{aligned} \tag{4.84}$$

$$\begin{aligned} Q_{MT}(t) + F_{MTTS}(t) + Q_{HTHP}(t) \cdot \delta_{HTHP}(t) = \\ P_{MTHP}(t) \cdot \delta_{MTHP}(t) + sum_i Q_{ICE,i}(t) + Q_{MTTS,MT}(t) \end{aligned} \tag{4.85}$$

$$Q_{HT}(t) = P_{HTH}(t) \cdot \delta_{HTH}(t) + P_{HTHP}(t) \cdot \delta_{HTHP}(t) \tag{4.86}$$

Where η_{GB} is the efficiency of the GB, η_{shaft} the efficiency of the shaft, η_{el} the efficiency of the electrical engine, $\eta_{freqconv}$ the efficiency of the frequency converters [246]. Lastly, a constraint has been set to ensure that the volume occupied by the additional power components installed on board (*i.e.* the ones not included in the base case layout) does not exceed the total volume occupied by the auxiliary ICEs (4 x Wärtsilä 6L32 [249]), increased by 10% (equal to 185.4 m^3). It should be noticed, however, that the volume of the hydrogen tank has not been included in such constraint, as hydrogen tanks are usually installed on the top deck to ensure sufficient ventilation [254].

Chapter 5

Results and discussion

In this section, the main results of the optimization models are presented and discussed for both the case studies outlined in Section 4. It should be noticed that some of the content reported hereafter may not be original content, but reproduced and/or adapted from previously published papers of the author during the course of the PhD. In particular, part of the contents in this section may have been reproduced or adapted from the following publications:

- **Dall'Armi, C.**, Micheli, D., Taccani, R. (2021). Comparison of different plant layouts and fuel storage solutions for fuel cells utilization on a small ferry. International Journal of Hydrogen Energy 46, 13878-13897. doi.org/10.1016/j.ijhydene.2021.02.138.

- Pivetta, D., **Dall'Armi, C.**, Taccani, R. (2021). Multi-objective optimization of hybrid PEMFC/Li-ion battery propulsion systems for small and medium size ferries. International Journal of Hydrogen Energy 46(72), 35949-35960. doi.org/10.1016/j.ijhydene.2021.02.124.

- **Dall'Armi, C.**, Pivetta, D., Taccani, R. (2021). Health-conscious optimization of long-term operation for hybrid PEMFC ship propulsion systems. Energies 14, no. 13:1813. https://doi.org/10.3390/en14133813.

- **Dall'Armi, C.**, Pivetta, D., Taccani, R. (2022). Uncertainty analysis of the optimal health-conscious operation of a hybrid PEMFC coastal ferry. International Journal of Hydrogen Energy 47(21), 11428-11440. doi.org/10.1016/j.ijhydene.2021.10.271.

- **Dall'Armi, C.**, Pivetta, D., Taccani, R. (2022). On optimal integration of PEMFC and low temperature waste heat recovery in a cruise ship energy system, ECOS 2022 - Proceedings of the 35th International Conference on Efficiency, Cost, Optimization, Simulation and Environmental Impact of Energy System, Copenhagen 3-7 July 2022, Denmark.

5.1 Hybrid PEMFC/LIB ferry: health-conscious energy management strategy

In this Section are presented and discussed the results of the optimization model described in Chapter 4, Section 4.1.2. While the proposed methodology has general validity, the specific case of a small size ferry has been chosen as case study, as reported in Section 4.1.1. The complete list of the parameters set for solving the optimization model is reported in Table 5.1. As for uncertain cost parameters, Table 5.1 reports here the mean values of the PERT distributions (see Figure 4.6), which have been used to find the optimal design of the ferry energy system.

Table 5.1: *Input parameters for the optimizations. Costs of FC, hydrogen, and LIB reported in the table refer here to the mean values of the PERT distribution characterizing the uncertain parameters.*

Parameter	Unit	Value	Refs.
c_{H2}	€/kWh	0.25	[36, 234, 235, 236]
c_{LIB}	€/kWh	933	[158, 188, 164, 239, 240, 241]
c_{FC}	€/kW	1222	[20, 188, 212, 237, 238]
Δv_{load}	$\mu V/kW$	0.0441	[188, 184, 148]
ΔP_{FC}	%	10	Assumed
Δv_{st-up}	$\mu V/cycle$	23.91	[188, 184, 148]
η_{LIB}	%	95	Assumed
F_{start}	%	10	Assumed
$I_{FC,max}$	A/cm^2	600	[150]
$I_{FC,min}$	A/cm^2	75	[150]
$k_{1,deg}$	$\mu V cm^2/A$	0.243	[188, 184, 148]
$k_{2,deg}$	μV	0.159	[188, 184, 148]
$k_{1,FC}$	$kWcm^2/A$	0.354	[148, 150, 226]
$k_{2,FC}$	kW	3.837	[148, 150, 226]
$k_{11,Ah}$	$1/KAh^2$	$-7.1 \cdot 10^{-9}$	[175, 229, 230]
$k_{21,Ah}$	$1/KAh$	$2.2 \cdot 10^{-4}$	[175, 229, 230]
$k_{31,Ah}$	$1/K$	0.033	[175, 229, 230]
$k_{12,Ah}$	$1/KAh^2$	$2.1 \cdot 10^{-6}$	[175, 229, 230]
$k_{22,Ah}$	$1/KAh$	-0.48	[175, 229, 230]
$k_{32,Ah}$	$1/K$	-8.885	[175, 229, 230]
SOC_{min}	%	20	[230]
SOC_{max}	%	90	[230]
V_{LIB}	m^3/kWh	0.0091	[158]
V_{FC}	m^3/kW	0.0313	[212]
V_{H2}	$m^3/kgH2$	0.025	[212]

Continued on next page

Table 5.1 – continued from previous page

Parameter	Unit	Value	Refs.
w_{LIB}	kg/kWh	8	[158]
w_{FC}	kg/kW	20	[212]
w_{H2}	kg/kg_{H2}	2.5	[212]
V_{max}	m^3	15.5	[80]
w_{max}	kg	7185	[80]

5.1.1 Optimal design and operation over a typical day of operation of the ferry

As for the optimal design of the hybrid PEMFC/LIB powertrain, by applying the phase 1 of the methodology, proposed in [190], with mean values of the uncertain input parameters c_{H2}, c_{FC}, and c_{batt} (reported in Table 4.2) it results an optimal size of 200 kW for PEMFC and 310 kWh for LIB. Such design has been used as input in the phase 2 and phase 3 optimizations. From the phase 1 optimization over one day of operation of the ferry it is also possible to retrieve the optimal operation of the plant, reported in Figure 5.1. If looking at the PEMFC operation, it results that for about 71% of time the PEMFC tend to avoid the operation at high power rates in order to avoid higher degradation rates, lower efficiency, and hence higher hydrogen consumption rates. However, for about 29% of time the operation of PEMFC at nominal power is allowed to avoid the increase of the LIB size, and hence costs. Lastly, from Figure 5.1 it can be observed how PEMFC avoid frequent load changes and/or start ups, as such operation would also increase their degradation rate, hence worsening the objective function.

5.1.2 Plant lifetime and daily operation cost

After determining the optimal design of the hybrid PEMFC/LIB power plant, iterative optimizations of the model have been run to analyze how the plant behaves during the entire lifetime (see phase 2 and phase 3 of the methodology in Section 4.1.2). More in detail, the estimation of the plant lifetime has been retrieved from the phase 3 optimization model outputs with reference to the average values of SOH_{FC} and SOH_{LIB}, calculated as the average value of the results obtained from the n_{MC} MC iterations of the phase 3 optimization model. Figure 5.2 shows the average SOH of PEMFC and LIB, and the average cost over the entire lifetime of the plant. It can be noticed that the proposed plant can operate for 23 consecutive months, *i.e.* 690 days. After this time, both PEMFC (black dots in Figure 5.2) and LIB (white dots in Figure 5.2)

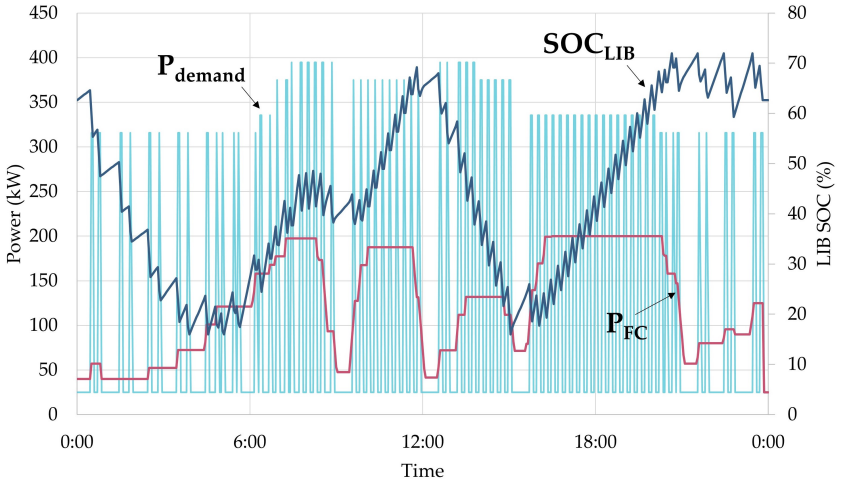

Figure 5.1: *Optimal operation of the ferry during a typical day. For each time step, the propulsion and auxiliary power demand of the ferry P_{demand}, the power output of PEMFC P_{FC}, and the SOC of the LIB SOC_{LIB} are reported.*

reach a SOH of 80% and hence the EoL. Contextually, from Figure 5.2 it can be inferred that the average operative cost of the ferry (diamonds in Figure 5.2) tends to increase, reaching a daily average cost at the 23^{rd} month that is about 16% higher than the daily operational cost at the 1^{st} month. Moreover, it should be noticed that the increase in the average cost has a non-linear trend (solid line in Figure 5.2). This is mainly due to the progressive decrease of PEMFC efficiency over their lifetime, and hence to the increase of the hydrogen consumption. The latter, increases by up to about 30% from the beginning to the end of the plant lifetime, from an average value over a typical operation day in the first month of 178 kg_{H2}/day to 233 kg_{H2}/day at the 23^{rd} month. It is important to stress that such aspect would influence not only the operation cost of the ferry, but also the design of the on board energy system in terms of volume occupied by the hydrogen tank. In the proposed analysis a constraint in the optimization model ensured that the overall volume of the energy system (including the hydrogen tank one) does not exceed te volume occupied by the traditional ICE-based energy system (see Equation 4.24). Further analyses on the volume required by the hydrogen storage system for different hydrogen storage types and in different scenarios can be found in the publication by the author [80], where a comparison with the traditional power system is also proposed.

As for costs, it is also interesting to see how the uncertainty on the input parameters affects the optimization model outputs. Figure 5.3 reports the boxplots of the objective function as retrieved from the n_{MC} MC iterations. The boxes contain the central 50% of cost distribution resulting for the n_{MC}

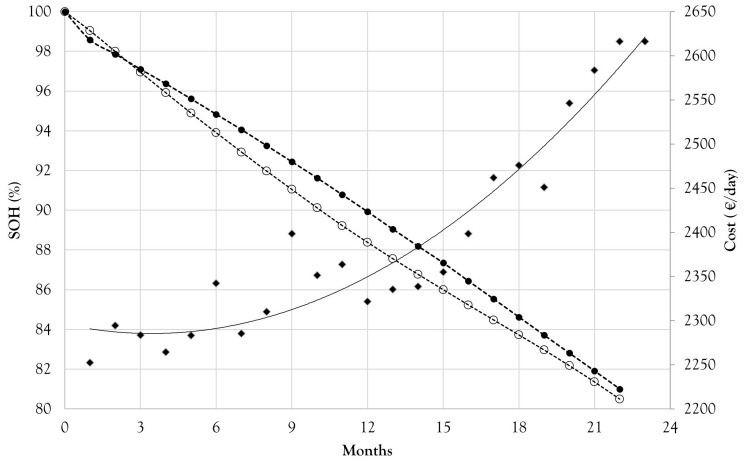

Figure 5.2: *Average daily operative cost (⧫) of the ferry over the entire plant lifetime, average SOH of LIB (○) and average SOH of PEMFC (●) over the plant lifetime. Average values have been calculated on the basis of the n_{MC} results of the MC iterations of the optimization model.*

optimization at each month. In other words, boxes extend from the first (25%) to the third quartile (75%) of each sample. The average values are represented by the solid lines in the boxes. The dots indicate the outliers, and the lines outside the boxes extend from the lower to the upper limit of the samples. In addition to the tendency of costs to increase over the plant lifetime already discussed, Figure 5.3 points out how the objective function results are affected by the variability of the input parameters. It can be observed that variability on the optimization results appears to increase with the progressive ageing of the plant. At the beginning of the plant lifetime, the central 50% of cost results are spread in a 500 € range, while at the end this amplitude increases by up to about 1000 € range. By knowing this trend in advance, it will be possible to take risk-aware decisions on the installation of this type of plant.

5.1.3 Optimal operation of batteries and fuel cells over the entire lifetime

As previously described for operation costs, the proposed methodology also allows to have an outlook on the variability of the optimal operation of the hybrid powertrain over the plant lifetime. Figure 5.4 reports the SOC of LIB over one typical day of operation, representative of one month. Similarly, Figure 5.5 shows the PEMFC power in a typical day. In both Figure 5.4 and Figure 5.5, the solid lines represent the average values of either SOC or P_{FC} at each time-step, while the light-blue areas indicate the uncertainty linked to the calculated values, expressed in terms of standard deviation, as

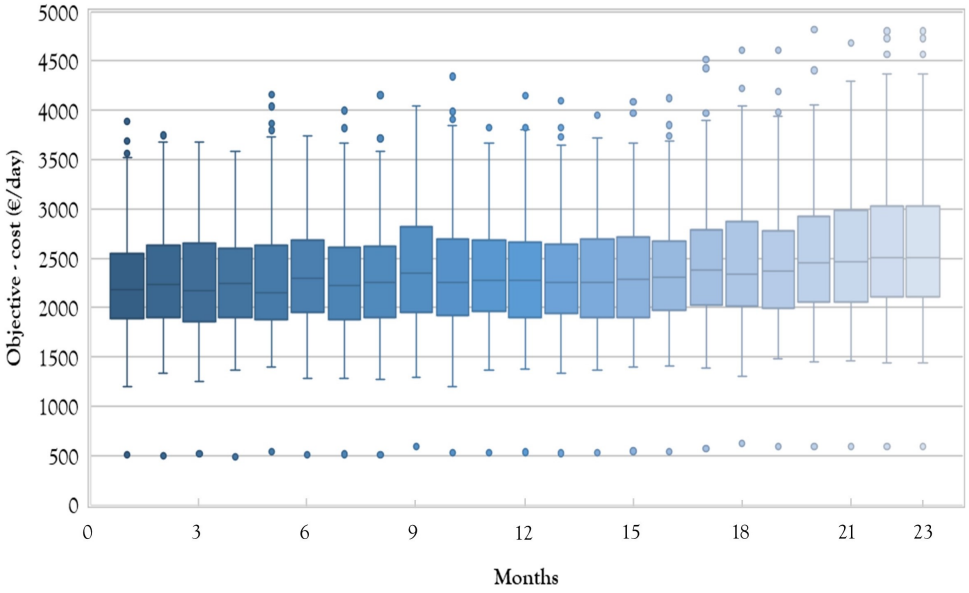

Figure 5.3: *Results of the operational cost of the ferry over the entire plant lifespan. Boxplots extend from the first quartile (25%) to the third quartile (75%) of the n_{MC} cost results obtained by the MC iterations of the optimization model for each month. Solid lines in the boxes represent the average cost at each month. Solid lines outside the boxes extend from the lower to the upper limit of the samples, and dots indicate the outliers.*

resulting from the n_{MC} values of the variables at each time-step. For the sake of simplicity in the graphical representations, results have been reported only for nine over 23 months of operation. For both LIB and PEMFC, it can be noticed that the variability in the optimal operation is higher at the beginning of the plant lifetime. It is interesting to notice that this trend is opposite to the one of the operation cost. For example, at the first month different input parameters can lead to even substantially different optimal operations of the plant, but this does not reflect in a high variability of the overall operation cost (Figure 5.3). In fact, at the beginning of the plant lifetime, the PEMFC are not degraded and hence can operate at high efficiency. As a consequence, even large variations in the cost of hydrogen would not cause large variations in the resulting cost. Also, at the first month both PEMFC and LIB are new, and hence the degradation rate is lower than the one at EoL: different operational pathways would hence not result in largely different cost outputs in terms of costs associated to the degradation rates. On the contrary, looking at the 23^{rd} month (*i.e.* the last month of operation), it can be seen that the optimal operation does not have a large variability despite the variability of input parameters. Nevertheless, the aged PEMFC have lower efficiency, and hence even a small variation in the hydrogen cost in input can result in a large variation of the operational cost. To better justify what said till now, the next section presents the GSA.

5.1.4 Global sensitivity analysis of optimization results

In order to identify the input parameters that influence the most the optimization results, the GSA has been conducted for every month. For each month, the n_{MC} results of the operational cost have been divided into two subsets: a behavioral subset B for costs under the median and a non-behavioral subset $\bar{B}$ for costs above the median. The results of this first step of the GSA have been reported for the first month in Figure 5.6 as an example, but similar results have been obtained for each month. Once obtained the B and $\bar{B}$ subsets of the objective functions, the corresponding samples of uncertain input parameters have been divided accordingly, and CDF have been derived for each parameter. Figure 5.7 shows the CDF of the behavioral and non-behavioral subsets of the uncertain parameters c_{FC}, c_{batt} and c_{H2} for the first, 10^{th} and 23^{rd} months. More in detail, the orange lines indicate the CDF of the input parameter values which led to cost result in the B subset, while the blue lines indicate the CDF of the input parameter values which led to cost result in the $\bar{B}$ subset. For each parameter, values of the k indicator (Equation 4.49 in Chapter 4) are reported in the boxes. It can be noticed that for all the months the most influent parameter is the cost of hydrogen c_{H2}, while c_{FC} and c_{batt} have k values that are similar to the critical value D (0.19). Moreover, the

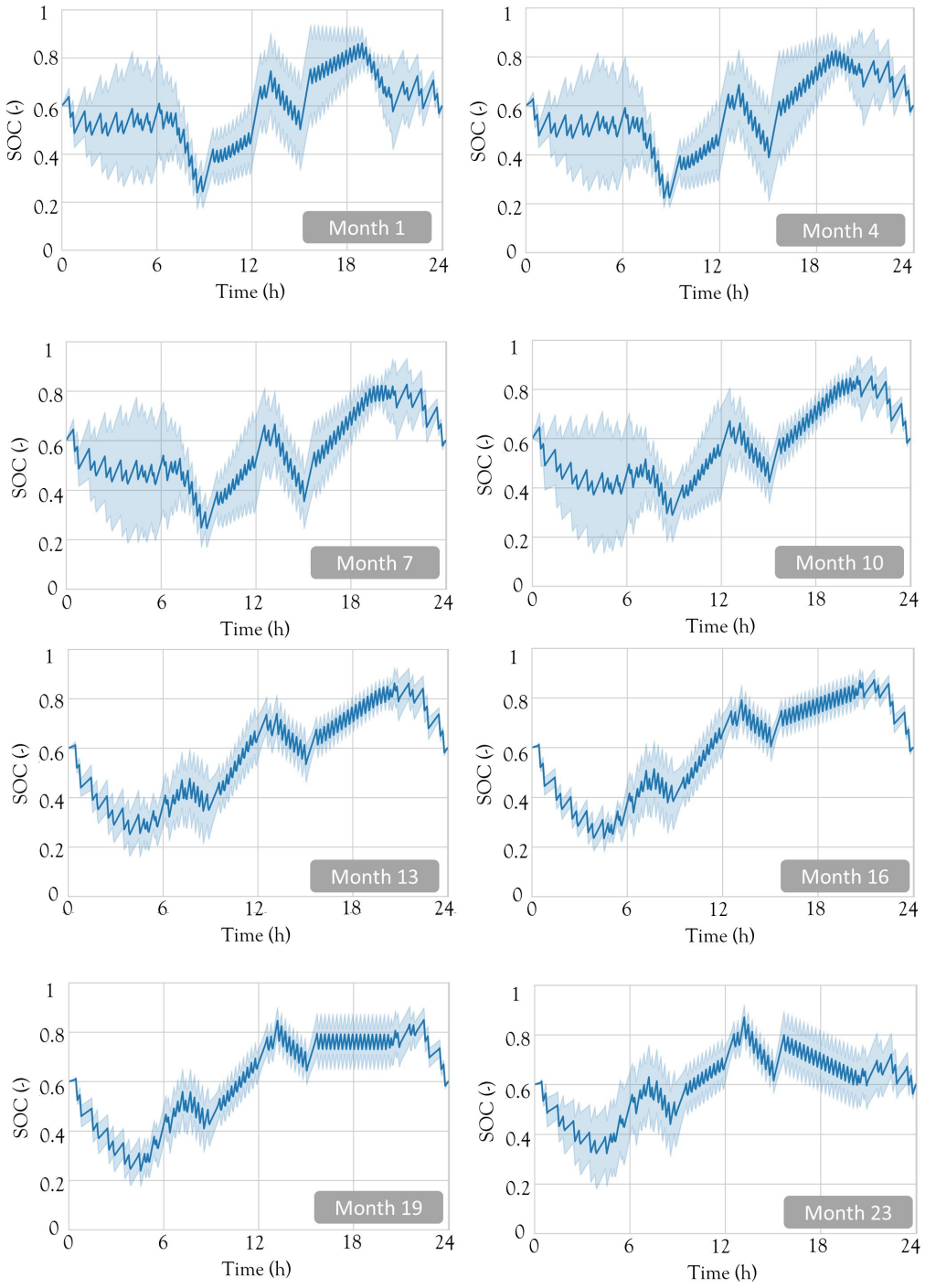

Figure 5.4: *Optimal SOC of LIB over a typical day of operation, representative of each month. Solid line represents the average value of SOC at each time-step. Light-blue area indicates the uncertainty linked to the calculated value, expressed in terms of standard deviation, as resulting from the n_{MC} values of the variables at each time-step.*

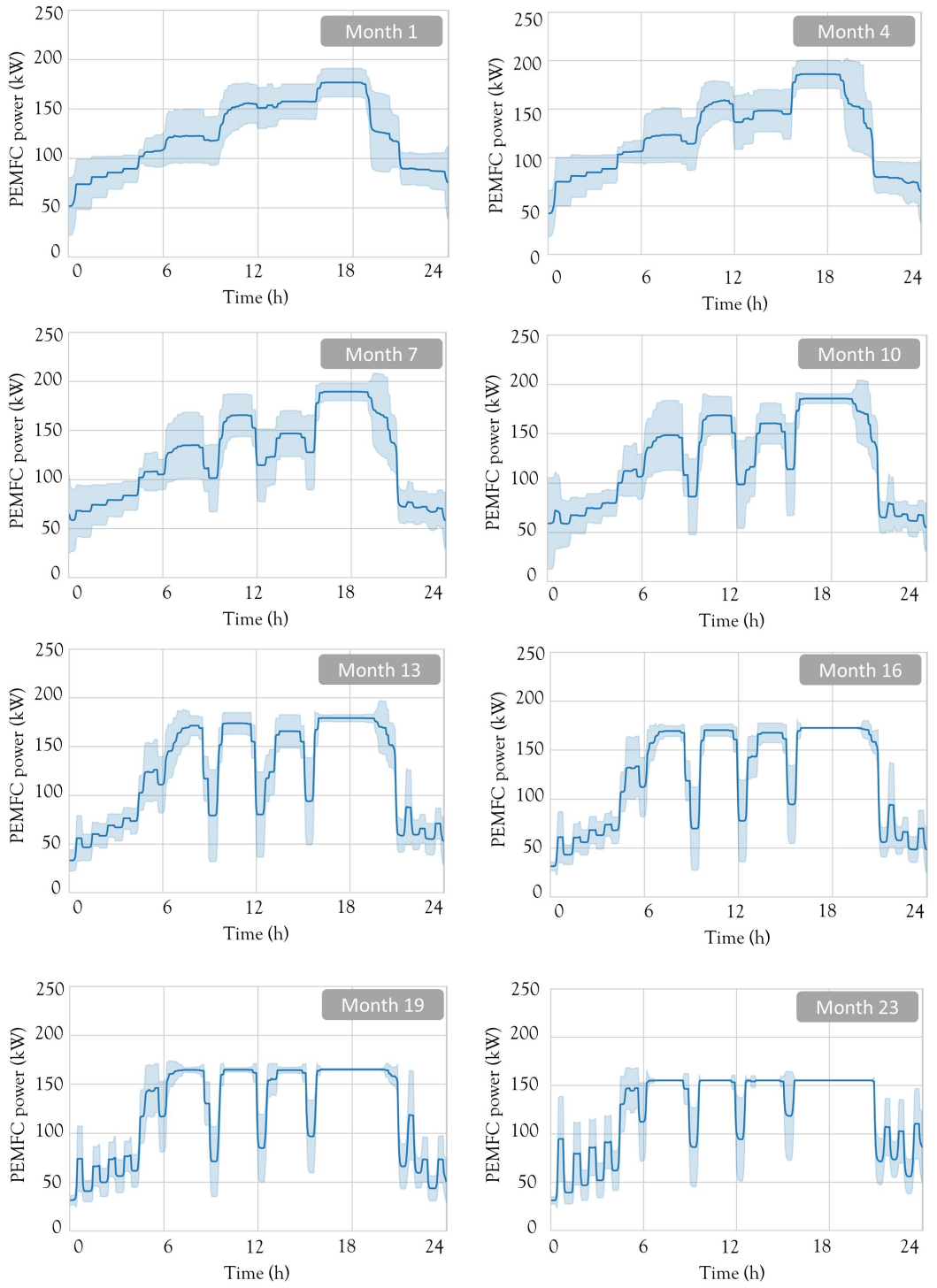

Figure 5.5: *Optimal PEMFC power over a typical operation day, representative of each month. Solid line represents the average value of P_{FC} at each time-step. Light-blue area indicates the uncertainty linked to the calculated value, expressed in terms of standard deviation, as resulting from the n_{MC} values of the variables at each time-step.*

analysis throughout the whole plant lifetime also points out that the influence of c_{H2} on the objective function increases with the passing of time (higher values of k). This is due to the progressive performance degradation of the plant, in particular the PEMFC degradation, that causes a decrease in the average efficiency and hence an increase in the consumption of hydrogen per day. Such considerations also explain the increase of costs with the passing of time, as seen in Section 5.1.2.

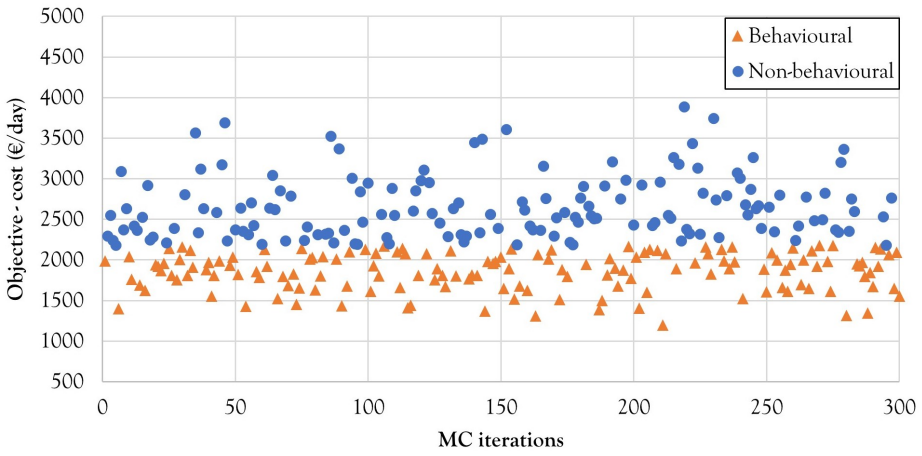

Figure 5.6: *Results of the MC filtering for the first month of vessel operation. Orange triangles indicate the behavioral subset of the n_{MC} cost results (cost below the median). Blue dots represent the cost results of the non-behavioral subset (cost above the median).*

5.2 On optimal integration of PEMFC and low temperature waste heat recovery in a cruise ship energy system

In this section, the main results of the optimization model outlined in Section 4.2.2 are presented and discussed. Also in this case, although the developed methodology has general validity, it is here applied to a cruise ship chosen as case study, as described in Section 4.2.1. Table 5.2 reports the complete list of parameters set to solve the optimization model. To limit the overall computational effort required for the yearly optimization of the whole energy systems, the optimization has been run for a representative month, composed by a number of typical winter, summer, and mid-season days (see Figure 4.8) that reflects the shares of the seasons over the entire year. In this case, the year was composed by 182 winter days, 62 summer days, and 121 mid-season days

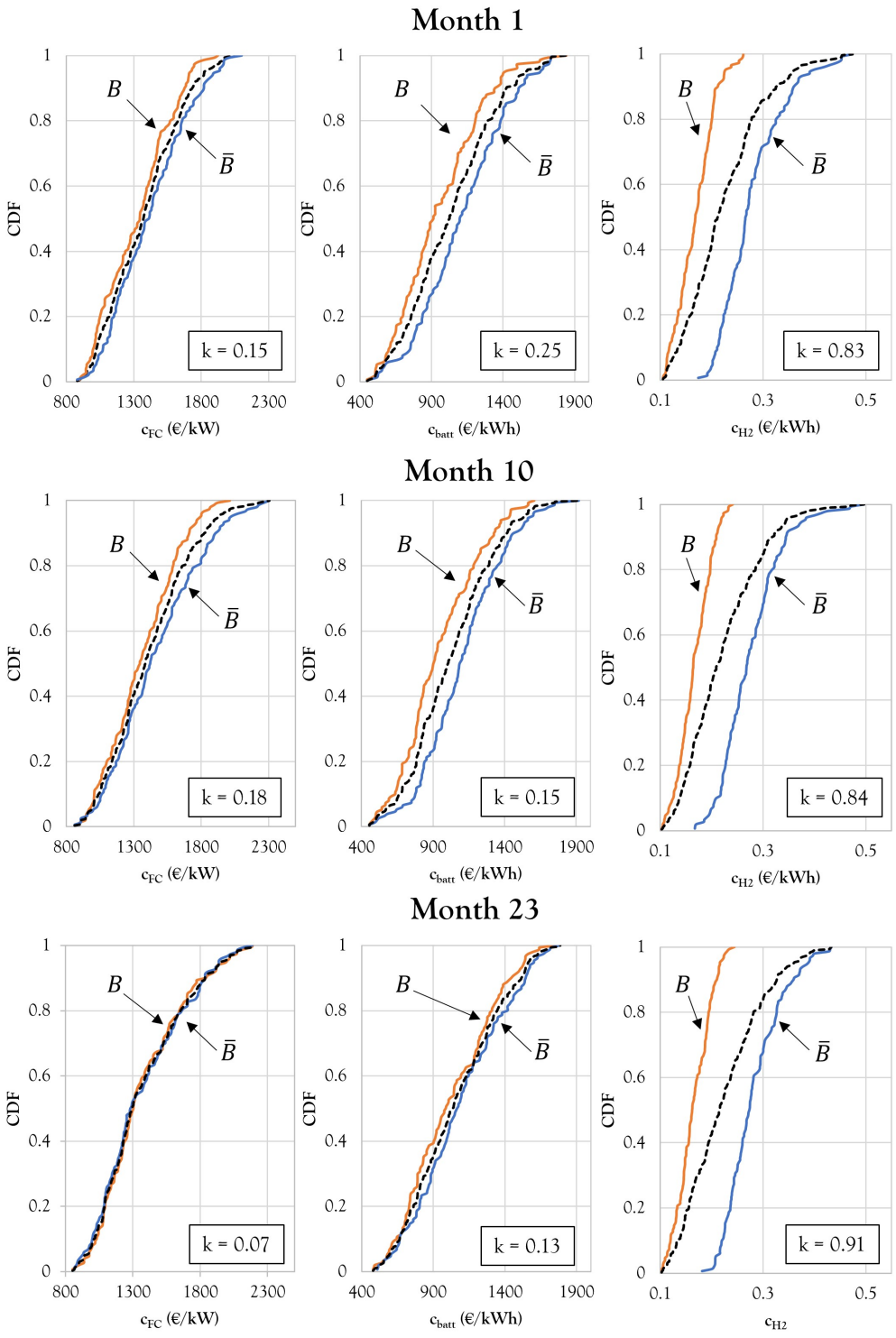

Figure 5.7: *GSA results for* 1^{st}, 10^{th} *and* 23^{rd} *months of operation. The orange lines represent the cumulative distribution functions of the input parameter values which led to cost result in the B (behavioral) subset. The blue lines indicate the cumulative distribution functions of the input parameter values which lead to cost result in the* $\bar{B}$*(non-behavioral) subset. The dashed black lines represent the cumulative distribution functions of the entire sample of the input parameters.*

[246], corresponding to about 50%, 17%, and 33% of the whole year duration, respectively. Considering a 30-day month, the subdivision among the seasons results in 15 winter days, 5 summer days, and 10 mid-season days. A 4% gap on the optimal results has been set for the optimizations, and a 3% relative tolerance has been allowed on the first priority objective (see Section 4.2.2). In the next sections are reported the optimization parameters set to solve the model, the results in terms of the energy system synthesis and design, and the results in terms of optimal operation of the plant.

Table 5.2: *Input parameters for the optimization.*

Parameter	**Unit**	**Value**	**Refs.**
$c_{FC,capex}$	€/kW	1250	[20, 188, 212, 237, 238]
$c_{LIB,capex}$	€/kWh	933	[158, 188, 164, 239, 240, 241]
$c_{AH,capex}$	€/kW	25	[255]
$c_{ABSC,capex}$	€/kW	300	[256]
$c_{TS,capex}$	€/m^3	17.1	[219]
$c_{MTHP,capex}$	€/kW	400	[257]
$c_{HTHP,capex}$	€/kW	60	[257]
c_{MDO}	€/kWh	0.0843	[37]
c_{H2}	€/kWh	0.25	[36, 234, 235, 236]
$c_{ICE,main}$	€/kWh	0.015	[246]
c_{AH}	€/kWh	0.006	[246]
c_{CC}	€/kWh	0.005	[246]
c_{FC}	€/kWh	0.1	Assumed
c_{LIB}	€/kWh	0.1	Assumed
c_{ABSC}	€/kWh	0.0025	[246]
c_{MTHP}	€/kWh	0.02	Assumed
c_{HTHP}	€/kWh	0.04	Assumed
k_{1ICE}	1/kW	2.162	Calculated
k_{2ICE}	kW	482.7	Calculated
k_{3ICE}	1/kW	0.9386	Calculated
k_{4ICE}	kW	445.2	Calculated
P_{ICE}^{MAX}	kW	5850	[248]
$load_{ICE,min}$	-	0.3	Assumed
$load_{ICE,max}$	-	0.9	Assumed
k_{1FC}	1/kW	2.5023	Calculated
k_{2FC}	kW	-440.65	Calculated
k_{3FC}	1/kW	1.5023	Calculated
k_{4FC}	kW	-440.65	Calculated
P_{FC}^{MAX}	kW	2000	Assumed
$load_{FC,min}$	-	0.1	Assumed
$load_{FC,max}$	-	0.95	Assumed
V_{FC}	m^3/kW	0.03125	[212]

Continued on next page

Table 5.2 – continued from previous page

Parameter	Unit	Value	Refs.
k_{1CC}	$1/kW$	0.2841	Calculated
k_{2CC}	kW	69.181	Calculated
P_{CC}^{MAX}	kW	2000	Assumed
$load_{CC,min}$	-	0	Assumed
$load_{CC,max}$	-	0.9	Assumed
COP_{ABSC}	-	0.67	[246]
P_{ABSC}^{MAX}	kW	4217	[258]
$load_{ABSC,min}$	-	0	Assumed
$load_{ABSC,max}$	-	0.95	Assumed
η_{TS}	%	98	[219]
ρ_{TS}	kg/m^3	1000	-
$c_{p_{TS}}$	kWh/kg	0.00162	-
$T_{LTTS,hot}$	K	318.15	Assumed
$T_{LTTS,cold}$	K	298.15	Assumed
$T_{MTTS,hot}$	K	343.15	Assumed
$T_{MTTS,cold}$	K	318.15	Assumed
TS_{min}	-	0.1	[219]
TS_{max}	-	0.9	[219]
η_{LIB}	%	95	Assumed
SOC_{min}	-	0.2	Assumed
SOC_{max}	-	0.9	Assumed
V_{LIB}	m^3/kWh	0.0091	[158]
COP_{MTHP}	-	4.22	[251]
P_{MTHP}^{MAX}	kW	590.3	[251]
$MTHP_{min}$	-	0.2	Assumed
$MTHPmax$	-	0.9	Assumed
COP_{HTHP}	-	3	[253]
P_{HTHP}^{MAX}	kW	590.3	Assumed
$HTHP_{min}$	-	0.2	Assumed
$HTHP_{max}$	-	0.9	Assumed
k_{1AH}	$1/kW$	1.3293	Calculated
k_{2AH}	kW	-22.188	Calculated
P_{AH}^{MAX}	kW	1125	Assumed
AH_{min}	-	0.05	Assumed
AH_{max}	-	0.9	Assumed
$V_{ICE,aux}$	m^3	42.1	[249]
η_{GB}	%	98	[246]
η_{gen}	%	97	[246]
η_{el}	%	96	[246]
$\eta_{freqconv}$	%	98	[246]
η_{shaft}	%	98	[246]

5.2.1 Optimal design, costs, and fuel consumption

Figure 5.8 reports the optimal synthesis of the system as resulting from the solution of the optimization problem, while detailed data on the components' sizes, operation and investment costs, and on the fuel consumption are reported in Table 5.3. From Figure 5.8 and Table 5.3 it can be noticed that LTTS and the ABSC are not encompassed in the optimal design of the ship energy system. With regard to the LTTS, it should be noticed that the optimal system of the plant includes a MTTS tank of about 60 m^3 capacity, which can also cover the LT heat demand. Hence, it is not convenient to invest on a LTTS. As for the ABSC, in this case it is not convenient to install it as the system already encompasses a CC for covering the cooling power demand. In fact, although an ABSC could guarantee higher amounts of heat recovered, the seasonal characteristics of the ship power demand, *i.e.* only 5% summer days, does not justify such additional investment. With reference to the other components, it can be retrieved from Table 5.3 that the optimal configuration of the ship energy system encompasses both MTHPs (2 x 590.3 kW) and HTHPs (1 x 590.3 kW), as in this way it is possible to fulfill the ship heating demand at MT and HT, while reducing the MDO consumption, *i.e.* the primary objective of the optimization. The electrical power demand of the ship, including the additional electrical power demand from HPs, is supplied by 4 MW of PEMFC.

Table 5.3: *Optimization results: synthesis and design data of the main components of the plant, CAPEX, and OPEX.*

Variable name	**Units**	**Value**
PEMFC installed power	MW	4
LIB installed capacity	kWh	76.6
HTH installed capacity	kW	0
LTH installed capacity	kW	3 x 1125
CC installed power	kW	2000
ABSC installed power	kW	0
LTTS capacity	m3	0
MTTS capacity	m3	59.6
MTHP installed power	kW	2 x 590.3
HTHP installed power	kW	1 x 590.3
CAPEX	M€	9.0
OPEX	M€/year	14.9
MDO consumption	ton/year	4032
H_2 consumption	ton/year	1104

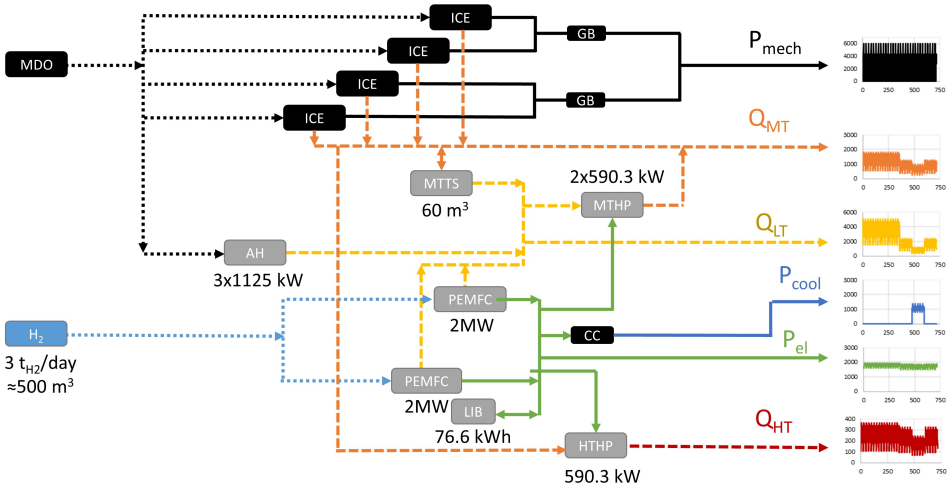

Figure 5.8: *Optimal synthesis of the proposed cruise ship energy system. Black boxes indicate the components that were already encompassed in the base case layout, grey boxes indicate the components that should be included in the energy system according to the results of the proposed multi-objective optimization. The value of the hydrogen consumption per day and the relative volume refer to the average value calculated from the cumulative consumption over the representative month.*

The new energy system results in a total CAPital EXpenditure (CAPEX) of about 9 M€. From Figure 5.9, which reports the shares of the components' investment costs on the overall CAPEX, it can be noticed that PEMFC are responsible for about 89% of the global CAPEX, as they are, today, the technology with the highest cost (see Table 5.2). Future reductions in the investment cost of PEMFC will hence have a strong impact on the overall CAPEX of this type of energy systems. In addition, it should be noticed that such CAPEX only refers to the investment costs of the single components, while installation costs, costs linked to the additional pipes and connections that may be needed on board, and certification costs for marine use of the components, are not included in the proposed calculations. Such additional costs may indeed contribute to a sensible increase in the estimated costs, and hence further analyses should investigate also these aspects.

With reference to the OPerational EXpenditure (OPEX), the new system results to have a global OPEX of about 15 M€/year. From the breakdown of the energy system's OPEX reported in Figure 5.10, it can be retrieved that hydrogen fuel is responsible of the 55% of the total OPEX. While it is evident that a reduction of hydrogen fuel costs in the future could positively impact the results, it should also be noticed that such a trend may be even strengthen in the future if penalties on the use of fossil fuels and further restrictions on

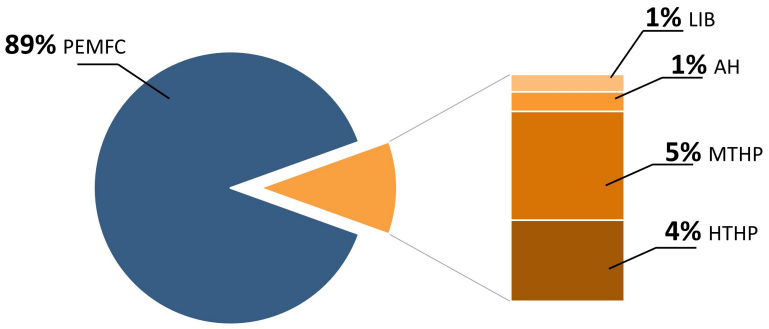

Figure 5.9: *Breakdown of the total CAPEX (9 M€) as resulting from the multi-objective optimization over the representative month.*

pollutant and GHG emissions will be imposed. In facts, it can be observed in Figure 5.10 that a remarkable share (29%) of the OPEX is referred to the MDO consumption, which amounts to about 4032 ton/year. Of these, only the 7% is consumed by LTH, while the rest is related to the ICE for propulsion. This aspect highlights that although the proposed system allows to reduce the MDO consumption by about 53% with respect to the base case layout (Figure 4.9), to achieve higher decarbonization rates it is necessary to act also on the propulsion side.

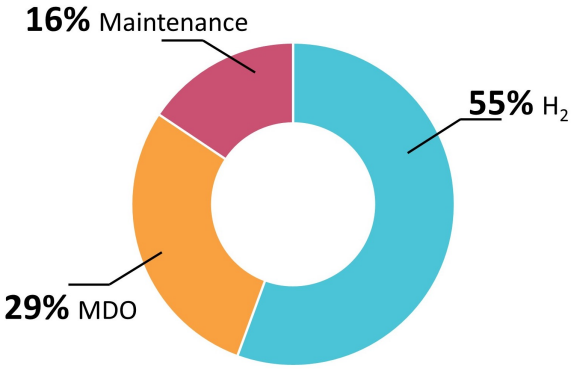

Figure 5.10: *Breakdown of the total OPEX (14.9 M€/year) as resulting from the multi-objective optimization over the representative month.*

5.2.2 Optimal operation

Figure 5.11 reports the optimal operation of the ship power plant with reference to electrical power (Figure 5.11 on the top) and LT heating power demand and supply (Figure 5.11 on the bottom). Looking at the plot on the top part of Figure 5.11 it can be noticed that the electrical power supply, *i.e.* the power

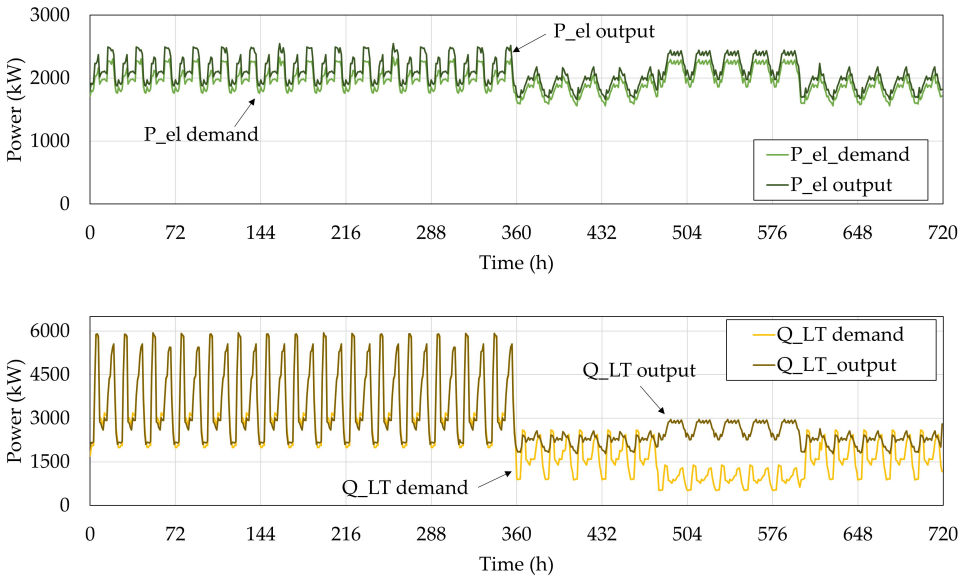

Figure 5.11: *Electrical power demand and supply part (top plot) and LT heating power demand and supply (bottom plot) over the representative month.*

output from the PEMFC, fulfills the ship electrical needs at each time step of the simulation, generally avoiding the operation at full power load (*i.e.* 4 MW) as this would decrease their efficiency and hence increase the operation costs related to hydrogen consumption. Moreover, it can be observed that for most of the time the electrical power demand on board is exceeded, as PEMFC must also contribute to the LT heating power supply. In fact, as reported in the bottom plot of Figure 5.11, it can be noticed how the PEMFC operation is also regulated to ensure that LT heating power needs are covered at each time step. It can be noticed that during the summer days (time step 480 to 600) there is a surplus of LT heat supplied by the system, as the PEMFC need to work at high power to cover the cooling power demands on board (electrical power required by the CC), but the LT heating power demand during the summer season generally does not exceed 1500 kW. Such surplus of LT heat could indeed be stored in a LTTS, which however is not encompassed in the system as it would increase the CAPEX and the volume occupied by the new components. Differently, during the winter days the LT heating power output from the PEMFC has to be integrated with LT heating power supply by the LTH and the MTTS, as reported in the breakdown of the LT heating power supply at each time step in Figure 5.12.

Figure 5.13 shows the breakdown of the LT heating power demand. It should be noticed that the higher LT heating power demand during the winter season is not only due to the higher levels of Q_{LT}, but also to the higher demand of LT heat by the MTHP in order to fulfill the MT heating power demand.

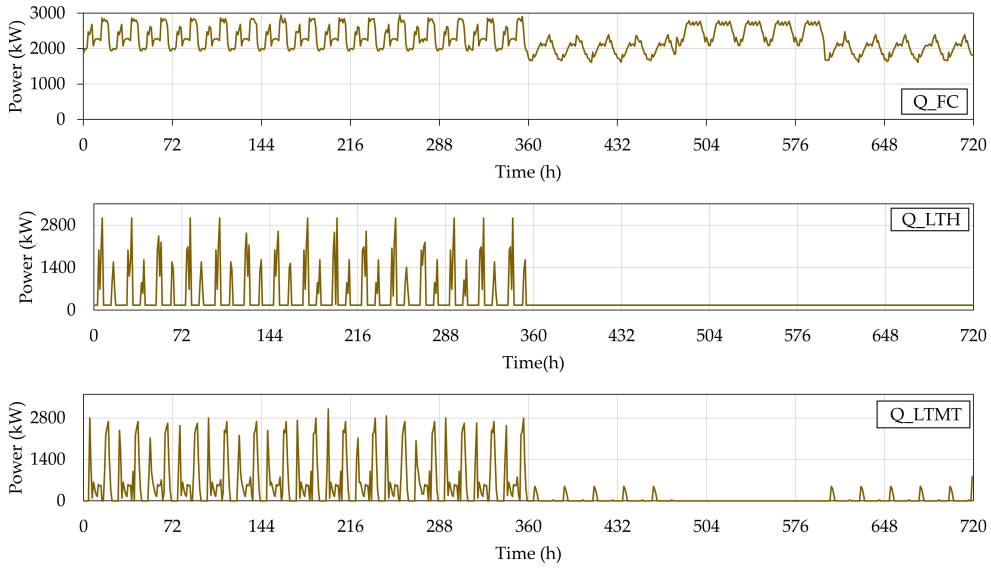

Figure 5.12: *Detailed components of the LT heating power supply from PEMFC (Q_{FC} in the top plot), LTH (Q_{LTAH} in the plot at the center), MTTS (Q_{LTMT} in the bottom plot) over the representative month.*

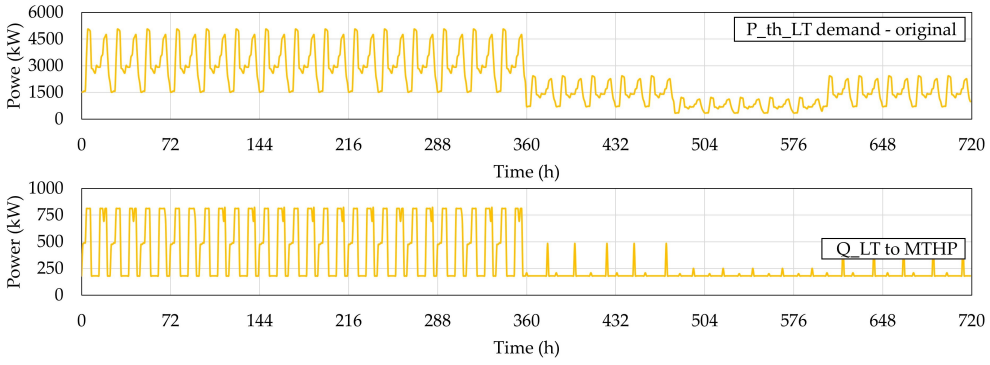

Figure 5.13: *Detailed components of the LT heating power demand on board over the representative month. It can be noticed that part of the heat is directed to the MTHP (Q_{LT} to MTHP in the bottom plot).*

Overall, the proposed analysis allows to quantitatively evaluate the possibility of recovering the PEMFC waste heat for an onboard ship energy system, optimizing the preliminary design and operation of the energy system. Nonetheless, it should be noticed that further analyses are needed to assess the technical feasibility of such power plant installation on board. For example, further analysis will be needed to ensure that the volume required by the whole heat recovery network on board does not exceed the total space available onboard. Hence, a detailed thermodynamic analysis on the whole heat surfaces required will further enhance this study. Similarly, a detailed analysis on the overall space required for the hydrogen system on board would be needed. In fact, while generally the projects on the use of hydrogen in shipping propose the installation of the hydrogen tank on the top deck of the ship, recent studies evaluated also other positioning options that may be advantageous in terms of ship stability and payload space availability on board while not compromising the safety levels on board [93]. In this respect, insights and recommendations on future research on the use of hydrogen fueled PEMFC power plants in shipping from an energy system engineering perspective are reported in the last Chapter of this thesis.

Chapter 6

Conclusions and recommendations for further research

6.1 Conclusions

In the general framework of research on actions and measures aimed at reducing the pollutant and greenhouse gas emissions from the maritime transport sector, this thesis focused on the use of PEMFC based energy systems, as they could potentially guarantee the zero-local emission navigation. In particular, the goal of the thesis was to develop a general methodology that allows to optimize the synthesis, design, and operation of PEMFC ship energy systems while taking into account the degradation of the plant over time, and the possibility to recover the low temperature waste heat from PEMFC on board. Such specific aim of the thesis derived from the literature analysis presented in Chapter 3, which highlighted two main research gaps regarding hydrogen PEMFC energy systems for maritime transportation. Firstly, the progressive degradation of both PEMFC and batteries in hybrid PEMFC systems needs to be taken into account in the definition of the energy management strategy of such systems. Some studies in the literature addressed such problem for land vehicles, but only few studies addressed this issue for ship energy systems. Moreover, studies in the literature usually do not account for the progressive impact of the power units degradation on the whole energy system operation over time, hence only partially investigating the problem. Secondly, the low temperature of PEMFC waste heat is a critical point for the use of PEMFC on board of large ships, such as cruise ships, as it could hamper the efficient waste heat recovery on board, making it difficult to cover the thermal needs of the vessel. Despite the key role that on board PEMFC waste heat

recovery may have in the establishment of maritime PEMFC in shipping, the literature review pointed out a lack of studies specifically investigating this issue. Hence, this thesis addressed such research gaps by applying an energy system approach, which focuses on the ship energy system as a whole rather than on the single components. A methodology of general validity has been developed to analyze and optimize the health conscious energy management strategy and on board PEMFC waste heat recovery, as described in Chapter 4. Two case studies have been taken for applying the methodology and analyzing the results: a small size passenger ferry and a passenger cruise ship. From the conducted analysis and the obtained results discussed in Chapter 5, the following conclusions can be drawn:

1. Taking into account PEMFC and LIB degradation over time is fundamental for a correct design and operation of hybrid PEMFC/LIB energy systems. The development of health-conscious energy management strategies can effectively improve the performance of hybrid PEMFC/LIB energy systems over time, ensuring not only the most effective operation in terms of costs and efficiency, but also avoiding stressful events that would decrease the overall lifetime of the plant.

2. The progressive ageing of PEMFC and LIB in hybrid PEMFC/LIB energy systems leads to the progressive decrease of the plant efficiency, with consequent increase in the vessel's hydrogen consumption. For the specific case study of a small size passenger ferry considered in this thesis, the hydrogen daily consumption at the last month of operation (23^{rd} month) resulted to be about 30% higher than the consumption at the first month of the vessel's operation. This reflects both on the daily operating cost of the vessel, which increases by up to 16% with the progressive plant degradation, and on the need to oversize the hydrogen storage system in order to ensure the daily navigation range of the ferry over the entire lifespan. Such an implication is thus jeopardizing the technical feasibility of directly installing on board the system, affecting also the cost and possible total loss of payload.

3. The uncertainty analysis is a powerful tool that can improve the understanding of the operation of hybrid PEMFC/LIB systems, allowing to obtain risk-aware information not only of the plant investment and operation costs over time, but also on the optimal plant operation.

4. The analysis of a cruise ship energy system including PEMFC with a system approach allows to obtain useful insights on the overall synthesis, design, and operation of such systems taking into account also the possibility to recover the PEMFC waste heat onboard. By including the possibility of recovering the PEMFC waste heat since the early design

phases of the energy system, it is possible to obtain alternative energy system configurations that meet the established objectives.

5. The proposed methodology for ship energy systems design and operation optimization applied to the specific case study of a passenger cruise ship highlighted that, if PEMFC are substituted to ICE for covering the auxiliary electric power demand on board, it is possible to cut the MDO consumption of the vessel by up to 53% if waste heat recovery from PEMFC is taken into account since the system design phase.

6. The use of high temperature heat pumps to supply the high temperature energy needs on board by enhancing the quality of the waste heat could be a viable option for future ship energy systems, although still affected by high investment costs.

Finally, it is worth emphasizing that the large-scale use of fuel cell-based low-emission ship energy systems depends on a variety factors. Beside the bottlenecks related to the still incomplete regulatory framework, the limited hydrogen availability, and the lack of an established hydrogen infrastructure, also other economic, environmental, and social aspects may play a critical role in the deployment of this type of technology and, more generally, in defining optimal decarbonization strategies for the maritime transport sector. With this in mind, it is believed that the analysis proposed in this thesis may help in enhancing the research and development on low to zero-emission PEMFC systems in shipping from an energy system engineering perspective. The extensive literature review conducted on this type of systems as well as the general methodology here proposed pose the basis for further research on this topic. In the next section, recommendations for future research on these subjects are outlined.

6.2 Recommendations for further research

On the basis of the findings and conclusions of this thesis, the following suggestions are proposed for future research on the topic:

- To integrate the fuel logistics in the energy system model.
- To include the certification costs in the models.
- To evaluate the possibility of cold energy recovery from cryogenic liquid hydrogen storage on board.
- To include in the models also other power sources (*e.g.* photovoltaic panels, wind assisted propulsion) and waste heat recovery technologies

(*e.g.* waste heat driven evaporative desalination systems, ORC) to further broaden the delimitations of the study.

- To perform detailed thermodynamic analyses of the low temperature waste heat recovery systems from PEMFC to assess the total heat exchange surfaces necessary on board.
- To explore the possibility of using also other logistic fuels on board.
- To extend the proposed PEMFC waste heat recovery analysis on board a cruise ship to the case of PEMFC propulsion.
- To account for vessels' operating profile uncertainties in order to investigate its impact on the energy systems design and operation.

List of publications

In the following it is reported the list of all the scientific publications developed during the PhD course, in chronological order. Publications are divided into papers published in peer-reviewed international journals, conference papers, and conference proceedings.

Journal papers:

- Taccani, R., Malabotti, S., **Dall'Armi, C.**, Micheli, D. (2020). High energy density storage of gaseous marine fuels: An innovative concept and its application to a hydrogen powered ferry. International Shipbuilding Progress, 67(1), 33-56. DOI:10.3233/ISP-190274.

- **Dall'Armi, C.**, Micheli, D., Taccani, R. (2021). Comparison of different plant layouts and fuel storage solutions for fuel cells utilization on a small ferry. International Journal of Hydrogen Energy 46, 13878-13897. doi.org/10.1016/j.ijhydene.2021.02.138.

- Pivetta, D., **Dall'Armi, C.**., Taccani, R. (2021). Multi-objective optimization of hybrid PEMFC/Li-ion battery propulsion systems for small and medium size ferries. International Journal of Hydrogen Energy 46(72), 35949-35960. doi.org/10.1016/j.ijhydene.2021.02.124.

- **Dall'Armi, C.**, Pivetta, D., Taccani, R. (2021). Health-conscious optimization of long-term operation for hybrid PEMFC ship propulsion systems. Energies 14, no. 13:1813. https://doi.org/10.3390/en14133813.

- **Dall'Armi, C.**, Pivetta, D., Taccani, R. (2022). Uncertainty analysis of the optimal health-conscious operation of a hybrid PEMFC coastal ferry. International Journal of Hydrogen Energy 47(21), 11428-11440. doi.org/10.1016/j.ijhydene.2021.10.271.

- Pivetta, D., **Dall'Armi, C.**, Taccani, R. (2022). Multi-Objective Optimization of a Hydrogen Hub for the Decarbonization of a Port Industrial Area, Journal of Marine Science and Application 10(2), 231, doi.org/10.3390/jmse10020231.

Conference papers:

- Pivetta, D., **Dall'Armi, C.**, Taccani, R .(2021). Strategies for the decarbonization of a port industrial area: design and operation optimization of a hydrogen hub. ECOS 2021 - Proceedings of the 34th International Conference on Efficiency, Cost, Optimization, Simulation and Environmental Impact of Energy System, Taormina, Italy.

- Bernardini, A., Lavagnini, I., **Dall'Armi, C**., Pivetta, D., Taccani, R., Cadenaro, F., Roiaz, M., Crucil, M., Chinese, T., Malabotti, S., Zanelli, M. (2022). The REShiP project: Renewable energy for ship propulsion, NAV 2022 - 21st International Conference on ship and maritime research, 15-17 June 2022, Genoa - La Spezia, Italy.

- **Dall'Armi, C.**, Pivetta, D., Taccani, R. (2022). On optimal integration of PEMFC and low temperature waste heat recovery in a cruise ship energy system, ECOS 2022 - Proceedings of the 35th International Conference on Efficiency, Cost, Optimization, Simulation and Environmental Impact of Energy System, Copenhagen 3-7 July 2022, Denmark.

- Pivetta, D., Volpato, g., Carraro, G., **Dall'Armi, C.**, Da Lio, L., Lazzaretto, A., Taccani, R. (2022). Identification of decarbonization strategies in an industrial port area using a MILP multi-objective optimization, ECOS 2022 - Proceedings of the 35th International Conference on Efficiency, Cost, Optimization, Simulation and Environmental Impact of Energy System, Copenhagen 3-7 July 2022, Denmark.

Conference proceedings:

- Taccani, R., **Dall'Armi, C.**, Zuliani, N., Micheli, D. (2019). Comparison of different plant layouts and fuel storage solutions for fuel cells utilization on a small ferry. 8th European Fuel Cell Piero Lunghi Conference.

- **Dall'Armi, C.**, Micheli, D., Zuliani, N., Taccani, R. (2020). Fuels choice analysis for hybrid fuel cells-batteries propulsion systems of a small size ferry. Oral presentation at the International Conference HYPOTHESIS XV - HYdrogen POwer THeoretical and Engineering Solutions International Symposium.

- **Dall'Armi, C.**, Pivetta, D., Micheli, D., Taccani, R. (2021). Health-conscious multi objective optimization of fuel cells/battery ship propulsion system. Oral presentation at the 1st International Conference WOCST -World Online Conference on Sustainable Technologies.

- **Dall'Armi, C.**, Pivetta, D., Taccani, R. (2021). Hybrid PEMFC/lithium-ion battery propulsion systems for zero-emission Ro-Pax ferries in Croatia: a multi-objective optimization approach. Oral presentation at the International Conference 1st Regional Hydrogen Energy Conference, Croatia (online), 27-29 Sept. 2021.

- Pivetta, D., **Dall'Armi, C.**, Taccani, R. (2021). Overview on decarbonization of port infrastructures in view of alternative fuels for shipping. 3rd International Conference on Modelling and Optimization of Ship Energy Systems.

- Pivetta, D., **Dall'Armi, C.**, Taccani, R. (2021). Ports as hydrogen hubs: an uncertainty analysis for the design and operation optimization. HYPOTHESIS XVI - HYdrogen POwer THeoretical and Engineering Solutions International Symposium.

- Pivetta, D., **Dall'Armi, C.**, Volpato, G., Carraro, G., Da Lio, L., Lazzaretto, A., Taccani, R. (2022). Energy and economic analysis of the local hydrogen production via electrolysis for industrial port districts". 2nd International Conference WOCST - World Online Conference on Sustainable Technologies.

- Pivetta, D., Del Mondo, F., **Dall'Armi, C.**, Bogar, M., Zuliani, N., Taccani, R. (2022). Technical insights and perspectives on hydrogen valleys deployment as enablers of European clean energy transition. HYPOTHESIS XVII - HYdrogen POwer THeoretical and Engineering Solutions International Symposium.

Appendix A

List of projects on fuel cells in shipping

Table A.1 reports the list of the main projects on the use of FC in shipping since 2000. For each project, the following information has been cataloged: ship name, project country, start and end date, state of the vessel (*operating* and *not operating*), vessel type, FC type, logistic fuel, type of EESS, and funding.

Table A.1: *Main projects on the use of FC in shipping available since 2000. Distinction is made between operating (•) and not-operating (○) projects, where the operating ones refer to the cases where the vessel navigated at least once. (N.A. = Not Available).*

Project name	Country	Start date	End date	Operating	Vessel type & name	FC type & rated power	Logistic fuel	Fuel storage	EESS type & capacity	Funding	Refs.
FLAGSHIPS	FRA	2019	2022	•	Tugboat, Zulu	LT-PEMFC, 400 kW	H_2	CH_2	Batteries	4,999,978 € public; 1,766,833 private	[259, 260, 261]
	NOR	2019	2022	○	RoPax (<200 pax), MF Hilde	LT-PEMFC, 600 kW	H_2	CH_2, 250 bar, 600 kg	Batteries, 500 kWh		
ShipFC	NOR	2020	2025	○	Research vessel, Viking Energy	SOFC, 2 MW	NH_3	Liquid NH_3	N.A.	9,975,477 € public; 3,203,578 € private	[44, 262, 263]
Maranda	FIN	2017	2021	•	Research vessel, Aranda	LT-PEMFC, 170 kW	H_2	CH_2, 350 bar, 83 kg	Batteries	2,939,460 € public; 765,297 € private	[264, 265]
NØé	FRA	2015	2020	○	RoPax(<200 pax)	LT-PEMFC, 2 MW	H_2	N.A.	N.A.	N.A.	[137, 266]

Continued on next page

Table A.1 – continued from previous page

Project name	Country	Start date	End date	Operating	Vessel type & name	FC type & rated power	Logistic fuel	Fuel storage	EESS type & capacity	Funding	Refs.
HYSEAS III	GB-SCT	2018	2021	○	RoPax(<200 pax)	LT-PEMFC, 600 kW	H_2	CH_2, 350 bar	LIB, 768 kWh	N.A. public; 2,932,520 € private	[267, 268]
Zeff (part of Pilot-E)	NOR	2018	2020	○	RoPax(>200 pax)	LT-PEMFC, 2.2 MW	$H -$ ”	CH_2	Batteries, 50 kWh	1,040,000 € public	[269, 136]
SeaShuttle (part of Pilot-E)	NOR	2018	-	○	Container vessel, Seashuttle	N.A.	H_2	N.A.	N.A.	6,000,000 € public	[269, 270]
Kamine boat	JPN	2015	2018	•	Small boat, Kamine	LT-PEMFC, 60 kW	H_2	CH_2	LIB, 60 kWh	N.A.	[271, 272]
ULSTEIN SX190 Zero Emission DP2	NOR	2019	2022	○	Research vessel, SX190	LT-PEMFC, 2 MW	H_2	CH_2	N.A.	N.A.	[135, 273]
FreeCO2ast (Part of Pilot-E)	NOR	2018	2023	○	RoPax(>200 pax)	LT-PEMFC. 3.2 MW	H_2	LH_2, 3.5 t	Batteries	N.A.	[274, 275]

Continued on next page

Table A.1 – continued from previous page

Project name	Country	Start date	End date	Operating	Vessel type & name	FC type & rated power	Logistic fuel	Fuel storage	EESS type & capacity	Funding	Refs.
e4ships - (Elektra) and Elektra 2	DEU	2017	2024	•	Tugboat, Elektra	LT-PEMFC,300 kW	H_2	CH_2,500 bar, 750kg	NMC, 2.5 MWh	(1,178,317€)+2,773,475 € public; (373,922 €)+5,108,037 € private	[276, 277, 278]
e4ships - (RiverCell 1) and RiverCell 2	DEU	2017	2021	○	RoPax(<200 pax), RiverCell	HT-PEMFC	MeOH, LNG optional	N.A.	(2,125,598 €)+1,852,793€ public; (2,052,343€)+1,779,538€ private	[276, 279]	
e4ships - Pa-X-ell	DEU	2009	2016	•	RoPax(>200 pax), MS Mariella	HT-PEMFC, 60 kW	MeOH	MeOH liquid	11,281,533€ public; 12,221,685 € private	[276, 280, 281]	
e4ships - Pa-X-ell 2	DEU	2017	2022	○	Cruise ship, AIDAnova	HT-PEMFC	MeOH, LNG optional	MeOH, liquid	N.A.	6,012,875€public; 5,529,202€ private	[276, 280, 281]
e4ships - (SchiBZ) and SchiBZ 2	DEU	2009	2019	•	Cargo vessel, MS Forester	SOFC, 50 kW	Diesel	Diesel, liquid	N.A.	8,072,158€ public;5,615,288 € private	[276, 280]

Continued on next page

Table A.1 – continued from previous page

Project name	Country	Start date	End date	Operating	Vessel type & name	FC type & rated power	Logistic fuel	Fuel storage	EESS type & capacity	Funding	Refs.
e4ships - Multi-SchiBZ	DEU	2018	2020	○	Cargo vessel, MS Forester	SOFC, 50 kW	Diesel, LNG optional	Diesel, liquid	N.A.	7,164,821€ public; 2,673,251€ private	[276, 282]
Greenfuel - Innogy	DEU	2017	2018	•	Small boat, MS Innogy	HT-PEMFC, 35 kW	MeOH	MeOH, liquid 330 l	Batteries, 100 kWh	N.A.	[281, 283]
RØdne E-Maran	NOR	2019	2023	○	RoPax (<200 pax)	LT-PEMFC, 500-750 kW	H_2	LH_2	LTO	N.A.	[284]
HydroCat	NL	2019	2022	•	Research vessel, Hydrocat 48	LT-PEMFC, 1.5 MW	N.A.	N.A.	N.A.	359,373 €public	[285, 286]
Zero V	USA	2017	Present	○	Research Vessel, ZeroV	LT-PEMFC,1.8 MW	H_2	LH_2,1100 kg	Batteries	N.A.	[287, 234]
Race for water	FRA, CHE	2017	2021	•	Small boat, Race for water	LT-PEMFC, 60 kW	H_2	CH_2,350 bar, 200 kg	LIB, 745 kWh	N.A.	[288]
Hynovar	FRA	2017	2021	○	RoPax (>200 pax)	LT-PEMFC	H_2	CH_2, 350 bar, 260 kg	N.A:	N.A.	[289]

Continued on next page

Table A.1 – continued from previous page

Project name	Country	Start date	End date	Operating	Vessel type & name	FC type & rated power	Logistic fuel	Fuel storage	EESS type & capacity	Funding	Refs.
Pilot Future Proof Shipping	NLD, BE	2020	2022	○	Container vessel	LT-PEMFC, 825 kW	H_2	CH_2,300 bar, 1000 kg	LIB,504 kWh	N.A.	[290, 291]
Greenyacht Hydrogen Viking	NOR	2020	2022	○	Small boat, hydrogen Viking	LT-PEMFC	H_2	N.A.	Batteries	N.A.	[292]
Norled Hydra	NOR	2019	2021	○	RoPax (>200 pax), MF Hydra	LT-PEMFC,400 kW	H_2	LH_2,3.8 t	Batteries	5,000,000€ public	[293, 294]
Energy observer	FRA	2017	2024	•	Small boat, Energy Observer	LT-PEMFC, 22 kW	H_2	CH_2,350 bar, 65 kg	LIB, 112 kWh	N.A.	[295]
Sea Change (ex Water-go-round)	USA	2020	2021	•	RoPax (<200 pax), Sea Change	LT-PEMFC, 360 kW	H_2	CH_2,250 bar, 264 kg	LIB, 100 kWh	2,640,000 € public;4,400,000 € private	[296, 74]
SF Breeze	USA	2015	2019	○	RoPax (<200 pax), SF Breeze	LT-PEMFC, 4.9 MW	H_2	LH_2, 1.2 t	-	N.A.	[297]

Continued on next page

Table A.1 – continued from previous page

Project name	Country	Start date	End date	Operating	Vessel type & name	FC type & rated power	Logistic fuel	Fuel storage	EESS type & capacity	Funding	Refs.
Aero 42	NOR	2019	2023	○	RoPax (>200 pax), Aero	LT-PEMFC, 2.8 MW	H_2	CH_2,250 bar, 612 kg	LIB, 672 kWh	N.A.	[298, 299]
Fellowship Viking Lady	NOR	2003	2018	•	Tanker ship, Viking Lady	MCFC,320 kW	LNG	LNG	N.A.	9,450,000 € public; 11,550,000 € private	[73, 300]
METHAPU Undine	SWE	2006	2010	•	Cargo vessel, Undine	SOFC, 250 kW(20 kW demonstrator)	MeOH	MeOH, liquid	N.A.	1,000,000 € public; 930,300 € private	[301, 302]
ZemShip Alsterwasser	DEU	2006	2013	•	Small boat, FCS Alsterwasser	LT-PEMFC, 100 kW	H_2	CH_2,350 bar, 50 kg	Lead gel battery, 360 Ah	2,384,424 € public; 2,773,924 € private	[303]
Nemo H2	NLD	2008	2011	•	RoPax(< 200 pax), Nemo H2	LT-PEMFC 60-70 kW	H_2	CH_2,350 bar, 24 kg	Lead acid battery, 55 kWh	N.A.	[71, 304]

Continued on next page

Table A.1 – continued from previous page

Project name	Country	Start date	End date	Operating	Vessel type & name	FC type & rated power	Logistic fuel	Fuel storage	EESS type & capacity	Funding	Refs.
Hornblower hybrid	USA	2012	Present	•	RoPax (>200 pax), Hornblower	LT-PEMFC, 32 kW	H_2	CH_2	N.A.	N.A.	[305]
Hydrogenesis	GBR	2012	Pesent	•	Small boat, Hydrogenesis	LT-PEMFC, 12 kW	H_2	CH_2,350 bar	N.A.	N.A.	[306, 307]
Royal Caribbean class icon	USA	2017	2026	○	Cruise ship	N.A.	LNG	LNG	N.A.	N.A:	[308]
MC-WAP	ITA	2005	2011	•	Medium & large vessels	MCFC, 500 kW (150 kW demonstrator)	Disel	Diesel, liquid	N.A.	9,899,413€ public; 6,048,207 € private	[309, 310]
FELICITAS	DEU	2005	2008	○	Different applications considered, among which marine	LT-PEMFC, 80 kW; SOFC,250 kW	H_2 for PEMFC & NG for SOFC	N.A. for PEMFC, LNG for SOFC	N.A.	7,943,597 € public; 4,615,926 € private	[311, 312]

Continued on next page

Table A.1 – continued from previous page

Project name	Country	Start date	End date	Operating	Vessel type & name	FC type & rated power	Logistic fuel	Fuel storage	EESS type & capacity	Funding	Refs.
FCSHIP	NOR	2002	2004	○	RopPax (both > and z 200 pax)	LT-PEMFC, HT-PEMFC, SOFC, MCFC; kW propulsion, 1 MW APU	H_2, diesel, NG	CH_2 for small ferry; LNG, diesel or LH_2 for large ferry	N.A.	1,405,563 e public; 1,142,938 € private	[313]
DESIRE	NLD	2001	2004	•	Study only on diesel reforming	MCFC, 25 kW demonstrator	diesel	-	-	N.A.	[314]
SMART H2	ISL, CAN	2007	2010	•	RoPax (<200 pax),Elding	LT-PEMFC, 10 kW	H_2	CH_2,350 bar	Batteries	N.A.	[315, 316]
NEW-H-SHIP	ISL	2004	2005	○	RoPax (<200 px), NEW-H-SHIP	LT-PEMFC, MCFC	N.A.	N.A.	N.A.	265,582 € public; 249,292 € private	[317, 318]
Cobalt 233 Zet	DEU,CHE	2007	2018	•	Small boat, Cobalt 233 Zet	LT-PEMFC, 24 kW	H_2	CH_2, 350 bar	N.A.	N.a:	[71, 319]

Continued on next page

Table A.1 – continued from previous page

Project name	Country	Start date	End date	Operating	Vessel type & name	FC type & rated power	Logistic fuel	Fuel storage	EESS type & capacity	Funding	Refs.
Redrock ferry project	SWE	2021	2023	○	RoPax (<200 pax), Beluga	N.A.	N.A.	N.A.	LTO	N.A.	[320, 321]
e5 Tug	JPN	2019	2022	○	Tugboat, e5 Tug	N.A.	H_2	N.A.	Batteries	N.A.	[322, 323]
Toshiba fuel cell ship	JPN	2020	2024	○	RoPax(<200 pax)	N.A.	H_2	N.A.	Batteries	N.A.	[324, 325]
Aqua	NLD	2020	-	○	Yacht, Aqua	LT-PEMFC, 4 MW	H_2	LH_2	LIB, 1.5 MWh	N.A.	[326]
GKP7H2	NOR	2016	2019	○	RoPax(< 200 pax), GKP7H2	1.2 MW, no data on type	H_2	CH_2,250 bar, 450 kg	N.A.	N.A.	[327, 328]
Tourist boat Busan	KOR	2016	-	•	Small boat, Gold green Hygen	LT-PEMFC, 56 kW	H_2	CH_2,350 bar, 25 kg	LIB, 47 kWh	N.A.	[329]
Jules Verne 2	FRA	2018	-	•	Small boat, Jules Verne 2	LT-PEMFC, 10 kW	H_2	CH_2	Batteries	678,000 € public	[330, 331]

Continued on next page

Table A.1 – continued from previous page

Project name	Country	Start date	End date	Operating	Vessel type & name	FC type & rated power	Logistic fuel	Fuel storage	EESS type & capacity	Funding	Refs.
HySHIP	NOR	2020	2024	○	RoPax (>200 pax), Topeka	LT-PEMFC, 3 MW	H_2	LH_2	Batteries, 1 MWh	8,000,000 € public; 21,730,000 € private	[332, 333]
NABCAT (part of Pilot-E	NOR	2021	2024	○	Farming boat, NABCAT	N.A.	N.A.	N.A.	N.A.	2,800,000 € public	[334]
TecBIA project - ZEUS - SZero Emission Ultimate Ship	ITA	2020	2022	○	Researc vessel, ZEUS	LT-PEMFC, 140 kW	H_2	MH, 50 kg	Batteries, 40 kWH	6,823,677 € public; 209,417 € private	[335, 336]
REShip	ITA	2019	2022	○	RoPax (<200 Pax)	LT-PEMFC, 600 kW	H_2	LH_2	LIB, 657 kWh	475,459 € public; 214,531 € private	[93]
Hydrogenia	KOR	2021	-	•	Small boat, Hydrogenia	N.A.	H_2	N.A.	Batteries	N.A.	[337, 338]
SOFC4Maritime	SWE	2020	-	○	N.A.	SOFC	H_2, NH_3, LNG	N.A.	N.A.	1,110,000 € public; 1,220,000 € private	[339, 340]

Continued on next page

Table A.1 – continued from previous page

Project name	Country	Start date	End date	Operating	Vessel type & name	FC type & rated power	Logistic fuel	Fuel storage	EESS type & capacity	Funding	Refs.
H2SHIPS	NLD,FRA	2019	2022	○	Small boat (NLD); Inland cargo vesse (FRA)	N.A.	H_2	MH (NLD); N.A. for FRA	N.A.	3,470,000 € public; 2,860,000 € private	[341]
ECO Ship 2050	JPN	2018	-	○	RoPax (>200 pax)	SOFC	H_2	LH_2,1900 m^3	N.A.	N.A.	[342, 343]
Green Pearl River	CHN	2020	2021	○	Container vessel inland river	LT-PEMFC, 500 kW	H_2	CH_2,350 bar	LIB, 1 MWh	N.A.	[344, 345]
Wind hunter	JPN	2020	-	•	Small boat, WINZ MARU	N.A.	H_2	MH	N.A.	N.A.	[346]
Yanmar EX38A FC	JPN	2020	-	•	Small boat	LT-PEMFC, 250 kW	H_2	CH_2,700 bar	N.A.	N.A.	[347, 348]
Shimpo	JPN	2018	2021	•	Small boat	LT-PEMFC,60 kW	H_2	CH_2	LIB, 60 kWh	N.A.	[349]

Continued on next page

Table A.1 – continued from previous page

Project name	Country	Start date	End date	Operating	Vessel type & name	FC type & rated power	Logistic fuel	Fuel storage	EESS type & capacity	Funding	Refs.
US-SSFC	USA	2000	2011	•	Naval ship	LT-PEMFC,2.5 MW (only 625 kW tested on board)	diesel	diesel, liquid	N.A.	N.A.	[71]
Bulk cargo-2000	CHN	2019	2021	○	Bulk carrier	LT-PEMFC, 540 kW	H_2	N.A.	LIB, 1 MWh	N.A.	[350]

Appendix B

Convergence analysis to assess the appropriate number of Monte Carlo iterations

Figure B.1 shows the average daily operation cost resulting from the uncertainty analysis performed with different numbers of MC iterations. It can be inferred that the choice of performing the uncertainty analysis with n_{MC}=300 represents a good trade-off between the quality of the obtained results and the overall computational effort.

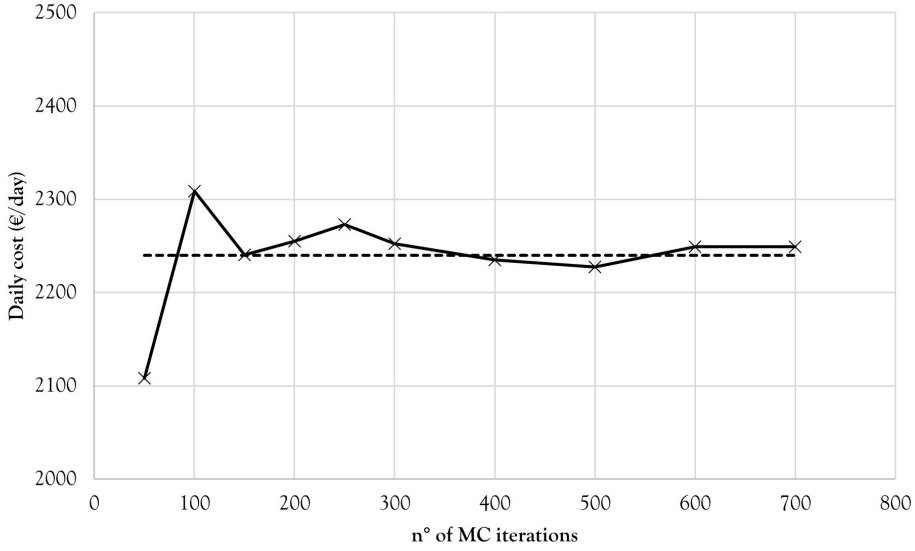

Figure B.1: *Average daily operation cost obtained by performing the uncertainty analysis with increasing numbers of MC iterations. The solid line represents the daily average cost at varying numbers of MC iterations. The dashed line indicates the average value of daily cost among the different numbers of MC iterations.*

Bibliography

[1] International Maritime Organization. Fourth IMO GHG Study 2020 - Executive Summary. Technical report.

[2] Marketa Pape. Sustainable maritime fuels - Fit for 55 package: theFuelEU Maritime proposal. Technical report, European Parliament.

[3] IMO -Energy Efficiency Measures. Available at `https://www.imo.org/en/OurWork/Environment/Pages/Technical-and-Operational-Measures.aspx`, Accessed on 2022-08-23.

[4] DNV GL. Navigating the regulatory environment - cruise insights - DNV. Available at `https://www.dnv.com/expert-story/maritime-impact/navigating-the-regulatory-environment.html`, Accessed on 2022-08-23.

[5] DNV. Fit for 55 – New EU GHG regulations for ships coming soon. Available at `https://www.dnv.com/news/fit-for-55-new-eu-ghg-regulations-for-ships-coming-soon-208746`, Accessed on 2022-08-31.

[6] Associazione Termotecnica Italiana (ATI). Transizione energetica e 4.0 nel settore navale: sfide e opportunità - webinar 27/05/2022. Technical report, Associazione Termotecnica Italiana (ATI)„ 2022.

[7] Chia-Wen Carmen Hsieh and Claus Felby. Biofuels for the marine shipping sector Biofuels for the marine shipping sector An overview and analysis of sector infrastructure, fuel technologies and regulations. 2017.

[8] Francesco Baldi, Andrea Coraddu, and Maria Mondejar, editors. *Sustainable energy systems on ships - Novel technologies for low carbon shipping*. Elsevier, 2022.

[9] Sotiria Lagouvardou, Harilaos N. Psaraftis, and Thalis Zis. A Literature Survey on Market-Based Measures for the Decarbonization of Shipping. *Sustainability 2020, Vol. 12, Page 3953*, (10):3953, may.

[10] Evert A. Bouman, Elizabeth Lindstad, Agathe I. Rialland, and Anders H. Strømman. State-of-the-art technologies, measures, and potential for re-

ducing GHG emissions from shipping – A review. *Transportation Research Part D: Transport and Environment*, 52:408–421, may 2017.

[11] IRENA. A pathway to decarbonise the shipping sector by 2050. Technical report, International Renewable Energy Agency, Abu Dhabi, 2021. www.irena.org.

[12] Jasper Faber, H. Wang, D. Nelissen, B. Russel, and D. Amand. Marginal abatement costs and cost effectiveness of energy efficiency measures. *International Maritime Organization, London, UK*.

[13] Haakon Lindstad and Gunnar S. Eskeland. Low carbon maritime transport: How speed, size and slenderness amounts to substantial capital energy substitution. *Transportation Research Part D: Transport and Environment*, 41:244–256, dec 2015.

[14] Z. L. Yang, D. Zhang, O. Caglayan, I. D. Jenkinson, S. Bonsall, J. Wang, M. Huang, and X. P. Yan. Selection of techniques for reducing shipping NOx and SOx emissions. *Transportation Research Part D: Transport and Environment*, 17(6):478–486, aug 2012.

[15] Dmytro Konovalov, Eugeniy Trushliakov, Mykola Radchenko, Halina Kobalava, and Vitaliy Maksymov. Research of the aerothermopressor cooling system of charge air of a marine internal combustion engine under variable climatic conditions of operation. *Lecture Notes in Mechanical Engineering*, pages 520–529, 2020. https://link.springer.com/chapter/10.1007/978-3-030-40724-7_53.

[16] Fabian Tillig, Wengang Mao, and Jonas W Ringsberg. Systems modelling for energy-efficient shipping. *Chalmers University of Technology*, 2015.

[17] Omer Berkehan Inal, Jean Frédéric Charpentier, and Cengiz Deniz. Hybrid power and propulsion systems for ships: Current status and future challenges. *Renewable and Sustainable Energy Reviews*, 156:111965, mar 2022.

[18] Todd Chou, Vasileios Kosmas, Michele Acciaro, and Katharina Renken. A Comeback of Wind Power in Shipping: An Economic and Operational Review on the Wind-Assisted Ship Propulsion Technology. *Sustainability 2021, Vol. 13, Page 1880*, 13(4):1880, feb 2021. https://www.mdpi.com/2071-1050/13/4/1880/htm https://www.mdpi.com/2071-1050/13/4/1880.

[19] Mphatso N. Nyanya, Huy B. Vu, Alessandro Schönborn, and Aykut I. Ölçer. Wind and solar assisted ship propulsion optimisation and its appli-

cation to a bulk carrier. *Sustainable Energy Technologies and Assessments*, 47:101397, oct 2021.

[20] L. van Biert, M. Godjevac, K. Visser, and P. V. Aravind. A review of fuel cell systems for maritime applications. *Journal of Power Sources*, 327:345–364, sep 2016.

[21] José E. Gutierrez-Romero, Jerónimo Esteve-Pérez, and Blas Zamora. Implementing Onshore Power Supply from renewable energy sources for requirements of ships at berth. *Applied Energy*, 255, dec 2019.

[22] Mohamed Elmi Radwan, Jihong Chen, Zheng Wan, Tianxiao Zheng, Chengying Hua, and Xiaoling Huang. Critical barriers to the introduction of shore power supply for green port development: case of Djibouti container terminals. *Clean Technologies and Environmental Policy*, 21(6):1293–1306, aug 2019.

[23] Thalis Zis, Robin Jacob North, Panagiotis Angeloudis, Washington Yotto Ochieng, and Michael Geoffrey Harrison Bell. Evaluation of cold ironing and speed reduction policies to reduce ship emissions near and at ports. *Maritime Economics and Logistics*, 16(4):371–398, dec 2014. https://link.springer.com/article/10.1057/mel.2014.6.

[24] Yuzhe Zhao, Yujun Fan, Kjetil Fagerholt, and Jingmiao Zhou. Reducing sulfur and nitrogen emissions in shipping economically. *Transportation Research Part D: Transport and Environment*, 90:102641, jan 2021.

[25] M.I. Lamas and C.G. Rodriguez. Emissions from Marine Engines and NOx Reduction Methods. *Journal of Maritime Research*, 2012. https://www.jmr.unican.es/index.php/jmr/article/view/172.

[26] Martin Hjorth Simonsen, Erik Larsson, Wengang Mao, and Jonas W. Ringsberg. State-of-the-Art Within Ship Weather Routing. oct 2015.

[27] Thalis P.V. Zis, Harilaos N. Psaraftis, and Li Ding. Ship weather routing: A taxonomy and survey. *Ocean Engineering*, 213:107697, oct 2020.

[28] Yifan Wang, Laurence A Wright, and Max Bergman. A Comparative Review of Alternative Fuels for the Maritime Sector: Economic, Technology, and Policy Challenges for Clean Energy Implementation. *World 2021, Vol. 2, Pages 456-481*, 2(4):456–481, oct 2021. https://www.mdpi.com/2673-4060/2/4/29/htm https://www.mdpi.com/2673-4060/2/4/29.

[29] Levent Bilgili. Comparative assessment of alternative marine fuels in life cycle perspective. *Renewable and Sustainable Energy Reviews*, 144, jul 2021.

[30] Hui Xing, Charles Stuart, Stephen Spence, and Hua Chen. Alternative fuel options for low carbon maritime transportation: Pathways to 2050. *Journal of Cleaner Production*, 297, may 2021.

[31] DNV-GL. LNG as ship fuel - the fture today. Technical report, 2014. www.dnvgl.com.

[32] Rodolfo Taccani, Stefano Malabotti, Chiara Dall'Armi, and Diego Micheli. High energy density storage of gaseous marine fuels: An innovative concept and its application to a hydrogen powered ferry. *International Shipbuilding Progress*, 67(1):33–56, jan 2020.

[33] Fabio Burel, Rodolfo Taccani, and Nicola Zuliani. Improving sustainability of maritime transport through utilization of Liquefied Natural Gas (LNG) for propulsion. *Energy*, 57:412–420, aug 2013.

[34] Sergey Ushakov, Dag Stenersen, and Per Magne Einang. Methane slip from gas fuelled ships: a comprehensive summary based on measurement data. *Journal of Marine Science and Technology (Japan)*, 24(4):1308–1325, dec 2019. https://link.springer.com/article/10.1007/s00773-018-00622-z.

[35] Francesco Baldi, Stefano Moret, Kari Tammi, and François Maréchal. The role of solid oxide fuel cells in future ship energy systems. *Energy*, 194:116811, mar 2020.

[36] Assessment of selected alternative fuels and technologies in shipping. Technical report, DNV-GL. https://www.dnv.com/maritime/publications/alternative-fuel-assessment-download.html.

[37] DNV. Alternative Fuels Insight. Available at `https://afi.dnv.com/`, Accessed on 2022-09-01.

[38] C. Zamfirescu and I. Dincer. Using ammonia as a sustainable fuel. *Journal of Power Sources*, 185(1):459–465, oct 2008.

[39] Yusuf Bicer, Ibrahim Dincer, Greg Vezina, and Frank Raso. Impact Assessment and Environmental Evaluation of Various Ammonia Production Processes. *Environmental Management*, 59(5):842–855, may 2017. https://link.springer.com/article/10.1007/s00267-017-0831-6.

[40] Arda Yapicioglu and Ibrahim Dincer. A review on clean ammonia as a potential fuel for power generators. *Renewable and Sustainable Energy Reviews*, 103:96–108, apr 2019.

[41] Ghassan Chehade and Ibrahim Dincer. Progress in green ammonia production as potential carbon-free fuel. *Fuel*, 299:120845, sep 2021.

[42] Kyunghwa Kim, Gilltae Roh, Wook Kim, and Kangwoo Chun. A Preliminary Study on an Alternative Ship Propulsion System Fueled by Ammonia: Environmental and Economic Assessments. *Journal of Marine Science and Engineering 2020, Vol. 8, Page 183*, 8(3):183, mar 2020. https://www.mdpi.com/2077-1312/8/3/183/htm https://www.mdpi.com/2077-1312/8/3/183.

[43] Charles J. McKinlay, Stephen R. Turnock, and Dominic A. Hudson. Route to zero emission shipping: Hydrogen, ammonia or methanol? *International Journal of Hydrogen Energy*, 46(55):28282–28297, aug 2021.

[44] ShipFC Project website - European Commission. Available at `https://cordis.europa.eu/project/id/875156`, Accessed on 2022-09-01.

[45] Herie J. Soto, Woo Kum Lee, J. W. Van Zee, and Mahesh Murthy. Effect of transient ammonia concentrations on PEMFC performance. *Electrochemical and Solid-State Letters*, 6(7):A133, jul 2003. https://iopscience.iop.org/article/10.1149/1.1574651 https://iopscience.iop.org/article/10.1149/1.1574651/meta.

[46] Nikoletta L. Trivyza, Michail Cheliotis, Evangelos Boulougouris, and Gerasimos Theotokatos. Safety and Reliability Analysis of an Ammonia-Powered Fuel-Cell System. *Safety 2021, Vol. 7, Page 80*, 7(4):80, nov 2021. https://www.mdpi.com/2313-576X/7/4/80/htm https://www.mdpi.com/2313-576X/7/4/80.

[47] Daniel Sheldon. Methanol production-a technical history. *Johnson Matthey Technology Review*, 61(3):172–182, 2017. https://www.technology.matthey.com/wp-content/uploads/pdf/169-264-jmtr-jul2017.pdf#page=6.

[48] Marc Alvarado. The changing face of the global methanol industry. *IHS Chemical Bulletin*, 2016. www.ihs.com.

[49] Martin Svanberg, Joanne Ellis, Joakim Lundgren, and Ingvar Landälv. Renewable methanol as a fuel for the shipping industry. *Renewable and Sustainable Energy Reviews*, 94:1217–1228, oct 2018.

[50] Selma Brynolf, Erik Fridell, and Karin Andersson. Environmental assessment of marine fuels: liquefied natural gas, liquefied biogas, methanol and bio-methanol. *Journal of Cleaner Production*, 74:86–95, jul 2014.

[51] International Maritime Organization (IMO). Methanol as marine fuel: Environmental benefits, technology readiness, and economic feasibility. Technical report, IMO - International Maritime Organization, 2016. www.dnvgl.com.

[52] Mark Penfold. Methanol as a Marine Fuel. Technical report, ABS - American Bureau of Shipping, 2018.

[53] Laurens Van Hoecke, Ludovic Laffineur, Roy Campe, Patrice Perreault, Sammy W. Verbruggen, and Silvia Lenaerts. Challenges in the use of hydrogen for maritime applications. *Energy & Environmental Science*, (2):815–843, feb.

[54] J Klier, M Rattey, G Kaiser, M Klupsch, A Kade, M Schneider, and R Herzog. A new cryogenic high-pressure H2 test area: First results. In *12th Cryogenics 2012 - IIR International Conference*, Dresden, Germany, 2012.

[55] American Bureau of Shipping (ABS). Requirements for Methanol and Ethanol Fueled Vessels. Technical report, 2022. www.eagle.org.

[56] Murat Ciniviz and Huseyin Kose. Hydrogen use in internal combustion engines - a review. *International Journal of Automotive Engineering and Technologies*, 1(1):1–15, 2012. https://www.researchgate.net/publication/267711346.

[57] H. Barthelemy, M. Weber, and F. Barbier. Hydrogen storage: Recent improvements and industrial perspectives. *International Journal of Hydrogen Energy*, 42(11):7254–7262, mar 2017.

[58] Zhenzhou Wang, Yikun Wang, Sheida Afshan, and Johanna Hjalmarsson. A review of metallic tanks for H2 storage with a view to application in future green shipping. *International Journal of Hydrogen Energy*, 46(9):6151–6179, feb 2021.

[59] Hannah Hyunah Cho, Vladimir Strezov, and Tim J. Evans. Environmental Impact Assessment of Hydrogen Production Via Steam Methane Reforming Based on Emissions Data. *SSRN Electronic Journal*, aug 2022. https://papers.ssrn.com/abstract=4182267.

[60] Furat Dawood, Martin Anda, and G. M. Shafiullah. Hydrogen production for energy: An overview. *International Journal of Hydrogen Energy*, 45(7):3847–3869, feb 2020.

[61] Iea - International Energy Agency. Global Hydrogen Review 2022. 2022. www.iea.org/t&c/.

[62] Lindert van Biert, Kamil Mrozewski, and Pieter 't Hart. Public final report: Inventory of the application of Fuel Cells in the MARitime sector (FCMAR). Technical report, 2021. https://www.koersenvaart.nl/files/MIIP 007-2020 FCMAR 03022021.pdf.

[63] Hannu Aatola, Martti Larmi, Teemu Sarjovaara, and Seppo Mikkonen. Hydrotreated Vegetable Oil (HVO) as a Renewable Diesel Fuel: Trade-off between NO x , Particulate Emission, and Fuel Consumption of a Heavy Duty Engine. *SAE Int. J. Engines*, 1:1251–1262, 2008.

[64] Eliseo Curcio, Michele Miceli, and Blend Tiger. WHITEPAPER: Bio-Bunkers the Immediate Solution to the Energy Transition - Ship & Bunker. *Ship&Bunker*, 2022. https://shipandbunker.com/news/world/470041-whitepaper-bio-bunkers-the-immediate-solution-to-the-energy-transition.

[65] Theodora Tyrovola, George Dodos, Stamatis Kalligeros, and Fanourios Zannikos. The introduction of biofuels in marine sector. *Journal of Environmental Science and Engineering*, 6(8A):415–421, 2017. www.davidpublisher.com.

[66] Radoslav Radonja, Dragan Bebić, and Darko Glujić. Methanol and Ethanol as Alternative Fuels for Shipping. *Promet - Traffic&Transportation*, 31(3):321–327, jun 2019.

[67] L. G. Pereira, O. Cavalett, A. Bonomi, Y. Zhang, E. Warner, and H. L. Chum. Comparison of biofuel life-cycle GHG emissions assessment tools: The case studies of ethanol produced from sugarcane, corn, and wheat. *Renewable and Sustainable Energy Reviews*, 110:1–12, aug 2019.

[68] Muhammad Saleem. Possibility of utilizing agriculture biomass as a renewable and sustainable future energy source. *Heliyon*, 8(2):e08905, feb 2022.

[69] BioDME project website. Available at `http://www.biodme.eu/`, Accessed on 2022-09-20.

[70] ETIP Bioenergy website - BioDME production at industrial scale. Available at `https://www.etipbioenergy.eu/value-chains/products-end-use/products/biodme`, Accessed on 2022-09-20.

[71] T. Tronstad, H. H. Åstrand, G. P. Haugom, and L. Langfeldt. Study on the use of Fuel Cells in Shipping. Technical report, EMSA - European Maritime Safety Agency, 2017. https://www.emsa.europa.eu/publications/item/2921-emsa-study-on-the-use-of-fuel-cells-in-shipping.html.

[72] Matthew M. Mench. Fuel Cell Engines. *Fuel Cell Engines*, pages 1–515, apr 2008. https://onlinelibrary.wiley.com/doi/book/10.1002/9780470209769.

[73] José J. De-Troya, Carlos Álvarez, Carlos Fernández-Garrido, and Luis Carral. Analysing the possibilities of using fuel cells in ships. *International Journal of Hydrogen Energy*, 41(4):2853–2866, jan 2016.

[74] SW/TCH Maritime - Sea change hydrogen PEMFC ferry. Available at `https://www.switchmaritime.com/projects`, Accessed on 2022-09-20.

[75] Michail Cheliotis, Evangelos Boulougouris, Nikoletta L. Trivyza, Gerasimos Theotokatos, George Livanos, George Mantalos, Athanasios Stubos, Emmanuel Stamatakis, and Alexandros Venetsanos. Review on the Safe Use of Ammonia Fuel Cells in the Maritime Industry. *Energies 2021, Vol. 14, Page 3023*, 14(11):3023, may 2021. https://www.mdpi.com/1996-1073/14/11/3023/htm https://www.mdpi.com/1996-1073/14/11/3023.

[76] Marco Gianni, Andrea Pietra, and Rodolfo Taccani. Outlook of future implementation of PEMFC and SOFC onboard cruise ships. *E3S Web of Conferences*, page 04004, feb.

[77] Heiko Ammermann, Philipp Hoff, Mirela Atanasiu, Ovidiu Tisler, and Markus Kaufmann. Advancing Europe's Energy Systems- Stationary Fuel Cells in Distributed Generation. Technical report, mar 2015. https://www.h2knowledgecentre.com/content/researchpaper1118.

[78] Omer Berkehan Inal and Cengiz Deniz. Assessment of fuel cell types for ships: Based on multi-criteria decision analysis. *Journal of Cleaner Production*, 265:121734, aug 2020.

[79] S Saxena and A Verma. Introduction to fuel cell technology: A review. *International Advanced Research Journal in Science, Engineering and Technology*, pages 205–209.

[80] C. Dall'Armi, D. Micheli, and R. Taccani. Comparison of different plant layouts and fuel storage solutions for fuel cells utilization on a small ferry. *International Journal of Hydrogen Energy*, 46(26):13878–13897, apr 2021.

[81] Phatiphat Thounthong, Vibboon Chunkag, Panarit Sethakul, Bernard Davat, and Melika Hinaje. Comparative study of fuel-cell vehicle hybridization with battery or supercapacitor storage device. *IEEE Transactions on Vehicular Technology*, 58(8):3892–3904, 2009.

[82] R. D. Geertsma, R. R. Negenborn, K. Visser, and J. J. Hopman. Design and control of hybrid power and propulsion systems for smart ships: A review of developments. *Applied Energy*, 194:30–54, may 2017.

[83] Miikka Jaurola, Anders Hedin, Seppo Tikkanen, and Kalevi Huhtala. Optimising design and power management in energy-efficient marine vessel power systems: a literature review. *https://doi.org/10.1080/20464177.2018.1505584*, (2):92–101, may.

[84] Daniele Bosich, Giovanni Giadrossi, Stefano Pastore, and Giorgio Sulligoi. Weighted Bandwidth Method for Stability Assessment of Complex DC Power Systems on Ships. *Energies 2022, Vol. 15, Page 258*, 15(1):258, dec 2021. https://www.mdpi.com/1996-1073/15/1/258/htm https://www.mdpi.com/1996-1073/15/1/258.

[85] Rene Prenc, Aleksandar Cuculić, and Ivan Baumgartner. Advantages of using a DC power system on board ship. *Pomorski zbornik*, 52(1):83–97, dec 2016.

[86] Peng Wu and Richard Bucknall. Hybrid fuel cell and battery propulsion system modelling and multi-objective optimisation for a coastal ferry. *International Journal of Hydrogen Energy*, 45(4):3193–3208, jan 2020.

[87] Alexander Innes and Jason Monios. Identifying the unique challenges of installing cold ironing at small and medium ports – The case of aberdeen. *Transportation Research Part D: Transport and Environment*, 62:298–313, jul 2018.

[88] Hervé Barthélémy. Hydrogen storage – Industrial prospectives. *International Journal of Hydrogen Energy*, 37(22):17364–17372, nov 2012.

[89] D Stolten and B Emonts. *Hydrogen Science and Engineering, 2 Volume Set: Materials, Processes, Systems, and Technology*.

[90] Etienne Rivard, Michel Trudeau, and Karim Zaghib. Hydrogen Storage for Mobility: A Review. *Materials 2019, Vol. 12, Page 1973*, 12(12):1973, jun 2019. https://www.mdpi.com/1996-1944/12/12/1973/htm https://www.mdpi.com/1996-1944/12/12/1973.

[91] M. Cristina Galassi, Daniele Baraldi, Beatriz Acosta Iborra, and Pietro Moretto. CFD analysis of fast filling scenarios for 70 MPa hydrogen type IV tanks. *International Journal of Hydrogen Energy*, 37(8):6886–6892, apr 2012.

[92] M. Heitsch, D. Baraldi, and P. Moretto. Numerical investigations on the fast filling of hydrogen tanks. *International Journal of Hydrogen Energy*, 36(3):2606–2612, feb 2011.

[93] Alessandro Bernardini, Irene Lavagnini, Chiara Dall'Armi, Davide Pivetta, Rodolfo Taccani, Fabrizio Cadenaro, Matteo Roiaz, Maurizio

Crucil, Tancredi Chinese, Stefano Malabotti, and Michela Zanelli. The REShiP Project: Renewable Energy for Ship Propulsion. *Progress in Marine Science and Technology*, 6: Technol:692–701, aug 2022. https://ebooks.iospress.nl/doi/10.3233/PMST220081.

[94] NIST Chemistry WebBook. Available at `https://webbook.nist.gov/chemistry/`, Accessed on 2022-10-24.

[95] FuelCellWorks website - Kawasaki Completes World's First Liquefied Hydrogen Receiving Terminal-Kobe LH2 Terminal. Available at `https://fuelcellsworks.com/news/throwback-thursday-kawasaki-completes-worlds-first-liquefied-hydrogen-receiving-terminal-kobe-lh2-terminal/`, Accessed on 2022-09-07.

[96] Joseph W. Pratt and Leonard E. Klebanoff. Feasibility of the SF-BREEZE: a Zero-Emission, Hydrogen Fuel Cell, High-Speed Passenger Ferry. sep 2016. https://rosap.ntl.bts.gov/view/dot/51783.

[97] Norwegian future value chains for liquid hydrogen. Technical report, Cleantech, NCE Maritime.

[98] L. E. Klebanoff, J. W. Pratt, and C. B. LaFleur. Comparison of the safety-related physical and combustion properties of liquid hydrogen and liquid natural gas in the context of the SF-BREEZE high-speed fuel-cell ferry. *International Journal of Hydrogen Energy*, 42(1):757–774, jan 2017.

[99] Linde Engineering website. Available at `https://www.linde-engineering.com/en/index.html`, Accessed on 2022-09-07.

[100] CRYOSTAR website - Design and manufacturing of cryogenic equipment. Available at `https://cryostar.com/`, Accessed on 2022-09-07.

[101] Offshore Energy website - World's first liquid hydrogen bunkering facility for fuelling zero-emission ships revealed. Available at `https://www.offshore-energy.biz/worlds-first-liquid-hydrogen-bunkering-facility-for-fuelling-zero-emission-ships-revealed/`, Accessed on 2022-09-26.

[102] HySTRA website - CO2-free Hydrogen Energy Supply-chain Technology Research Association. Available at `https://www.hystra.or.jp/en/`, Accessed on 2022-10-24.

[103] Federico Ustolin, Alessandro Campari, and Rodolfo Taccani. An Extensive Review of Liquid Hydrogen in Transportation with Focus on the Maritime Sector. *Journal of Marine Science and Engineering 2022, Vol. 10, Page 1222*, 10(9):1222, sep 2022. https://www.mdpi.com/2077-1312/10/9/1222/htm https://www.mdpi.com/2077-1312/10/9/1222.

[104] Salvador M. Aceves, Guillaume Petitpas, Francisco Espinosa-Loza, Manyalibo J. Matthews, and Elias Ledesma-Orozco. Safe, long range, inexpensive and rapidly refuelable hydrogen vehicles with cryogenic pressure vessels. *International Journal of Hydrogen Energy*, 38(5):2480–2489, feb 2013.

[105] R. K. Ahluwalia, T. Q. Hua, J. K. Peng, S. Lasher, K. McKenney, J. Sinha, and M. Gardiner. Technical assessment of cryo-compressed hydrogen storage tank systems for automotive applications. *International Journal of Hydrogen Energy*, 35(9):4171–4184, may 2010.

[106] R.K. Ahluwalia, J.-K. Peng, and T.Q. Hua. Cryo-compressed hydrogen storage. *Compendium of Hydrogen Energy*, pages 119–145, jan 2016.

[107] R. K. Ahluwalia, J. K. Peng, H. S. Roh, T. Q. Hua, C. Houchins, and B. D. James. Supercritical cryo-compressed hydrogen storage for fuel cell electric buses. *International Journal of Hydrogen Energy*, 43(22):10215–10231, may 2018.

[108] Mykhaylo V. Lototskyy, Ivan Tolj, Lydia Pickering, Cordellia Sita, Frano Barbir, and Volodymyr Yartys. The use of metal hydrides in fuel cell applications. *Progress in Natural Science: Materials International*, 27(1):3–20, feb 2017.

[109] M. Cavo, E. Gadducci, D. Rattazzi, M. Rivarolo, and L. Magistri. Dynamic analysis of PEM fuel cells and metal hydrides on a zero-emission ship: A model-based approach. *International Journal of Hydrogen Energy*, 46(64):32630–32644, sep 2021.

[110] Matteo Cavo, Eleonora Gadducci, Massimo Rivarolo, Loredana Magistri, Andrea Dellacasa, Matteo Romanello, Gerardo Borgogna, and Christian Davico. Thermal integration of PEM Fuel Cells and metal hydrides storage system for Zero Emission Ultimate Ship (ZEUS). *E3S Web of Conferences*, page 04004.

[111] Sanjay Kumar, Ankur Jain, Hiroki Miyaoka, Takayuki Ichikawa, and Yoshitsugu Kojima. Study on the thermal decomposition of NaBH4 catalyzed by ZrCl4. *International Journal of Hydrogen Energy*, 42(35):22432–22437, aug 2017.

[112] Rahul Kumar, Abhi Karkamkar, Mark Bowden, and Tom Autrey. Solid-state hydrogen rich boron–nitrogen compounds for energy storage. *Chemical Society Reviews*, 48(21):5350–5380, oct 2019. https://pubs.rsc.org/en/content/articlehtml/2019/cs/c9cs00442d https://pubs.rsc.org/en/content/articlelanding/2019/cs/c9cs00442d.

[113] O. V. Netskina, E. S. Tayban, I. P. Prosvirin, O. V. Komova, and V. I. Simagina. Hydrogen storage systems based on solid-state NaBH4/Co composite: Effect of catalyst precursor on hydrogen generation rate. *Renewable Energy*, 151:278–285, may 2020.

[114] N. A.A. Rusman and M. Dahari. A review on the current progress of metal hydrides material for solid-state hydrogen storage applications. *International Journal of Hydrogen Energy*, 41(28):12108–12126, jul 2016.

[115] Jose Bellosta von Colbe, Jose Ramón Ares, Jussara Barale, Marcello Baricco, Craig Buckley, Giovanni Capurso, Noris Gallandat, David M. Grant, Matylda N. Guzik, Isaac Jacob, Emil H. Jensen, Torben Jensen, Julian Jepsen, Thomas Klassen, Mykhaylol V. Lototskyy, Kandavel Manickam, Amelia Montone, Julian Puszkiel, Sabrina Sartori, Drew A. Sheppard, Alastair Stuart, Gavin Walker, Colin J. Webb, Heena Yang, Volodymyr Yartys, Andreas Züttel, and Martin Dornheim. Application of hydrides in hydrogen storage and compression: Achievements, outlook and perspectives. *International Journal of Hydrogen Energy*, 44(15):7780–7808, mar 2019.

[116] D. Chabane, M. Ibrahim, F. Harel, A. Djerdir, D. Candusso, and O. Elkedim. Energy management of a thermally coupled fuel cell system and metal hydride tank. *International Journal of Hydrogen Energy*, 44(50):27553–27563, oct 2019.

[117] Farshid Mahmoodi and Rahbar Rahimi. Experimental and numerical investigating a new configured thermal coupling between metal hydride tank and PEM fuel cell using heat pipes. *Applied Thermal Engineering*, 178:115490, sep 2020.

[118] Billur Sakintuna, Farida Lamari-Darkrim, and Michael Hirscher. Metal hydride materials for solid hydrogen storage: A review. *International Journal of Hydrogen Energy*, 32(9):1121–1140, jun 2007.

[119] A. I. Bevan, A. Züttel, D. Book, and I. R. Harris. Performance of a metal hydride store on the "Ross Barlow" hydrogen powered canal boat. *Faraday Discussions*, (0):353–367, aug.

[120] Renju Zacharia and Sami Ullah Rather. Review of solid state hydrogen storage methods adopting different kinds of novel materials. *Journal of Nanomaterials*, 2015, 2015.

[121] Jianfeng Zhang, Zhinian Li, Yuanfang Wu, Xiumei Guo, Jianhua Ye, Baolong Yuan, Shumao Wang, and Lijun Jiang. Recent advances on the thermal destabilization of Mg-based hydrogen storage materials. *RSC Advances*, (1):408–428, jan.

[122] C. Fiori, A. Dell'Era, F. Zuccari, A. Santiangeli, A. D'Orazio, and F. Orecchini. Hydrides for submarine applications: Overview and identification of optimal alloys for air independent propulsion maximization. *International Journal of Hydrogen Energy*, 40(35):11879–11889, sep 2015.

[123] Ahad Al-Enazi, Eric C. Okonkwo, Yusuf Bicer, and Tareq Al-Ansari. A review of cleaner alternative fuels for maritime transportation. *Energy Reports*, 7:1962–1985, nov 2021.

[124] Boris Stolz, Maximilian Held, Gil Georges, and Konstantinos Boulouchos. Techno-economic analysis of renewable fuels for ships carrying bulk cargo in Europe. *Nature Energy 2022 7:2*, 7(2):203–212, jan 2022. https://www.nature.com/articles/s41560-021-00957-9.

[125] Päivi T. Aakko-Saksa, Chris Cook, Jari Kiviaho, and Timo Repo. Liquid organic hydrogen carriers for transportation and storing of renewable energy – Review and discussion. *Journal of Power Sources*, 396:803–823, aug 2018.

[126] Daniel Teichmann, Wolfgang Arlt, and Peter Wasserscheid. Liquid Organic Hydrogen Carriers as an efficient vector for the transport and storage of renewable energy. *International Journal of Hydrogen Energy*, 37(23):18118–18132, dec 2012.

[127] Qi Long Zhu and Qiang Xu. Liquid organic and inorganic chemical hydrides for high-capacity hydrogen storage. *Energy & Environmental Science*, (2):478–512, feb.

[128] Nicole Brückner, Katharina Obesser, Andreas Bösmann, Daniel Teichmann, Wolfgang Arlt, Jennifer Dungs, and Peter Wasserscheid. Evaluation of Industrially Applied Heat-Transfer Fluids as Liquid Organic Hydrogen Carrier Systems. *ChemSusChem*, (1):229–235, jan.

[129] Satoshi Nagatake, Takuma Higo, Shuhei Ogo, Yukihiro Sugiura, Ryo Watanabe, Choji Fukuhara, and Yasushi Sekine. Dehydrogenation of Methylcyclohexane over Pt/TiO2 Catalyst. *Catalysis Letters*, 146(1):54–60, jan 2016. https://link.springer.com/article/10.1007/s10562-015-1623-3.

[130] Patrick Preuster, Alexander Alekseev, and Peter Wasserscheid. Hydrogen Storage Technologies for Future Energy Systems. *https://doi.org/10.1146/annurev-chembioeng-060816-101334*, pages 445–471, jun.

[131] Patrick Preuster, Qingping Fang, Roland Peters, Robert Deja, Van Nhu Nguyen, Ludger Blum, Detlef Stolten, and Peter Wasserscheid. Solid oxide fuel cell operating on liquid organic hydrogen carrier-based hydrogen –

making full use of heat integration potentials. *International Journal of Hydrogen Energy*, 43(3):1758–1768, jan 2018.

[132] Weiyu Shi, Baolian Yi, Ming Hou, and Zhigang Shao. The effect of H2S and CO mixtures on PEMFC performance. *International Journal of Hydrogen Energy*, 32(17):4412–4417, dec 2007.

[133] Thomas Luschtinetz, Andreas Sklarow, and Johannes Gulden. Degradation Effects on PEM Fuel Cells Supplied with Hydrogen from a LOHC System. *Applied Mechanics and Materials*, 839:165–169, jun 2016. https://www.scientific.net/AMM.839.165.

[134] Walther Grot. Commercial Membrane Types. *Fluorinated Ionomers*, pages 185–199, 2011.

[135] Ulstein website - SX190 Zero emission DP2. Available at `https://ulstein.com/vessel-design/sx190`, Accessed on 2022-09-07.

[136] NCE Maritime Cleantech website - ZeFF: Towards zero emission fast ferries. Available at `https://maritimecleantech.no/event/introducing-the-worlds-first-zero-emission-fast-ferry/`, Accessed on 2022-09-07.

[137] Mer et Marine website - Nøé - Barillec's zero emission vessel. Available at `https://www.meretmarine.com/fr/construction-navale/noe-barillec-s-zero-emissions-vessel`, Accessed on 2022-09-07.

[138] B. Viswanath Sasank, N. Rajalakshmi, and K. S. Dhathathreyan. Performance analysis of polymer electrolyte membrane (PEM) fuel cell stack operated under marine environmental conditions. *Journal of Marine Science and Technology (Japan)*, 21(3):471–478, sep 2016. https://link.springer.com/article/10.1007/s00773-016-0369-y.

[139] Wei Mon Yan, Xiao Dong Wang, Sen Sin Mei, Xiao Feng Peng, Yi Fan Guo, and Ay Su. Effects of operating temperatures on performance and pressure drops for a 256 cm2 proton exchange membrane fuel cell: An experimental study. *Journal of Power Sources*, 185(2):1040–1048, dec 2008.

[140] Andrea Pietra, Marco Gianni, Nicola Zuliani, Stefano Malabotti, and Rodolfo Taccani. Experimental characterization of a PEM fuel cell for marine power generation. *E3S Web of Conferences*, page 05002.

[141] Huy Quoc Nguyen and Bahman Shabani. Proton exchange membrane fuel cells heat recovery opportunities for combined heating/cooling and power applications. *Energy Conversion and Management*, 204:112328, jan 2020.

[142] M. R. Islam, B. Shabani, G. Rosengarten, and J. Andrews. The potential of using nanofluids in PEM fuel cell cooling systems: A review. *Renewable and Sustainable Energy Reviews*, 48:523–539, aug 2015.

[143] Mohamed H.S. Bargal, Mohamed A.A. Abdelkareem, Qi Tao, Jing Li, Jianpeng Shi, and Yiping Wang. Liquid cooling techniques in proton exchange membrane fuel cell stacks: A detailed survey. *Alexandria Engineering Journal*, 59(2):635–655, apr 2020.

[144] Zhemin Du, Congmin Liu, Junxiang Zhai, Xiuying Guo, Yalin Xiong, Wei Su, and Guangli He. A Review of Hydrogen Purification Technologies for Fuel Cell Vehicles. *Catalysts 2021, Vol. 11, Page 393*, 11(3):393, mar 2021. https://www.mdpi.com/2073-4344/11/3/393/htm https://www.mdpi.com/2073-4344/11/3/393.

[145] Jinfeng Wu, Xiao Zi Yuan, Jonathan J. Martin, Haijiang Wang, Jiujun Zhang, Jun Shen, Shaohong Wu, and Walter Merida. A review of PEM fuel cell durability: Degradation mechanisms and mitigation strategies. *Journal of Power Sources*, 184(1):104–119, sep 2008.

[146] Jennifer Péron, Yannig Nedellec, Deborah J. Jones, and Jacques Rozière. The effect of dissolution, migration and precipitation of platinum in Nafion®-based membrane electrode assemblies during fuel cell operation at high potential. *Journal of Power Sources*, 185(2):1209–1217, dec 2008.

[147] L. Franck-Lacaze, C. Bonnet, E. Choi, J. Moss, S. Pontvianne, H. Poirot, R. Datta, and F. Lapicque. Ageing of PEMFC's due to operation at low current density: Investigation of oxidative degradation. *International Journal of Hydrogen Energy*, 35(19):10472–10481, oct 2010.

[148] Tom Fletcher, Rob Thring, and Martin Watkinson. An Energy Management Strategy to concurrently optimise fuel consumption & PEM fuel cell lifetime in a hybrid vehicle. *International Journal of Hydrogen Energy*, 41(46):21503–21515, dec 2016.

[149] Shengsheng Zhang, Xiaozi Yuan, Haijiang Wang, Walter Mérida, Hong Zhu, Jun Shen, Shaohong Wu, and Jiujun Zhang. A review of accelerated stress tests of MEA durability in PEM fuel cells. *International Journal of Hydrogen Energy*, 34(1):388–404, jan 2009.

[150] Guangjin Wang, Fei Huang, Yi Yu, Sheng Wen, and Zhengkai Tu. Degradation behavior of a proton exchange membrane fuel cell stack under dynamic cycles between idling and rated condition. *International Journal of Hydrogen Energy*, 43(9):4471–4481, mar 2018.

[151] S. J.C. Cleghorn, D. K. Mayfield, D. A. Moore, J. C. Moore, G. Rusch, T. W. Sherman, N. T. Sisofo, and U. Beuscher. A polymer electrolyte fuel cell life test: 3 years of continuous operation. *Journal of Power Sources*, 158(1):446–454, jul 2006.

[152] Manik Mayur, Mathias Gerard, Pascal Schott, and Wolfgang G. Bessler. Lifetime Prediction of a Polymer Electrolyte Membrane Fuel Cell under Automotive Load Cycling Using a Physically-Based Catalyst Degradation Model. *Energies 2018, Vol. 11, Page 2054*, 11(8):2054, aug 2018. https://www.mdpi.com/1996-1073/11/8/2054/htm https://www.mdpi.com/1996-1073/11/8/2054.

[153] Charles Lorenzo, David Bouquain, Samuel Hibon, and Daniel Hissel. Synthesis of degradation mechanisms and of their impacts on degradation rates on proton-exchange membrane fuel cells and lithium-ion nickel–manganese–cobalt batteries in hybrid transport applications. *Reliability Engineering & System Safety*, 212:107369, aug 2021.

[154] E. Brightman and G. Hinds. In situ mapping of potential transients during start-up and shut-down of a polymer electrolyte membrane fuel cell. *Journal of Power Sources*, 267:160–170, dec 2014.

[155] Meiling Yue, Samir Jemei, Rafael Gouriveau, and Noureddine Zerhouni. Review on health-conscious energy management strategies for fuel cell hybrid electric vehicles: Degradation models and strategies. *International Journal of Hydrogen Energy*, 44(13):6844–6861, mar 2019.

[156] Ahmad Baroutaji, Arun Arjunan, Mohamad Ramadan, John Robinson, Abed Alaswad, Mohammad Ali Abdelkareem, and Abdul Ghani Olabi. Advancements and prospects of thermal management and waste heat recovery of PEMFC. *International Journal of Thermofluids*, 9:100064, 2021. https://doi.org/10.1016/j.ijft.2021.100064.

[157] Hoda Ahmadi, Mehdi Rafiei, Moseyeb Afshari-Igder, Meysam Gheisarnejad, and Mohammad Hassan Khooban. An Energy Efficient Solution for Fuel Cell Heat Recovery in Zero-Emission Ferry Boats: Deep Deterministic Policy Gradient. *IEEE Transactions on Vehicular Technology*, 70(8):7571–7581, 2021.

[158] EMSA - European Maritime Safety Agency. Study on Electrical Energy Storage for Ships. Technical report, 2021. https://www.emsa.europa.eu/publications/item/3895-study-on-electrical-energy-storage-for-ships.html.

[159] Ander González, Eider Goikolea, Jon Andoni Barrena, and Roman Mysyk. Review on supercapacitors: Technologies and materials. *Renewable and Sustainable Energy Reviews*, 58:1189–1206, may 2016.

[160] Fabio Ongaro, Stefano Saggini, and Paolo Mattavelli. Li-Ion battery-supercapacitor hybrid storage system for a long lifetime, photovoltaic-based wireless sensor network. *IEEE Transactions on Power Electronics*, 27(9):3944–3952, 2012.

[161] Nolann G. Williams, Dongping Lu, James R. McVey, and Robert J. Cavagnaro. A Comparative Analysis of Lithium-Ion Battery Chemistries for Cold-Climate Maritime Applications. jun 2021. https://www.osti.gov/servlets/purl/1844295/.

[162] Arumugam Manthiram. An Outlook on Lithium Ion Battery Technology. *ACS Central Science*, 3(10):1063–1069, oct 2017. https://pubs.acs.org/doi/full/10.1021/acscentsci.7b00288.

[163] Namireddy Praveen Reddy, Mehdi Karbalaye Zadeh, Christoph Alexander Thieme, Roger Skjetne, Asgeir Johan Sorensen, Svein Aanond Aanondsen, Morten Breivik, and Egil Eide. Zero-Emission Autonomous Ferries for Urban Water Transport: Cheaper, Cleaner Alternative to Bridges and Manned Vessels. *IEEE Electrification Magazine*, 7(4):32–45, dec 2019.

[164] P Wu and RWG Bucknall. Marine propulsion using battery power. *In: (Proceedings) Shipping in Changing Climates Conference 2016. (2016)*, nov 2016.

[165] XALT Energy website. Available at `https://www.xaltenergy.com/marine7`, Accessd on 2022-09-26.

[166] Leclanché website. Available at `https://www.leclanche.com/solutions/e-transport-solutions/e-marine/`, Accessed on 2022-09-26.

[167] Kyunghwa Kim, Juwan An, Kido Park, Gilltae Roh, and Kangwoo Chun. Analysis of a Supercapacitor/Battery Hybrid Power System for a Bulk Carrier. *Applied Sciences 2019, Vol. 9, Page 1547*, 9(8):1547, apr 2019. https://www.mdpi.com/2076-3417/9/8/1547/htm https://www.mdpi.com/2076-3417/9/8/1547.

[168] Alon Oz, Danny Gelman, Emanuelle Goren, Neta Shomrat, Sioma Baltianski, and Yoed Tsur. A novel approach for supercapacitors degradation characterization. *Journal of Power Sources*, 355:74–82, jul 2017.

[169] Philippe Azaïs, Laurent Duclaux, Pierre Florian, Dominique Massiot, Maria Angeles Lillo-Rodenas, Angel Linares-Solano, Jean Paul Peres,

Christophe Jehoulet, and François Béguin. Causes of supercapacitors ageing in organic electrolyte. *Journal of Power Sources*, 171(2):1046–1053, sep 2007.

[170] M. Zhu, C. J. Weber, Y. Yang, M. Konuma, U. Starke, K. Kern, and A. M. Bittner. Chemical and electrochemical ageing of carbon materials used in supercapacitor electrodes. *Carbon*, 46(14):1829–1840, nov 2008.

[171] Amrane Oukaour, Boubekeur Tala-Ighil, Monzer Alsakka, Hamid Gualous, Roland Gallay, and Bertrand Boudart. Calendar ageing and health diagnosis of supercapacitor. *Electric Power Systems Research*, 95:330–338, feb 2013.

[172] F. Naseri, S. Karimi, E. Farjah, and E. Schaltz. Supercapacitor management system: A comprehensive review of modeling, estimation, balancing, and protection techniques. *Renewable and Sustainable Energy Reviews*, 155:111913, mar 2022.

[173] Asmae El Mejdoubi, Amrane Oukaour, Hicham Chaoui, Hamid Gualous, Jalal Sabor, and Youssef Slamani. Prediction Aging Model for Supercapacitor's Calendar Life in Vehicular Applications. *IEEE Transactions on Vehicular Technology*, 65(6):4253–4263, jun 2016.

[174] Eduardo Redondo-Iglesias, Pascal Venet, and Serge Pelissier. Calendar and cycling ageing combination of batteries in electric vehicles. *Microelectronics Reliability*, 88-90:1212–1215, sep 2018.

[175] John Wang, Ping Liu, Jocelyn Hicks-Garner, Elena Sherman, Souren Soukiazian, Mark Verbrugge, Harshad Tataria, James Musser, and Peter Finamore. Cycle-life model for graphite-LiFePO4 cells. *Journal of Power Sources*, 196(8):3942–3948, apr 2011.

[176] Xuebing Han, Languang Lu, Yuejiu Zheng, Xuning Feng, Zhe Li, Jianqiu Li, and Minggao Ouyang. A review on the key issues of the lithium ion battery degradation among the whole life cycle. *eTransportation*, 1:100005, aug 2019.

[177] Christoph R. Birkl, Matthew R. Roberts, Euan McTurk, Peter G. Bruce, and David A. Howey. Degradation diagnostics for lithium ion cells. *Journal of Power Sources*, 341:373–386, feb 2017.

[178] Mohammad Shahjalal, Probir Kumar Roy, Tamanna Shams, Ashley Fly, Jahedul Islam Chowdhury, Md Rishad Ahmed, and Kailong Liu. A review on second-life of Li-ion batteries: prospects, challenges, and issues. *Energy*, 241:122881, feb 2022.

[179] Samuel Pelletier, Ola Jabali, Gilbert Laporte, and Marco Veneroni. Battery degradation and behaviour for electric vehicles: Review and numerical analyses of several models. *Transportation Research Part B: Methodological*, 103:158–187, sep 2017.

[180] Lanre Olatomiwa, Saad Mekhilef, M. S. Ismail, and M. Moghavvemi. Energy management strategies in hybrid renewable energy systems: A review. *Renewable and Sustainable Energy Reviews*, 62:821–835, 2016.

[181] Abba Lawan Bukar and Chee Wei Tan. A review on stand-alone photovoltaic-wind energy system with fuel cell: System optimization and energy management strategy. *Journal of Cleaner Production*, 221:73–88, jun 2019.

[182] Reducing emissions from the shipping sector. Available at `https://ec.europa.eu/clima/eu-action/transport-emissions/reducing-emissions-shipping-sector`, Accessed on 2022-08-23.

[183] Lorenzo Balestra and Ingrid Schjølberg. Energy management strategies for a zero-emission hybrid domestic ferry. *International Journal of Hydrogen Energy*, 46(77):38490–38503, nov 2021.

[184] Lorenzo Balestra and Ingrid Schjølberg. Modelling and simulation of a zero-emission hybrid power plant for a domestic ferry. *International Journal of Hydrogen Energy*, 46(18):10924–10938, mar 2021.

[185] Jingang Han, Jean Frederic Charpentier, and Tianhao Tang. An Energy Management System of a Fuel Cell/Battery Hybrid Boat. *Energies 2014, Vol. 7, Pages 2799-2820*, 7(5):2799–2820, apr 2014. https://www.mdpi.com/1996-1073/7/5/2799/htm https://www.mdpi.com/1996-1073/7/5/2799.

[186] Ameen M. Bassam, Alexander B. Phillips, Stephen R. Turnock, and Philip A. Wilson. An improved energy management strategy for a hybrid fuel cell/battery passenger vessel. *International Journal of Hydrogen Energy*, 41(47):22453–22464, dec 2016.

[187] Lisi Zhu, Jingang Han, Dongkai Peng, Tianzhen Wang, Tianhao Tang, and Jean Frederic Charpentier. Fuzzy logic based energy management strategy for a fuel cell/battery/ultra-capacitor hybrid ship. *2014 1st International Conference on Green Energy, ICGE 2014*, pages 107–112, 2014.

[188] Peng Wu and Richard Bucknall. Hybrid fuel cell and battery propulsion system modelling and multi-objective optimisation for a coastal ferry. *International Journal of Hydrogen Energy*, 45(4):3193–3208, jan 2020.

[189] Chiara Dall'armi, Davide Pivetta, and Rodolfo Taccani. Health-Conscious Optimization of Long-Term Operation for Hybrid PEMFC Ship Propulsion Systems. *Energies 2021, Vol. 14, Page 3813*, 14(13):3813, jun 2021. https://www.mdpi.com/1996-1073/14/13/3813/htm https://www.mdpi.com/1996-1073/14/13/3813.

[190] D. Pivetta, C. Dall'Armi, and R. Taccani. Multi-objective optimization of hybrid PEMFC/Li-ion battery propulsion systems for small and medium size ferries. *International Journal of Hydrogen Energy*, 46(72):35949–35960, oct 2021.

[191] C. Dall'Armi, D. Pivetta, and R. Taccani. Uncertainty analysis of the optimal health-conscious operation of a hybrid PEMFC coastal ferry. *International Journal of Hydrogen Energy*, 47(21):11428–11440, mar 2022.

[192] Daogui Tang, Enrico Zio, Yupeng Yuan, Jiangbin Zhao, and Xinping Yan. The energy management and optimization strategy for fuel cell hybrid ships. *2017 2nd International Conference on System Reliability and Safety, ICSRS 2017*, 2018-Janua:277–281, jan 2018.

[193] M. Rivarolo, D. Rattazzi, and L. Magistri. Best operative strategy for energy management of a cruise ship employing different distributed generation technologies. *International Journal of Hydrogen Energy*, 43(52):23500–23510, dec 2018.

[194] Hui Chen, Zehui Zhang, Cong Guan, and Haibo Gao. Optimization of sizing and frequency control in battery/supercapacitor hybrid energy storage system for fuel cell ship. *Energy*, 197:117285, apr 2020.

[195] Armin Letafat, Mehdi Rafiei, Morteza Sheikh, Mosayeb Afshari-Igder, Mohsen Banaei, Jalil Boudjadar, and Mohammad Hassan Khooban. Simultaneous energy management and optimal components sizing of a zero-emission ferry boat. *Journal of Energy Storage*, 28:101215, apr 2020.

[196] M. Rivarolo, D. Rattazzi, T. Lamberti, and L. Magistri. Clean energy production by PEM fuel cells on tourist ships: A time-dependent analysis. *International Journal of Hydrogen Energy*, 45(47):25747–25757, sep 2020.

[197] Mohsen Banaei, Fatemeh Ghanami, Mohammad Hassan Khooban, and Jalil Boudjadar. Cost-effective control of Roll-on/Roll-off Emission-Free Ships. *2021 25th International Conference on Methods and Models in Automation and Robotics, MMAR 2021*, pages 315–320, aug 2021.

[198] Saeed Hasanvand, Mehdi Rafiei, Meysam Gheisarnejad, and Mohammad Hassan Khooban. Reliable Power Scheduling of an Emission-Free

Ship: Multiobjective Deep Reinforcement Learning. *IEEE Transactions on Transportation Electrification*, 6(2):832–843, jun 2020.

[199] Navid Vafamand, Jalil Boudjadar, and Mohammad Hassan Khooban. Model predictive energy management in hybrid ferry grids. *Energy Reports*, 6:550–557, feb 2020.

[200] Peng Wu, Julius Partridge, and Richard Bucknall. Cost-effective reinforcement learning energy management for plug-in hybrid fuel cell and battery ships. *Applied Energy*, 275:115258, oct 2020.

[201] Peng Wu, Julius Partridge, Enrico Anderlini, Yuanchang Liu, and Richard Bucknall. Near-optimal energy management for plug-in hybrid fuel cell and battery propulsion using deep reinforcement learning. *International Journal of Hydrogen Energy*, 46(80):40022–40040, nov 2021.

[202] Hegazy Rezk, Ahmed M. Nassef, Mohammad Ali Abdelkareem, Abdul Hai Alami, and Ahmed Fathy. Comparison among various energy management strategies for reducing hydrogen consumption in a hybrid fuel cell/supercapacitor/battery system. *International Journal of Hydrogen Energy*, 46(8):6110–6126, jan 2021.

[203] DNV. Handbook for Hydrogen-fuelled Vessels. Technical report, 2021. https://www.dnv.com/maritime/publications/handbook-for-hydrogen-fuelled-vessels-download.html.

[204] American Bureau of Shipping. Guide for Fuel Cell Power Systems For Marine and Offshore Applications. 2019. www.eagle.org.

[205] Bureau Veritas. Ships using fuel cells. Technical report, 2022. https://erules.veristar.com/dy/data/bv/pdf/547-NR_2022-01.pdf.

[206] DNV-GL. Part 6 Additional class notations - Chapter 2 propulsion, power generation and auxiliary systems. Technical report, 2019. https://rules.dnv.com/docs/pdf/DNV/RU-SHIP/2019-10/DNVGL-RU-SHIP-Pt6Ch2.pdf.

[207] IMO. Interim Guidelines for the safety of ships using fuel cell power installations. Technical report, 2022.

[208] Bureau Veritas. Rules for the classification of steel ships. Technical report, 2021. https://erules.veristar.com/dy/data/bv/pdf/467-NR_Amd_2021-01.pdf.

[209] Lloyd Register's. Large battery installation guidance: a risk-based approach. Technical report, 2015. https://www.lr.org/en/latest-news/lr-issues-new-guidance-on-large-battery-installations/.

[210] Fuel Cells and Hydrogen Joint Undertaking. HyLAW Online Database. Available at https://www.hylaw.eu/, Accessed on 2022-09-27.

[211] Fuel Cells and Hydrogen Energy Association. Hydrogen Fuel Cell Codes & Standards. Available at https://www.fuelcellstandards.com/, Accessed on 2022-09-27.

[212] Data and assumptions – The Future of Hydrogen – Analysis - IEA. Available at https://www.iea.org/reports/the-future-of-hydrogen/data-and-assumptions, Accessed on 2022-09-27.

[213] Korean Register of Shipping. Guidance for Fuel Cell Systems on Board of Ships. 2022.

[214] American Bureau of Shipping. Guide for Use of Lithium-ion Batteries in the Marine and Offshore Industries 2022. 2022. www.eagle.org.

[215] MarineTraffic: Global Ship Tracking Intelligence | AIS Marine Traffic. Available at https://www.marinetraffic.com/en/ais/home/centerx:-12.0/centery:24.9/zoom:4, Accessed on 2022-09-09.

[216] Shuaian Wang and Qiang Meng. Sailing speed optimization for container ships in a liner shipping network. *Transportation Research Part E: Logistics and Transportation Review*, 48(3):701–714, may 2012.

[217] K. Ito, R. Yokoyama, and T. Shiba. Optimal Operation of a Diesel Engine Cogeneration Plant Including a Heat Storage Tank. *Journal of Engineering for Gas Turbines and Power*, (4):687–694, oct.

[218] S. Rech and A. Lazzaretto. Smart rules and thermal, electric and hydro storages for the optimum operation of a renewable energy system. *Energy*, 147:742–756, mar 2018.

[219] Sergio Rech. Smart Energy Systems: Guidelines for Modelling and Optimizing a Fleet of Units of Different Configurations. *Energies 2019, Vol. 12, Page 1320*, 12(7):1320, apr 2019. https://www.mdpi.com/1996-1073/12/7/1320/htm https://www.mdpi.com/1996-1073/12/7/1320.

[220] Python website. Available at https://www.python.org/, Accessed on 2022-09-09.

[221] Gurobi Optimization website. Available at https://www.gurobi.com/, Accessed on 2022-09-09.

[222] Cummins Inc. website. Available at https://www.cummins.com/new-power, Accessed on 2022-09-09.

[223] PowerCell website. Available at `https://powercell.se/en/start`, Accessed on 2022-09-09.

[224] Proton Motor website. Available at `https://www.proton-motor.de/`, Accessed on 2022-09-09.

[225] Nedstack website. Available at `https://nedstack.com/en`, Accessed on 2022-09-09.

[226] Huicui Chen, Pucheng Pei, and Mancun Song. Lifetime prediction and the economic lifetime of Proton Exchange Membrane fuel cells. *Applied Energy*, 142:154–163, mar 2015.

[227] Tobias S. Schmidt, Martin Beuse, Xiaojin Zhang, Bjarne Steffen, Simon F. Schneider, Alejandro Pena-Bello, Christian Bauer, and David Parra. Additional Emissions and Cost from Storing Electricity in Stationary Battery Systems. *Environmental Science and Technology*, 53(7):3379–3390, apr 2019. https://pubs.acs.org/doi/full/10.1021/acs.est.8b05313.

[228] Tom Terlouw, Tarek AlSkaif, Christian Bauer, and Wilfried van Sark. Multi-objective optimization of energy arbitrage in community energy storage systems using different battery technologies. *Applied Energy*, 239:356–372, apr 2019.

[229] Matthieu Dubarry, Nan Qin, and Paul Brooker. Calendar aging of commercial Li-ion cells of different chemistries – A review. *Current Opinion in Electrochemistry*, 9:106–113, jun 2018.

[230] Jens Groot. *State of health estimation of Li-ion batteries: ageing models*. PhD thesis, Chalmers University of technology, 2014.

[231] Georgios Mavromatidis, Kristina Orehounig, and Jan Carmeliet. Uncertainty and global sensitivity analysis for the optimal design of distributed energy systems. *Applied Energy*, 214:219–238, mar 2018.

[232] D. Vose. *Risk Analysis: A Quantitative Guide*. John wiley edition.

[233] Ivalin Petkov and Paolo Gabrielli. Power-to-hydrogen as seasonal energy storage: an uncertainty analysis for optimal design of low-carbon multi-energy systems. *Applied Energy*, 274:115197, sep 2020.

[234] R. T. Madsen, L. E. Klebanoff, S. A.M. Caughlan, J. W. Pratt, T. S. Leach, T. B. Appelgate, S. Z. Kelety, H. C. Wintervoll, G. P. Haugom, A. T.Y. Teo, and S. Ghosh. Feasibility of the Zero-V: A zero-emissions hydrogen fuel-cell coastal research vessel. *International Journal of Hydrogen Energy*, 45(46):25328–25343, sep 2020.

[235] Yuki Ishimoto, Mari Voldsund, Petter Nekså, Simon Roussanaly, David Berstad, and Stefania Osk Gardarsdottir. Large-scale production and transport of hydrogen from Norway to Europe and Japan: Value chain analysis and comparison of liquid hydrogen and ammonia as energy carriers. *International Journal of Hydrogen Energy*, 45(58):32865–32883, nov 2020.

[236] Wei Tao, Hongwei Cheng, Weilin Yao, Xionggang Lu, Qiuhua Zhu, Guangshi Li, and Zhongfu Zhou. Syngas production by CO2 reforming of coke oven gas over Ni/La2O3–ZrO2 catalysts. *International Journal of Hydrogen Energy*, 39(32):18650–18658, oct 2014.

[237] C Raucci. The potential of hydrogen to fuel international shipping. *Doctoral thesis, UCL (University College London).*, feb 2017.

[238] Iain Staffell and Richard Green. The cost of domestic fuel cell micro-CHP systems. *International Journal of Hydrogen Energy*, 38(2):1088–1102, jan 2013.

[239] Lebedeva N. Tsiropoulos I., Tarvydas D. Li-Ion Batteries for Mobility and Stationary Storage Applications—Scenarios for Costs and Market Growth. *JRC113360*.

[240] Zhibin Zhou, Mohamed Benbouzid, Jean Frédéric Charpentier, Franck Scuiller, and Tianhao Tang. A review of energy storage technologies for marine current energy systems. *Renewable and Sustainable Energy Reviews*, 18:390–400, feb 2013.

[241] Björn Nykvist and Måns Nilsson. Rapidly falling costs of battery packs for electric vehicles. *Nature Climate Change 2014 5:4*, 5(4):329–332, mar 2015. https://www.nature.com/articles/nclimate2564.

[242] Majdi I. Radaideh and Mohammad I. Radaideh. Application of Stochastic and Deterministic Techniques for Uncertainty Quantification and Sensitivity Analysis of Energy Systems. *International Journal of Energy Research*, 44(4):2517–2534, jan 2019. http://arxiv.org/abs/1901.05566 http://dx.doi.org/10.1002/er.4837.

[243] Patrick O'Connor and Andre Kleyner. *Practical Reliability Engineering*. Chichester.

[244] Georgios Mavromatidis. *Model-based design of distributed urban energy systems under uncertainty*. PhD thesis, Eidgenössische Technische Hochschule (ETH) Zürich, sep 2017.

[245] Francesco Baldi, Fredrik Ahlgren, Tuong Van Nguyen, Marcus Thern, and Karin Andersson. Energy and Exergy Analysis of a Cruise Ship. *Energies 2018, Vol. 11, Page 2508*, 11(10):2508, sep 2018. https://www.mdpi.com/1996-1073/11/10/2508/htm https://www.mdpi.com/1996-1073/11/10/2508.

[246] M. A. Ancona, F. Baldi, M. Bianchi, L. Branchini, F. Melino, A. Peretto, and J. Rosati. Efficiency improvement on a cruise ship: Load allocation optimization. *Energy Conversion and Management*, 164:42–58, may 2018.

[247] Wikipedia images. https://en.wikipedia.org/wiki/File:Birka_June_2013.jpg.

[248] Wärtsilä 46F - datasheet. Available at `https://www.wartsila.com/marine/products/engines-and-generating-sets/diesel-engines/wartsila-46f`, Accessed on 2022-09-15.

[249] Wärtsilä 32 - product guide. Technical report, 2021. https://www.wartsila.com/docs/default-source/product-files/engines/ms-engine/product-guide-o-e-w32.pdf.

[250] Waltteri Salmi, Juha Vanttola, Mia Elg, Maunu Kuosa, and Risto Lahdelma. Using waste heat of ship as energy source for an absorption refrigeration system. *Applied Thermal Engineering*, 115:501–516, mar 2017.

[251] Hiref website- KSW - Pompe di calore acqua/acqua per elevate temperature di evaporazione e condensazione. Available at `https://hiref.it/pompe-di-calore-acqua-acqua-ksw`, Accessed on 2022-09-15.

[252] Cordin Arpagaus, Frédéric Bless, Michael Uhlmann, Jürg Schiffmann, and Stefan S. Bertsch. High temperature heat pumps: Market overview, state of the art, research status, refrigerants, and application potentials. *Energy*, 152:985–1010, jun 2018.

[253] Dariusz Mikielewicz and Jan Wajs. Performance of the very high-temperature heat pump with low GWP working fluids. *Energy*, 182:460–470, sep 2019.

[254] Feng Li, Yupeng Yuan, Xinping Yan, Reza Malekian, and Zhixiong Li. A study on a numerical simulation of the leakage and diffusion of hydrogen in a fuel cell ship. *Renewable and Sustainable Energy Reviews*, 97:177–185, dec 2018.

[255] Nikoletta L Trivyza, Athanasios Rentizelas, and Gerasimos Theotokatos. Impact of carbon pricing on the cruise ship energy systems optimal configuration. 2019.

[256] Sarah Brückner, Selina Liu, Laia Miró, Michael Radspieler, Luisa F. Cabeza, and Eberhard Lävemann. Industrial waste heat recovery technologies: An economic analysis of heat transformation technologies. *Applied Energy*, 151:157–167, aug 2015.

[257] Chiara Magni, Sylvain Quoilin, and Alessia Arteconi. Classification of industrial thermal processes for the investigation of the electrification and flexibility potential. In *Proceedings of ECOS 2022 - 35th International Conference on Efficiency, Cost, Optimization, Simulation and Environmental Impact of Energy Systems*, pages 965–976, 2022.

[258] LG. LG HVAC solution - Absorption chiller. Available at `https://www.lg.com/global/business/download/resources/sac/Catalogue{\_}AbsorptionChillers{\_}ENG{\_}F.pdf`, Accessed on 2022-10-21.

[259] EU commission website - FLAGSHIPS project. Available at `https://cordis.europa.eu/project/id/826215`, Accessed on 2022-09-22.

[260] Ballard marine centre in Europe, supply deal for Norwegian ferry. *Fuel Cells Bulletin*, 2019(5):7, may 2019.

[261] Flagships website - Presenting the FLAGSHIPS H2 ferry. Available at `https://flagships.eu/2019/10/04/presenting-the-flagships-h2/`, Accessed on 2022-09-22.

[262] FuelCell works website - ShipFC project. Available at `https://fuelcellsworks.com/news/shipfc-consortium-awarded-e10-million-to-deliver-offshore-vessel-powered-by-fuel-cells-green-ammonia/`, Accessed on 2022-09-22.

[263] University of Strathclyde - ShipFC project. Available at `https://www.strath.ac.uk/research/maritimesafetyresearchcentre/projects/shipfc/`, Accessed on 2022-09-22.

[264] European Commisstion website - Maranda project. Available at `https://cordis.europa.eu/project/id/735717/results`, Accessed on 2022-09-22.

[265] Maranda project website. Available at `https://projectsites.vtt.fi/sites/maranda/`, Accessed on 2022-09-22.

[266] Vinci Energies website - Nøé Barillec. Available at `https://www.blue-growth.org/`, Accessed on 2022-09-22.

[267] European Commission website - HyseasIII project. Available at `https://cordis.europa.eu/project/id/769417`, Accessed on 2022-09-22.

[268] HySeasIII website. Available at https://www.hyseas3.eu/, Accessed on 2022-09-22.

[269] Hyon website - products and projects. Available at https://hyon.energy/products-projects, Accessed on 2022-09-22.

[270] FuelCellWorks website - SeaShuttle project. Available at https://fuelcellsworks.com/news/samskip-leads-way-in-norway-with-seashuttle-hydrogen-fuel-cell-container-sh/, Accessed on 2022-09-22.

[271] Ballard modules used in successful Yanmar boat test in Japan. *Fuel Cells Bulletin*, 2018(5):5–6, may 2018.

[272] Toyota Tsusho Corporation - Boat fuel cell systems. Available at https://www.toyota-tsusho.com/english/press/detail/180326/004178.html, Accessed on 2022-09-22.

[273] Ulstein website - SX190. Available at https://ulstein.com/vessel-design/sx190, Accessed on 2022-09-22.

[274] PowerCell website - zeroemisison website. Available at https://powercell.se/en/press-releases/A8434432E331DA67?releaseId=A8434432E331DA67, Accessed on 2022-09-22.

[275] PowerCell, Havyard to develop maritime zero-emission solution. *Fuel Cells Bulletin*, 2019(12):4, dec 2019.

[276] e4ships website. Available at https://www.e4ships.de/, Accessed on 2022-09-22.

[277] Elektra project to build zero-emissions canal pusher boat in Germany. *Fuel Cells Bulletin*, 2019(9):5–6, sep 2019.

[278] Ballard receives order from Behala to power German push boat. *Fuel Cells Bulletin*, 2019(11):7–8, nov 2019.

[279] NOW GmbH website - RiverCell 2. Available at https://www.now-gmbh.de/en/projectfinder/rivercell-2/, Accessed on 2022-09-22.

[280] German e4ships project reports on fuel cell maritime demos. *Fuel Cells Bulletin*, 2016(10):5, oct 2016.

[281] Serenergy, fischer fuel cells tested in e4ships project in Germany. *Fuel Cells Bulletin*, 2016(6):4, jun 2016.

[282] e4ships website - MultiSchiBZ project. Available at https://www.e4ships.de/deutsch/seeschifffahrt/multischibz/, Accessed on 2022-09-22.

[283] The innogy Green Fuel Project. Available at https://www.iere.jp/events/forum/2017-canada/Abstract/, Accessed on 2022-09-22.

[284] Jennifer Baumann, Lionel Boillot, Jogchum Buinsma, and Rafael D'Amore-Domenech. IEA Task 39 - Hydrogen in the Maritime. 2021.

[285] Windcat Workboats website - Hydrocat. Available at https://www.windcatworkboats.com/portfolio/hydrocat-mk3-5-h2/, Accessed on 2022-09-22.

[286] Offshore Wind - Hydrocat. Available at https://www.offshorewind.biz/2019/11/28/carbon-trust-picks-ctv-emissions-reduction-tech/, Accessed on 2022-09-22.

[287] Leonard E Klebanoff, Joseph W Pratt, Robert T Madsen, Sean A M Caughlan, Timothy S Leach, T Bruce Appelgate, Stephen Zoltan Kelety, Hans-Christian Wintervoll, Gerd Petra Haugom, and Anthony T Y Teo. Feasibility f the Zero-V : A Zero-Emission, hydrogen fuel-cell, coastal research vessel. Technical report, SANDIA, 2018. https://classic.ntis.gov/help/order-methods/.

[288] Race for Water website. Available at https://www.raceforwater.org/fr/, Accessed on 2022-09-22.

[289] Polemer website - Hynovar project. Available at https://www.polemermediterranee.com/Activites-Projets/Ports-logistique-et-transport-maritime/HYNOVAR, Accessed on 2022-09-26.

[290] Creating a zero-emissions shipping world Hydrogen powered inland container vessel. Technical report, Future Proof Shipping, 2019.

[291] Future Proof Shipping website. Available at https://futureproofshipping.com/projects/the-maas/, Accessed on 2022-09-26.

[292] Green Yacht website - Hydrogen Viking. Available at https://en.greenyacht.no/, Accessed on 2022-09-26.

[293] Annual report Norled AS. Technical report, 2020.

[294] Offshore energy website - MF Hydra LH2 powered ferry. Available at https://www.offshore-energy.biz/ballard-fuel-cells-for-worlds-largest-lh2-powered-ferry/, Accessed on 2022-09-26.

[295] Energy Observer website. Available at https://www.energy-observer.org/, Accessed on 2022-09-26.

[296] Ship technology website - Sea Change hydrogen ferry. Available at https://www.ship-technology.com/news/aam-switch-launch-hydrogen-ferry/, Accessed on 2022-09-26.

[297] Joseph W Pratt and Leonard E Klebanoff. Feasibility of the SF-BREEZE: a Zero-Emission, Hydrogen Fuel Cell, High-Speed Passenger Ferry. http://www.ntis.gov/search.

[298] Ocean Hyway Cluster website - Aero 42 vessel. Available at https://www.oceanhywaycluster.no/member-area-hydrogen-vessels/aero42?rq=aero42, Accessed on 2022-09-26.

[299] FuelCellWorks website - Aero42 project. Available at https://fuelcellsworks.com/news/brodrene-aa-presents-the-aero-a-newly-developed-hydrogen-fast-ferry-concept/, Accessed on 2022-09-26.

[300] Green Car Congress website - Fuel cells in shipping industry. Available at https://www.greencarcongress.com/2012/09/h2shipping-20120907.html, Accessed on 2022-09-26.

[301] METHAPU pr1. METHAPU prototypes methanol SOFC for ships. Fuel Cells Bull. 2008, 4–5 (2008).ototypes methanol SOFC for ships. *Fuel Cells Bulletin*, 2008(5):4–5, may 2008.

[302] European Commission website - METHAPU Project. Available at https://cordis.europa.eu/project/id/31414, Accessed on 2022-09-26.

[303] F Vogler and G Würsig. Fuel cells in maritime applications - Challenges, chances and experiences. 2011.

[304] Green light district website - Fuel cell boat through the canals. Available at http://thegreenlightdistrict.nl/2009/11/30/fuel-cell-boat-through-the-canals/, Accessed on 2022-09-26.

[305] Marine insight website - Hornblower hybrid ferry. Available at https://www.marineinsight.com/future-shipping/hornblower-hybrid-the-worlds-first-hydrogen-hybrid-ferry/, Accessed on 2022-09-26.

[306] Bristol Hydrogen Boats website. Available at http://www.bristolhydrogenboats.co.uk/, Accessed on 2022-09-26.

[307] Ship technology website - Hydrogenesis Passenger Ferry. Available at https://www.ship-technology.com/projects/hydrogenesis-passenger-ferry/, Accessed on 2022-09-26.

[308] FuelCellWorks website - Royal Caribbean Fleet Expansion Cruises To Clean Energy Future. Available at https://fuelcellsworks.com/news/royal-caribbean-fleet-expansion-cruises-to-clean-energy-future/, Accessed on 2022-09-26.

[309] European Commission website - MC WAP project. Available at https://cordis.europa.eu/project/id/19973, Accessed on 2022-09-26.

[310] European Commission website - TRIMIS - MC WAP project. Available at https://trimis.ec.europa.eu/project/molten-carbonate-fuel-cells-waterborne-application, Accessed on 2022-09-26.

[311] European Commission website - FELICITAS project final reoprt. Available at https://cordis.europa.eu/project/id/516270/reporting, Accessed on 2022-09-26.

[312] European Commission website - FELICITAS project. Available at https://cordis.europa.eu/project/id/516270/it, Accessed on 2022-09-26.

[313] European Commission website - FCSHIP project. Available at https://cordis.europa.eu/project/id/G3RD-CT-2002-00823/it, Accessed on 2022-09-26.

[314] S. Krummrich, B. Tuinstra, G. Kraaij, J. Roes, and H. Olgun. Diesel fuel processing for fuel cells—DESIRE. *Journal of Power Sources*, 160(1):500–504, sep 2006.

[315] Icelandic New Energy SMART-H2. 2008.

[316] Vicki P. McConnell. Now, voyager? The increasing marine use of fuel cells. *Fuel Cells Bulletin*, 2010(5):12–17, may 2010.

[317] European Commission website - New-H-Ship project. Available at https://cordis.europa.eu/article/id/87564-towards-hydrogenfuelled-ships, Accessed on 2022-09-26.

[318] Jón Björn Skúlason. NEW H SHIP Publishable final activity report. 2005.

[319] PresseBox website - Cobalt 233 ZET – Zero Emission Technology for Runabouts on Lake Constance. Available at https://www.pressebox.com/inactive/zebotec-gmbh/Cobalt-233-ZET-Zero-Emission-Technology-for-Runabouts-on-Lake-Constance/boxid/128356, Accessed on 2022-09-26.

[320] New Atlas website - World-first zero-emission catamaran set for service in Sweden. Available at https://newatlas.com/marine/world-first-zero-emission-catamaran-beluga24/, Accessed on 2022-09-26.

[321] Shippax website - High-speed emission free catamaran – BELUGA24. Available at https://www.shippax.com/en/press-releases/high-speed-emission-free-catamaran-beluga24.aspx, Accessed on 2022-09-26.

[322] TU website - e5tug ship. Available at https://www.tu.no/artikler/hydrogendrevet-taubat-i-2022/477792?key=l52R1wlE, Accessed on 2022-09-26.

[323] e5ship website. Available at https://e5ship.com/, Accessed on 2022-09-26.

[324] Ocean Hyway Cluster website - Toshiba Fuel Cell Ship. Available at https://www.oceanhywaycluster.no/member-area-hydrogen-vessels/toshiba?rq=toshiba, Accessd on 2022-09-26.

[325] Toshiba Energy Systems & Solutions website - Demonstration Project Begins for Commercialization of Vessels Equipped with High-power Fuel Cells. Available at https://www.global.toshiba/ww/news/energy/2020/09/news-20200901-01.html, Accessed on 2022-09-26.

[326] Sinot website - Aqua yacht. Available at https://sinot.com/aqua/, Accessedon 2022-09-26.

[327] Ocean Hyway Cluster website- GKP7H2. Available at https://www.oceanhywaycluster.no/projectlist/project-1, Accessed on 2022-09-26.

[328] Fredrik Aarskog and Olav Roald Hansen. Preliminary design of hydrogen-driven high speed passenger ferry. pages 14–15, 2018.

[329] Choeng Hoon Choi, Sungju Yu, In Su Han, Back Kyun Kho, Dong Gug Kang, Hyun Young Lee, Myung Soo Seo, Jin Woo Kong, Gwangyun Kim, Jong Woo Ahn, Sang Kyun Park, Dong Won Jang, Jung Ho Lee, and Minje Kim. Development and demonstration of PEM fuel-cell-battery hybrid system for propulsion of tourist boat. *International Journal of Hydrogen Energy*, 41(5):3591–3599, feb 2016.

[330] Elizabeth sea queen Swann website - Jules Verne 2 hydrogen boat. Available at http://www.elizabethqueenseaswann.com/HISTORY/LH2, Accessed on 2022-09-26.

[331] Energy Observer website - Jules Verne 2, a new hydrogen-powered passenger vessel. Available at https://www.energy-observer.org/inno

vations/jules-verne-2-navibus-nantes-hydrogen-propulsion, Accessed on 2022-09-26.

[332] Hyship website. Available at https://hyship.eu/, Accessed on 2022-09-26.

[333] ETH Zurich sus.lab website - HyShip. Available at https://www.suslab.ch/hyship, Accessed on 2022-09-26.

[334] FuelCellsWorks - ENOVA supports the aquaculture industry's first hydrogen fuel cell powered boat. Available at https://fuelcellsworks.com/news/enova-supports-the-aquaculture-industrys-first-hydrogen-boat/, Accessed on 2022-09-26.

[335] Matteo Cavo, Eleonora Gadducci, Massimo Rivarolo, Loredana Magistri, Andrea Dellacasa, Matteo Romanello, Gerardo Borgogna, and Christian Davico. Thermal integration of PEM Fuel Cells and metal hydrides storage system for Zero Emission Ultimate Ship (ZEUS). *E3S Web of Conferences*, 334:04004, 2022.

[336] Fincantieri website - Fincantieri: impostata unità sperimentale Zeus. Available at https://www.fincantieri.com/it/media/comunicati-stampa-e-news/2020/fincantieri-impostata-unita-sperimentale-zeus/, Accessed on 2022-09-26.

[337] Danfoss website - Hydrogenia vessel. Available at https://www.danfoss.com/en/about-danfoss/news/dps/south-korea-s-first-commercialized-hydrogen-electric-boat-officially-unveiled/, Accessed on 2022-09-26.

[338] Offshore energy website - Hydrogenia vessel. Available at https://www.offshore-energy.biz/vinssens-hydrogen-electric-vessel-hydrogenia-unveiled/, Accessed on 2022-09-26.

[339] Energiforskning website - SOFC4Maritime. Available at https://energiforskning.dk/en/node/16089, Accessed on 2022-09-26.

[340] Offshore Energy website - SOFC4Maritime fuel cell project. Available at https://www.offshore-energy.biz/abs-takes-part-in-sofc4maritime-fuel-cell-development-project/, Accessed on 2022-09-26.

[341] H2Ships website. Available at https://h2ships.org/, Accessed on 2022-09-26.

[342] NYK Line website - NYK super Eco Ship. Available at https://www.nyk.com/english/esg/envi/ecoship/, Accessed on 2022-09-26.

[343] Offshore Energy website - NYK Super Eco Ship 2050. Available at https://www.offshore-energy.biz/nyk-steps-into-the-future-with-super-eco-ship-2050/, Accessed on 2022-09-26.

[344] The Maritime Executive website - China Takes Steps in Hydrogen Fuel Cell Development. Available at https://www.maritime-executive.com/article/china-takes-steps-in-hydrogen-fuel-cell-development, Accessed on 2022-09-26.

[345] Offshore Energy website - CCS awards China's 1st hydrogen fuel cell type approval. Available at https://www.offshore-energy.biz/ccs-awards-chinas-1st-hydrogen-fuel-cell-type-approval/, Accessed on 2022-09-26.

[346] Mitsui O.S.K. Lines website - Wind hunter project. Available at https://www.mol.co.jp/en/pr/2020/20080.html, Accessed on 2022-09-26.

[347] Yanmar demos marine hydrogen fuel cell system in boat test. *Fuel Cells Bulletin*, 2021(4):8, apr 2021.

[348] Electric Hybrid Marine Technology website - Yanmar undertakes hydrogen fuel cell field tests |. Available at https://www.electrichybridmarinetechnology.com/news/environmental/yanmar-undertakes-hydrogen-fuel-cell-field-tests.html, Accessed on 2022-09-26.

[349] Yanmar Marine website -YANMAR Cooperates in Field test of Hydrogen Fuel Cell-Powered Boat. Available at https://www.yanmarmarine.eu/News-detail/yanmar-cooperates-in-field-test-of-hydrogen-fuel-cellpowered-boat-095/, Accessed on 2022-09-26.

[350] Zhipeng Zhan. Current status and future development of ful cell ships in China. *Journal of Physics: Conference Series*, page 12061, 2022.

Aknowledgements

Firstly, I would like to thank my supervisor, Prof. Rodolfo Taccani, for the insightful comments and guidance during the PhD. I would also like to thank Prof. Diego Micheli for the advice and encouragement in moving my first steps as a PhD student. My sincere gratitude goes also to Prof. Andrea Lazzaretto, for encouraging me in engaging in a PhD course and for all the advice during these years. My thanks goes to the reviewers of the thesis, whose suggestions helped me in improving the manuscript. I thank also Ing. Irene Lavagnini for the fruitful cooperation in the framework of the research project REShiP. A huge thanks goes to my colleagues of the Enesys lab, for the insightful discussions and collaborations, but also for the relaxed environment in the office and for sharing the addiction to caffeine and chocolates. In particular, a special thank goes to Davide Pivetta for all the inspiring discussions on A3 sheets, for the hard work before deadlines, and for all the fun we had in these years. Infine, il ringraziamento più grande va alla mia famiglia e ai miei amici, per il supporto continuo e incondizionato in tutti questi anni. Soprattutto, un enorme grazie a Fabrizio, il mio tifoso numero 1, per tutti gli incoraggiamenti, le risate e la pazienza in questi anni.